

Alma Mater Studiorum – Università di Bologna

FACOLTA' DI INGEGNERIA

**DOTTORATO DI RICERCA IN
BIOINGEGNERIA**

Ciclo XXII

Settore scientifico-disciplinare di afferenza: ING-INF/06

Tesi di Dottorato

**PERCEZIONE DELLA DIREZIONE DEL
PROPRIO MOVIMENTO: DALLA
REGISTRAZIONE DELL'ATTIVITA'
CORTICALE AL MODELLO
COMPUTAZIONALE**

Candidato: Ing. Chiara Carrozzini

Supervisore: Chiar.mo Prof. Ing. Angelo Cappello
Co-supervisor: Chiar.mi Prof. Salvatore Squatrito,
Dott.ssa Milena Raffi (Dip. Fisiologia
Umana e Generale, Bologna)
Controrelatore: Chiar.mo Prof. Ing. Mauro Ursino

Esame finale anno 2010

Acknowledgements

I am grateful to Prof. Angelo Cappello, my official advisor, for providing the intellectual and personal support to the project and for financially supporting part of my graduate research. He constantly followed my progresses and always helped me with his suggestions, that improved significantly the theoretical and mathematical aspects of this thesis. I admire the way he encouraged me and helped me in becoming a more independent researcher, without even making me notice it.

Neuroscience is a vast field: without the guidance provided by Prof. Salvatore Squatrito and Milena Raffi I would have easily got lost. Their knowledge and passion for research have always been a constant source of motivation. I have always enjoyed the discussions with them, because every day I could learn something new. Prof. Squatrito helped me understand the importance of devotion to research and uprightness. Milena, with her constant good humor and smile, cheered up the long days of experiments and data analysis in the lab. I would also thank Andrea Meoni for sharing his knowledge and kindness on animal caring.

I would also mention Prof. Mauro Ursino, who was the first who introduced me to Neuroscience and neuronal model network during the University years with clarity and professionalism.

Abstract

The main aim of this thesis is strongly interdisciplinary: it involves and presumes a knowledge on Neurophysiology, to understand the mechanisms that undergo the studied phenomena, a knowledge and experience on Electronics, necessary during the hardware experimental set-up to acquire neuronal data, on Informatics and programming to write the code necessary to control the behaviours of the subjects during experiments and the visual presentation of stimuli. At last, neuronal and statistical models should be well known to help in interpreting data.

The project started with an accurate bibliographic research: until now the mechanism of perception of heading (or direction of motion) are still poorly known. The main interest is to understand how the integration of visual information relative to our motion with eye position information happens.

To investigate the cortical response to visual stimuli in motion and the integration with eye position, we decided to study an animal model, using Optic Flow expansion and contraction as visual stimuli.

In the first chapter of the thesis, the basic aims of the research project are presented, together with the reasons why it's interesting and important to study perception of motion. Moreover, this chapter describes the methods my research group thought to be more adequate to contribute to scientific community and underlines my personal contribute to the project.

The second chapter presents an overview on useful knowledge to follow the main part of the thesis: it starts with a brief introduction on central nervous system, on cortical functions, then it presents more deeply associations areas, which are the main target of our study. Furthermore, it tries to explain why studies on animal models are necessary to understand mechanism at a cellular level, that could not be addressed on any other way. In the second part of the chapter, basics on electrophysiology and cellular communication are presented, together with traditional neuronal data analysis methods.

The third chapter is intended to be a helpful resource for future works in the laboratory: it presents the hardware used for experimental sessions, how to control animal behaviour during the experiments by means of C routines and a software, and how to present visual stimuli on a screen.

The fourth chapter is the main core of the research project and the thesis. In the methods, experimental paradigms, visual stimuli and data analysis are presented. In the results, cellular response of area P_{EC} to visual stimuli in motion combined with different eye positions are shown. In brief, this study led to the identification of different cellular behaviour in relation to focus of expansion (the direction of motion given by the optic flow pattern) and eye position. The originality and importance of the results are pointed out in the conclusions: this is the first study aimed to investigate perception of motion in this particular cortical area. In the last paragraph, a neuronal network model is presented: the aim is simulating cellular pre-saccadic and post-saccadic response of neuron in area P_{EC}, during eye movement tasks.

The same data presented in chapter four, are further analysed in chapter fifth. The analysis started from the observation of the neuronal responses during 1s time period in which the visual stimulation was the same. It was clear that cells activities showed oscillations in time, that had been neglected by the previous analysis based on mean firing frequency. Results distinguished two cellular behaviour by their response characteristics: some neurons showed oscillations that changed depending on eye and optic flow position, while others kept the same oscillations characteristics independent of the stimulus.

The last chapter discusses the results of the research project, comments the originality and interdisciplinary of the study and proposes some future developments.

List of Figures

	Pag.
Figure 1: Optic Flow as seen from an airplane	7
Figure 2: Optic Flow of a fly flying forward and rotating	8
Figure 3: Optic Flow pattern as seen by a fly flying forward and rotating	9
Figure 4: Optic Flow while hovering	10
Figure 5: A collection of retinal-flow fields	13
Figure 6: Central nervous system	22
Figure 7: Four areas of the cerebral cortex	23
Figure 8: The six layers of the cortex	26
Figure 9: Orientation sensitivity of columns in the striate cortex	27
Figure 10: Two cytoarchitectonic maps of the cortex	28
Figure 11: Main areas of the brain	33
Figure 12: Comparison between human and macaque brains	37
Figure 13: Area MST, VIP, 7a, STP and PEc in the macaque brain	39
Figure 14: Typical neuron physiology	42
Figure 15: Schematic of recording technique used with behaving monkey	45
Figure 16: Example of a raster plot	49
Figure 17: Temporal averaging of neural spikes to calculate mean firing rate	51
Figure 18: Mean firing rate calculated over several trials	52
Figure 19: Example of a neuronal network	53
Figure 20: Two general kinds of connections between neurons	55
Figure 21: Symmetric cross-correlogram of two cells activity	56
Figure 22: Another symmetric cross-correlogram	57
Figure 23: Cross-correlogram with a peak	57
Figure 24: Experimental paradigms	67
Figure 25: Behavioral protocol	72
Figure 26: Retinotopic, retinotopic eye-position and non retinotopic tasks	75
Figure 27: Text file format generated by the acquisition system	76
Figure 28: Output text files with mean frequencies over time	78
Figure 29: Two conditions of stimulation	81
Figure 30: Venn diagram and results	84

Figure 31: Response of a PEc neuron to luminous bar and translational visual stimuli	86
Figure 32: Response of a PEc neuron to all stimuli	87
Figure 33: Spike density plot (50 ms bin) and regression planes for FP/FOE positions of non-retinotopic EP test in two cells	91
Figure 34: Comparison of the same retinal stimulation at different eye positions	93
Figure 35: Comparison of the same retinal stimulation at different eye positions, by means of a total least square linear regression method	94
Figure 36: Comparison of regression planes in retinotopic and non-retinotopic EP tests, in four cells	96
Figure 37: Anatomy of the recording regions	97
Figure 38: Saccade behavioural task	98
Figure 39: Directional curve of real data and simulated	105
Figure 40: Experimental paradigm	109
Figure 41: Output text file of the acquisition system	115
Figure 42: Raster plot of the activity of a neuron	116
Figure 43: Raster plot of the activity of a neuron during the presentation of a particular combination of FOE/FP positions	116
Figure 44: Spline interpolation of the PSTH discrete values, for the response to expansion optic flow	118
Figure 45: Spline interpolation of the PSTH discrete values, for the response to contraction optic flow	118
Figure 46: Spline interpolation of the PSTH discrete values, for the response to expansion optic flow	120
Figure 47: Spline interpolation of the PSTH discrete values, for the response to contraction optic flow	120

Table of Contents

Acknowledgements	i
Abstract	ii
List of Figures	iv
1. Introduction	1
1.1. Overall aim	1
1.2. Why study perception of motion?	2
1.3. Perception of motion	5
1.4. Main contribution and organization	18
2. Background	19
2.1. Animal research in brain studies	21
2.2. Organization of the nervous system	21
2.2.1. Association areas	31
2.3. Non-human primates vs. human brain.....	34
2.3.1. Perception of motion in the macaque cerebral cortex	38
2.4. Electrophysiology.....	42
2.5. Neural data analysis.....	47
3. Hardware and software for neurophysiologic experiment with behaving monkey	59
3.1. Hardware for neural data acquisition	59
3.2. Behaviour control during experiments	61
3.3. Visual stimuli presentation	64
4. Multimodal representation of optic flow processing in monkey area PEc	69
4.1. Methods	70
4.1.1. Experimental paradigm and stimuli.....	70
4.1.2. Data analysis.....	76
4.2. Results	82
4.3. Conclusions and discussion.....	99

4.4. Model of a neuronal network for eye position coding.....	103
4.4.1. Experimental paradigm	104
4.4.2. Data analysis.....	105
4.4.3. Results and neuronal model	107
5. Spike train oscillation modulated by optic flow stimuli in area P _{Ec}	111
5.1. Methods.....	114
5.1.1. Experimental paradigm and stimuli.....	114
5.1.2. Data Analysis	116
5.2. Results	122
5.3. Conclusions and Discussion	123
7. Overall Conclusions and Discussion	127
Bibliography.....	133

1. Introduction

“ The body, by the place which at each moment it occupies in the universe, indicates the parts and the aspects of matter on which we can lay hold: our perception, which exactly measures our virtual action on things, thus limits itself to the objects which actually influence our organs and prepare our movements.”

Henri Bergson

This chapter has the aim of introducing the topic of the thesis: first, the overall aim of the research project is presented, then the reason why it is important to study mechanisms of the perception of motion is discussed. The third paragraph concentrates on how perception of motion has been studied until now. The last paragraph presents the personal contribution of the author to the research project.

1.1. Overall aim

The principal subject of this work is the investigation of the mechanism of the visual perception of space and motion. There's a question researcher and scientists of many fields have tried for a long time to address: how do we see the world around us?

“The questions is at once a theoretical one, a factual one and a practical one. The theories to be considered have to do with the history of philosophy and psychology. The facts come from psychology, physics and physiology. The applications extend to art, aviation, photography and mountain-climbing.” (Gibson 1950)

The problem of visual perception has a long history and scientists concentrated on the need of explaining why things are seen. It has long been known that vision depends on retinal picture, but these static images seem inadequate when compared with the result we perceive of scenes with depth, distance, solidity. The most amazing aspect of vision is how the third dimension that characterizes the world we live in is restored in perception. But vision also provides a major source of information for the control of self-motion. It’s very difficult to walk to a goal with eyes closed. The visual motion we experience as a result of walking, running, driving, is a powerful signal to control the parameters of our own movements.

A main question is: how can men perceive the direction of their motion?

1.2. Why study perception of motion?

The theoretical approach to understand how visual perception happens started at the beginning of world war II, concomitantly with a sudden need to understand the perception of depth and distance applied to aviation. A critical task was to evaluate the distance from the ground while landing.

Researchers defined a list of *cues* for the perception of distance, classified in monocular and binocular. The “air theory” seemed to underlie the earlier researches: subjects were in darks rooms in which points, lines and subjects were presented. Later, the “ground theory” was hypothesized: there’s no perception of space without the perception of a continuous background surface. The experimenter started to study not the differences between two

object, but the variation in stimulation corresponding to a continuous background.

The main principles of such theory are:

- The elementary impressions of a visual world are those of surfaces (conceived as background) and edges (outline or figure against the background)
- Every variable in visual stimulation corresponds to a property of the spatial world.
- Many properties of visual space do not have any copy in the two-dimensional retinal image, but they may have correlates.
- The pattern of retinal images can be considered a stimulus.
- The problem of how we perceive the visual world can be divided into two separate problems: there's the perception of spatial world, of colours, textures, surfaces, slopes, edges, shapes, and then there's the world of significant things, as objects, places, people, symbols. The latter is too complex to be attended all at once, so our perception is selective.

When we look around in a room, we see a perfectly stable scene of floor and walls, with other familiar objects at defined locations and distances. This is the *visual world*. If we try to look at the same room in a different way, concentrating on areas or patches of colored surfaces, edges, with only one eye, and paying attention to the whole range of what we can see, the scene starts to appear different. This is the *visual field*. Let's underline the differences between these two visual perceptions.

The visual field has oval boundaries, even if hard to notice, it extends about 180° laterally and 150° up and down. If we close one eye, it even becomes smaller. It has a sharp, clear center but it loses details towards its boundaries:

it possesses a central-to-periphery gradient of clarity. The visual field shifts whenever the eyes perform a saccade, that is a rapid change of fixation point. If the shifts are wide, the head also moves in the same direction and as a result the boundaries of the visual field sweep across. In the field, as a projection, the background is not different from the objects, and every head movement produces a deformation of the visual field. In the visual field, the impression of distance never quite vanishes but it's quite reduced.

The visual world, in contrast, is not delimited: floors and walls are seen as a continuous and we're aware they extend backward behind our heads. Since it doesn't have any boundaries, it doesn't have a center. It is usually perceived with the eyes scanning around, so it's always clear and sharp. One of the most familiar characteristic of the visual world is its stability: things possess a direction not respect to the margin of the visual field but of an external frame of reference which seems incomprehensible on the basis of retinal images. In the visual world, natural visual scenes have many items that can be considered as background or figures, and we can perceive if an object is in front of another and it hides part of it. When the head moves, visual world is not distorted: objects remain constant despite changes in the observer's viewing position. Clear and certain distance perception is a characteristic only of the visual world.

When we interact with the environment, we're usually active. Our head never remains in a fixed position, the adjustments in posture produce some changes in the position of our eyes in space. Shifts of the images on our retina occur all the time during vision, but the result is that vision is enriched rather than spoiled. It must be noted that motion of the image produced by head movements it's not the same as that produced by eye movement: the former is a sensory correlate of locomotor behavior that deforms the image, while the latter is only a transpose of the image. All these information are important to determine what is called *heading direction*. Heading perception is the process of inferring the speed and direction of elements in a scene based on visual,

vestibular and proprioceptive inputs. Although this process appears straightforward to most observers, it has proven to be a difficult problem from a computational perspective, and extraordinarily difficult to explain in terms of neural processing.

1.3. Perception of motion

How can we perceive heading direction?

The visual information during locomotion, called Optic Flow (OF), is very important to perceive heading direction, and its value becomes apparent when OF is not matched to true locomotion. For instance, when the walls of a surrounding room are set into motion, toddlers that have just learned to walk fall, while adults modify their walking speed depending on OF (Lee 1980) (Prokop 1997). In stationary subjects, OF induces illusory feeling of self-motion and causes motion sickness after prolonged exposure.

The importance of OF for the control of heading and visual navigation was first recognized by J.J. Gibson. Over 60 years ago Gibson stated that we use optic flow (the pattern of motion flow available at the eye as an observer moves through their environment), rather than object position, to control our direction of locomotion. He noted that the visual motion in the optic array surrounding a moving observer radially expands out of a singular point along the direction of heading. This focus of expansion (FOE) position with respect to the fovea is a critical cue for heading perception. When the observer moves forward fixating his/her final destination, heading computation is a simple brain function (e. a. Warren 1988) (e. a. Warren 1991) (van den Berg 2000). Recovering heading from such an image would be trivial were it not for an issue called “rotational problem”: the problem is more difficult than Gibson’s analysis suggested. The analysis of motion in the optic array is complicated by the fact that the sensors of the visual systems, our eyes, are still respect to

the body: in real life, eye and head movements almost always occur together with the optic flow. Thus the observer experiences a retinal flow resulting from eye, head and body movements that change the FOE position with respect to the fovea. Eye rotation induces a coherent visual motion on the retina. To estimate heading accurately, the visual system must first decompose resulting complex vector fields into the component that is caused by the gaze shift and the component that results from our movement. Note that the visual system has to use retinal and not optic flow, as the basis of self-motion estimation.

How this is accomplished is not well understood yet, despite extensively studies. Different mechanisms have to be considered whether observer gazes at targets away from the FOE or he/she tracks a slowly moving object during locomotion. In any case, heading must be computed integrating retinal and extra-retinal signals.

Let's see some characteristic of Optic flow we experiment in life.

When we move, for example flying on a plane or driving a car, distant objects like clouds and mountains move so slowly they appear still. The objects that are closer, such as buildings and trees, appear to move backwards, with the closer objects moving faster than the distant objects. Very close objects, such as grass or small signs by the road, move so fast they whiz right by you.

There are clear mathematical relationships between the magnitude of the optic flow and where the object is in relation to you. If you double the speed which you travel, the optic flow you see will also double. If an object is brought twice as close to you, the optic flow will again double.

Also the optic flow will vary depending on the angle between your direction of travel and the direction of the object you are looking at. Suppose you are travelling forward. The optic flow is the fastest when the object is to your side by 90 degrees, or directly above or below you. If the object is brought closer to the forward or backward direction, the optic flow will be less. An object

directly in front of you will have no optic flow, and appear to stand still. However, since the edges of that forward object are not directly ahead of you, these edges will appear to move, and the object will appear to get larger.

In Figure 1 different OF are shown:

- A passenger looking downward would experience a strong optic flow pattern due to the ground and rocks on the ground. The optic flow is faster directly below the aircraft. It is especially fast where the tall rock protrudes from the ground.
- Looking forward from the cabin, there is another optic flow pattern due to the upcoming rock and anything else the aircraft might be approaching. The circle directly at the center shows the FOE. The FOE tells the specific direction of motion. This OF is larger to the right of the FOE, due to the large rock, while to the left it's smaller, due to the farther ground.
- Towards the upper left, the pilot would see no optic flow because this region of the visual field only has the sky.

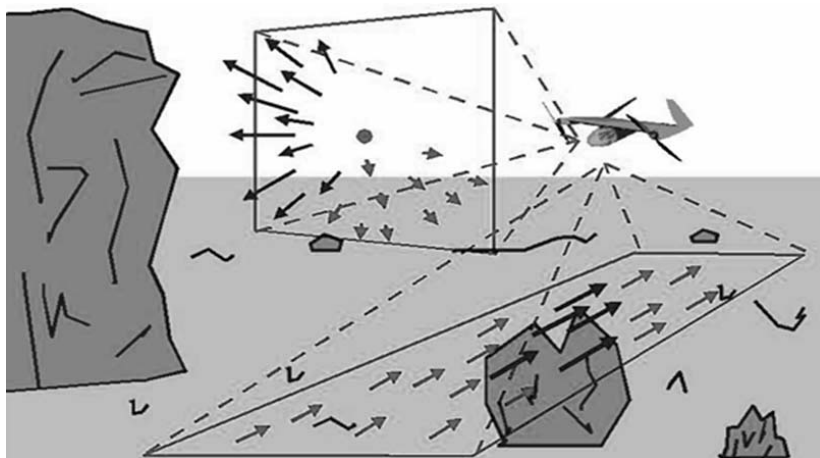


Figure 1: OF as seen from an airplane

Figure 2 shows an overhead view of a fly, and the resulting optic flows in the sideways direction. The figure on the left shows the dragon fly travelling forward. The optic flow travels from the forward to backward direction, and is generally faster sideways than in front. The figure on the right shows a fly rotating to the right. Here the optic flow is to the left in all directions. OF can be also much more complicated: if the fly were flying on a curved path, the optic flow patterns would be a combination of these two patterns.

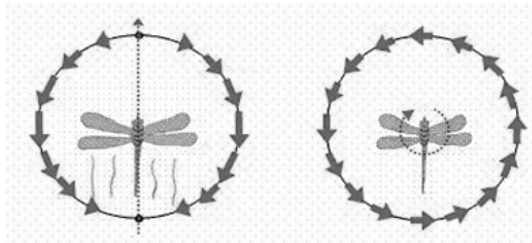


Figure 2: OF of a fly flying forward and rotating

Figure 3 shows the OF seen from the point of view of the fly, and with the 360 degree field of view flattened onto the screen. When travelling forward, the optic flow will diverge from the forward direction, flow backwards, and converge in the rear. When the fly is rotating, or yawing, to the right, the optic flow will be everywhere to the left. However in the directions along the axis of rotation, the optic flow will be zero.

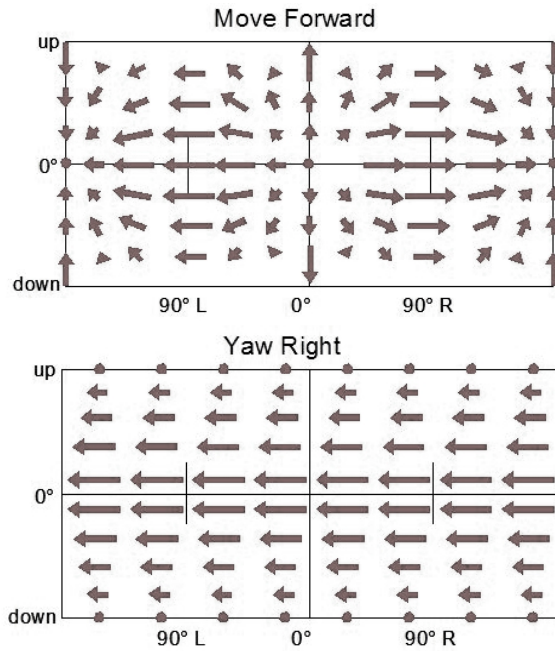


Figure 3: OF pattern as seen by the fly of fig. 2

As already said, sensing OF is useful when interacting with the world.

Suppose you want to hover in one place. The best way to achieve this is to try to keep the OF zero everywhere (Figure 4). This method will only work if the rest of the world is still. What if the “world” is moving? Flies solved this problem swaying with the same rhythm as moving branches or grass.

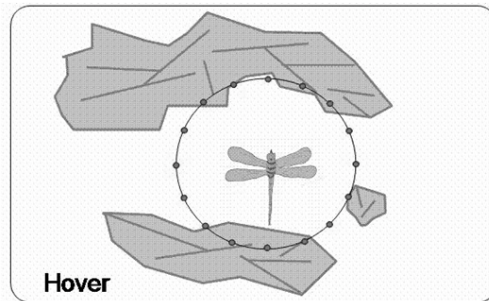


Figure 4: OF while hovering

In avoiding obstacles, a large optic flow on one side warns of an approaching object. The clue may also be that the FOE is inside the obstacles, and the optic flow is expanding rapidly.

The field of heading perception mechanism has been extensively studied and reviewed. A large body of experimental and theoretical evidence has built up in support of the optic flow hypothesis (Lappe M. 1999). Recently, the use of simple egocentric direction (the sum of extra-retinal gaze direction and retinal location) has been offered as an alternative source of visual information (Rushton, Harris, et al. 1998). In the real world, optic flow and egocentric-direction strategies both provide information that can be used to reach a target. When displacing prisms are placed over the eyes during locomotion, the information provided by optic flow and direction-based strategies can be dissociated (Rushton, Harris, et al. 1998). Displacing prisms shift the image of the world on the retina by an amount corresponding to the power of the prism. The result is that objects that appear to be straight ahead when viewed through the prisms, are actually positioned to one side of the observer's body midline. If observers use a simple egocentric-direction strategy to direct them to the target, then while wearing prisms they will attempt to walk directly towards the image of the target, rather than the target itself. The constant heading error (difference between the direction in which the participant is walking and the

actual direction of the target) induced by the prisms will cause them to walk a curved path. In contrast, flow-based locomotion strategies should be unaffected by prisms (apart from on the first step, when flow is not available). This is because displacing prisms do not change differential properties of the flow field such as the focus of expansion (FOE). Instead, they change the visual direction of the FOE. Thus, the FOE will still coincide with the image of the target to which one wants to walk and if FOE is used to control locomotion, the observer should walk along a straight path to the target. Rushton et al.'s study (1998) was the first to use the prism technique to dissociate egocentric direction from flow. The study has now been replicated and extended by several groups (Rogers e Allison 1999) (Rogers e Dalton 1999) (Wood 2000) (Harris e Carrè 2001) (e. a. Warren 2001).

It is now generally agreed that under some circumstances, participants walk a curved path and make heading errors consistent with the use of perceived egocentric direction. The debate now centers around how scene structure and optic flow information influence locomotion in addition to simple egocentric direction (Fajen e Warren 2000).

It has been argued that structure and flow cues could act directly, for example through the use of classic optic flow strategies (e. a. Warren 2001) and the use of motion parallax (Harris e Carrè 2001) or indirectly, by influencing the perception of egocentric direction (Rushton e Salvucci 2001).

For example, both static scene structure and changing structure (flow) are known to have an effect on perceived direction. Such an effect could play a part in the control of locomotion in addition to the possible direct use of flow to guide locomotion.

Heading detection during eye rotation

Experimental investigations of visual self motion perception have benefited from the availability of specialized 3D graphic workstations that can simulate motion through an environment in real time. The most basic experiment use linear movement in simple random-dot environments. The resulting visual motion is presented on a screen in front of a subject and heading judgements are determined either as a just noticeable difference or by a pointing response. For these simple linear movements without eye rotation FOE can be used as an indicator of heading. Accuracy is largely independent of the 3D layout and density of the dots (e. a. Warren 1988). Large errors occur when the FOE is outside the visible area of the screen (Crowell 1991). The estimation of the FOE is mostly based on the pattern of directions of the individual dot movements, less on their speeds (e. a. Warren 1991).

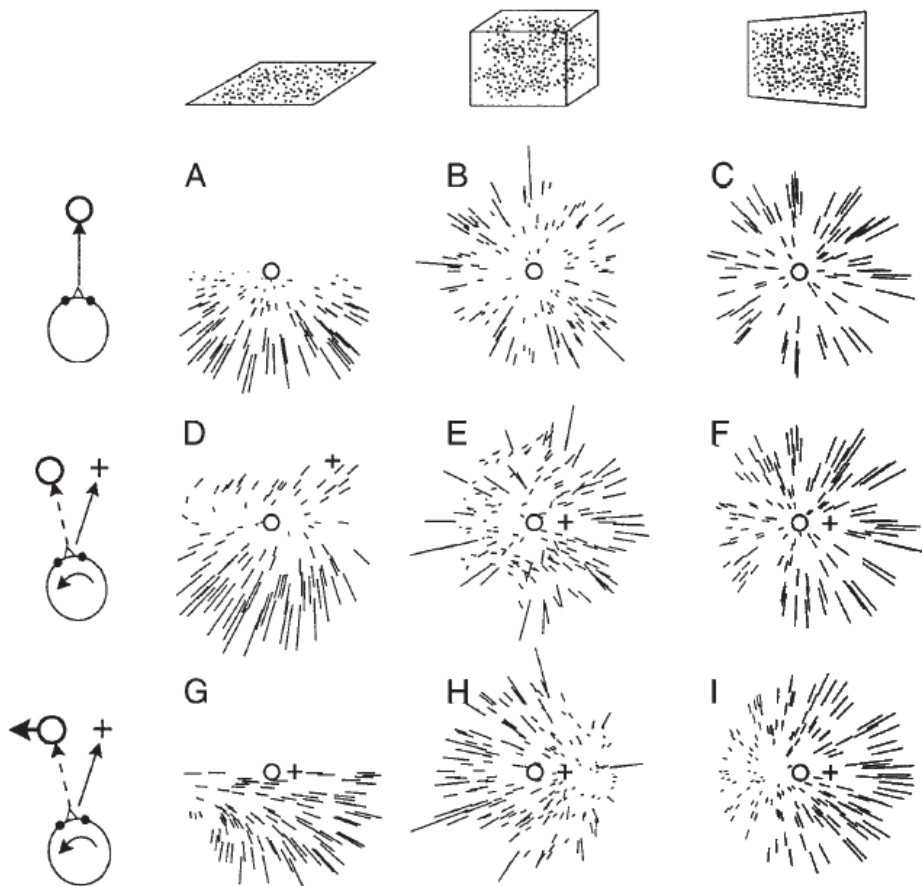


Figure 5: A collection of retinal-flow fields. The retinal flow experienced by a moving observer depends on translation, eye rotation, and the composition of the environment. Columns represent different environments: a flat horizontal plane (the ‘ground plane’), a 3-D volume of random dots, and a vertical wall. Rows represent different combinations of observer translation and eye rotation. (A–C) Pure forward movement in the absence of eye movement. The flow consists of a radial expansion. All motion is away from the focus of expansion (circle) which indicates heading. (D–F) Forward movement while gaze is directed towards an element in the environment. Heading is indicated by a cross, direction of gaze by a circle. An eye rotation is necessary to stabilize gaze onto the target element. The direction of this eye movement is coupled to the motion of the observer because it is along a flow line away from the heading point. Retinal flow becomes a superposition of the visual motion induced by forward movement and that induced by eye movement. The singular point no longer corresponds to heading, which is now on the target element in the direction of gaze, because

this point is stabilized on the retina. In the ground plane (D), the retinal flow obtains a spiralling structure. (E) demonstrates motion parallax: dots near the observer move fast and follow an expansion pattern. Their motion is dominated by the forward movement. Dots far from the observer move more slowly and in a more laminar, unidirectional pattern. Their motion is dominated by the eye rotation. The vertical wall (F) is a special case: the uniform motion introduced by the eye movement transforms the flow field such that a new center of expansion appears in the direction of gaze (circle). Often human subjects confuse this flow field with that of a pure forward movement (C) . The only difference between the two is the distribution of speeds in the periphery. (G-I) Forward movement (cross) with an eye rotation that tracks a horizontally moving target (circle). This target is not attached to the environment, thus the direction of the eye movement is uncoupled from heading. In G and I eye movement is towards the left, in H to the right. The flow field in G is reminiscent of the flow experienced during movement in a curve and human subjects sometimes confuse.

Visual versus extraretinal mechanisms

Eye rotation or combined eye-head rotation induce additional retinal image motion which modify the retinal flow pattern and uncouples retinal from optic flow. This upsets the use of solely FOE as an indicator of heading. Hence, a different strategy should be used. Two alternatives have been proposed. First, eye and eye-head rotations are usually accompanied by non visual or extraretinal signals. These encompass proprioceptive or vestibular signals or an internal copy of motor commands (“efference copy”). This hypothesis assume that extraretinal signals are used to compensate for the rotational components of retinal flow and to calculate the FOE.

The second hypothesis starts from the idea that retinal flow itself contains enough information to separate translational and rotational components. Studies on the contribution of visual and extravisual signals usually involve the paradigm of simulated eye movements (Rieger 1985) (e. a. Cutting 1986). The idea is to present retinal flow normally experience during combined translation and eye rotation to the stationary eye. In this case only visual

mechanism of heading perception can be used, because no extraretinal signals participate when the eye position is fixed.

During eye rotations and active head rotations heading errors are small. However, this result does not by itself prove that extraretinal signals are required because both extraretinal and visual signals are available (and congruent) in this situation. In the simulated eye movement paradigm, the conflict case, results are more variable. The initial study by Warren and Hannon (Warren e Hannon 1990) showed small errors, comparable to those observed during real eye movements, provided that the simulated scene contained large depth variations. Warren and Hannon modelled their stimuli after normal locomotor behavior. They simulated rather slow (up to 1.5 deg/s) eye movements that stabilized gaze on an environmental target. Banks and colleagues (Banks e Royden 1994) (e. a. Banks 1996) used higher rotation rates and simulated pursuit of an independently moving target. They found much larger errors, up to 15 degrees for rotation rates of 5 deg/s. They suggested that direct visual estimation of heading can only be performed for very slow eye movements. At rotation rates greater than 1 deg/s extraretinal information would be required.

The true heading performance and the prediction for an observer that ignores the rotation and simply estimates the FOE in the retinal flow can be compared. The former would correspond to pure visual heading detection, the latter to complete reliance on extraretinal input.

Path perception

The above descriptions assume linear motion and a rotational component induced by eye movement. However, a combination of translational and rotational self-motion also arises during movement along a curved path. In this case the rotation axis is not in the eye but at the center of the motion curve. This creates a further problem for heading detection from retinal flow

because the flow field cannot specify the location of the rotation axis and hence the origin of the rotational component. The retinal flow is ambiguous in that respect. Decomposition of the retinal flow in rotational and translational components only specifies the momentary retinal heading. To relate this to a path in the visual scene requires additional transformations which can give rise to additional errors (Stone e Perrone 1997) . In principle, curved movements can be distinguished from straight movements (Turano e Wang 1994). Observers can discriminate whether an object is on their future curved path with similar precision as during linear movement (e. a. Warren 1991). Sometimes, however, subjects erroneously perceive curved motion paths where linear motion is presented. When pure expansion patterns differ with respect to the average speed of motion in the left and right hemifields, a curved self-motion towards the side with the lower speed is perceived.

Combining retinal flow with information about the environment

Another factor that could influence heading judgements is information about 3-D scene layout. Knowledge of the depth structure of the scene could aid the separation of translation and rotation, because the motion of objects in the flow depends on their distance from the observer. The motion of distant points can be used to estimate rotation while the motion of near points is more useful to obtain translational information. Independent knowledge about the depth structure of the scene is normally available through binocular vision.

Dynamic properties and saccadic eye movements

Saccadic gaze shifts disrupt the retinal flow and change the retinal projection of the direction of heading on average twice per second. Heading judgements are possible for presentation times as short as 228– 400 ms, that is, within the time available between two saccades. Yet, visual search for the heading

direction is only rarely accomplished in a single saccade, indicating that heading direction is usually processed across successive saccadic intervals. But there might be different temporal dynamics of visual and extraretinal contributions to heading perception. Grigo and Lappe suggested that heading detection in the typical time interval between two saccades uses visual mechanisms and that extraretinal inputs become important only at a later time or during longer fixations or eye pursuits (Grigo e Lappe 1998).

OF is the distribution of apparent velocities of movement of brightness patterns in an image and can give important information about the spatial arrangement of the objects viewed and the rate of change of this arrangement. So, many works concentrated also on OF images analysis. Discontinuities in the optical flow can help in segmenting images into regions that correspond to different objects. Attempts have been made to perform such segmentation using differences between successive image frames. Some recent papers have considered the problem of recovering the motions of objects relative to the viewer from the optical flow (Hadani, Ishai e Gur 1980) (Koenderink e van Doorn 1974) (Longuet-Higgins e Prazdny 1980).

In some cases information about the shape of an object may also be recovered (Koenderink e van Doorn 1974) (Clocksin 1980).

One of the major functions of visual perception is to enable us to interact with and move around in our environment. A crucial task for a mobile animal such as ourselves is to be able to walk or run precisely towards (or away from) an object of interest.

1.4. Main contribution and organization

My personal contribution to the research project I was part of during these three years of PhD studies is underlined in each Chapter. To summarize:

- I followed the initial experimental hardware setup with the new equipment for the neuronal data acquisition. This included hardware installation and test of the performances compared to the old acquisition system (see Chapter 3).
- I wrote the C language routines to show the visual stimuli on the screen and to control the behavior of the animal during the training and the experimental sessions. These routines also control neural data recording and synchronization with visual stimuli. (see Chapter 3)
- I performed most of data analysis, by means of MatLAB routines. This included basic and more advanced statistical analysis as well as the implementation of neuronal models (see Chapter 2, 4 & 5).
- I am the second author of the article under review that was written to public the results of the main experiments carried on (see Chapter 4).

2. Background

This chapter consists of five sections, beginning with some thoughts about the use of animal in scientific research. A brief description of the central nervous system, cerebral cortex and association areas follows. The third paragraph concentrates on the analogies and differences between the human and other primates brain. Then, some brief notes about electrophysiology are explained, and at last some traditional neuronal data analysis are presented.

2.1. Animal research in brain studies

It's always hard to speak and write about animal research. This section cannot be exhaustive on the topic, it just wants to be a starting point for meditation.

Most of people are emotionally involved when they hear word as vivisection or animal research, because they think it's an act of violence without any therapeutic aim.

In the last years many animalists raised the debate over the use of animals in biomedical and behavioural research, disputing the value and necessity of these studies and promoting alternative methods. These activities raised confusion and doubts in people's minds over the importance of animal research.

But scientists agree that when there's no other way to encourage the progress of scientific knowledge, animal studies are necessary.

From a recent study by National Academy of Science (NAS) and the Institute of Medicine in the USA (IOM) it's been found that 94% of animals in research do not suffer from experimentation, or at least they are given drugs to

relieve pain. The remaining 6% are exposed to pain only because involved in drug research against pain.

Animals are mainly subjects of three sort of studies: biomedical research, teaching and pharmaceutical.

Biomedical research helps to understand how biological systems work. It's based over the "experimental physiology", founded by Claude Bernard. A scientific study, to be valid, needs to follow two rules: every variable must be controlled and results must be repeatable. It can be basic research or applied. Applied research has more practical and understandable aims, but it leans on basic research knowledge. We cannot say one is more important than the other.

In teaching, animal experiments are necessary for surgeons and veterinaries to acquire the skills to operate on patients, as well as new for knowing the effects of new drugs.

Animalists stand up to the idea that we can learn only from studies on humans, because other species differ too much from us. This is not true, especially because scientists choose a particular species for a study because they know it may have similar response to humans. Dogs for example were of unbelievable value for kidney transplant, for studying heart disease, for better understanding how insulin is involved in diabetes.

Animalists also insist that there are alternatives to animal research: in vitro research and computer simulation. They both helped a lot researchers in the last decades, but first isolated cells will never react as cells in a living body. Some in vitro results may have nothing to do with real cellular behavior. Regarding computer simulation, the main problem is that a model is good only when supported by a deep knowledge of reality: most of biological mechanisms are still unknown, so no model can simulate their behavior.

When speaking of studies on non human primates, the objection is even stronger: animalists believe primates can feel the same sufferance as humans. This may be true, but this similarity makes them even more precious: they can get most of the same disease we have, their immune system is quite similar to ours, they have extraordinary intellectual and social abilities and in some motor act they are even better than humans. Primates are used only in 0.5% of animal studies, but their contribution is enormous: they helped to find the vaccine against polio and hepatitis, to study hypertension, Parkinson disease. It's true, there might be chances that the animals suffer, but this has nothing to do with maltreatment: scientists try their best to avoid every stress and pain in animals.

Scientists agree that animal research is necessary for reducing pain and illness in humans, and most progresses made by medicine in the past involved animal research. And most of all, scientists are aware there are no other choices.

2.2. Organization of the nervous system

This chapter aims to introduce some basics about the nervous system. The anatomy of the brain and the pattern of its interconnections appear (and are) rather complex, but the functional organization of the nervous system is governed by a relatively simple set of principles that make the anatomy more comprehensible.

All our behavior are governed by the central nervous system, which consist in the spinal cords and the brain. The main brain divisions are the cerebellum, the brain stem and the cerebral hemispheres. The cerebral hemispheres are interconnected by the corpus callosum and consist of the cerebral cortex, the white matter, the basal ganglia, the amygdale and the hippocampus.

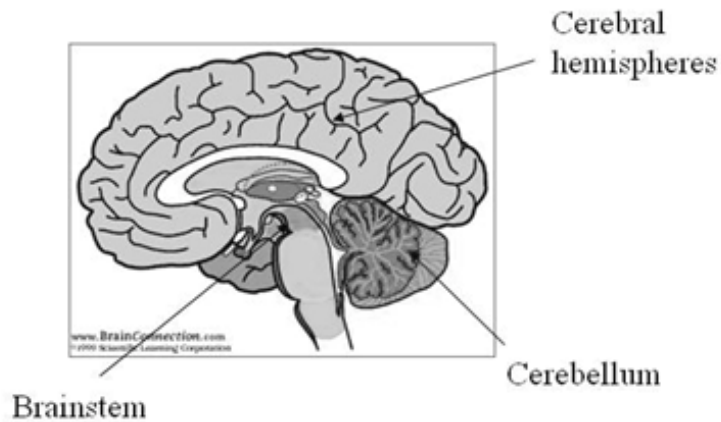


Figure 6: Central nervous system

The description of the nervous system divisions goes beyond the aim of this work, so I'll concentrate only on the cerebral cortex.

The cerebral cortex is the highly folded sheet of grey matter encasing the brain, home to most higher cognitive functions. Its thickness varies significantly by cortical region, changes across the human life-span, and is affected in multiple disease and disorders.

The brain operations responsible for our cognitive abilities occur primarily in the furrowed gray matter that cover the cerebral hemispheres. Humans have the most elaborated cerebral cortex, highly convoluted in shape, with many sulci that separates the regions. It's 2-4mm thick, but thanks to the convolutions (*gyri* and *sulci*) the surface area is incredibly larger than other primates. The cerebral cortex is divided into four lobes: frontal, parietal, temporal and occipital.

The frontal lobe is largely concerned with planning future actions and controlling movements, the parietal lobe with somatic sensation, sensory integration and relating our body with extrapersonal space, the occipital lobe

is involved in vision and the temporal lobe with hearing. The deep structures (hippocampus and amygdala) are involved in memory, learning and emotions.



Figure 7: Four areas of the cerebral cortex: frontal, parietal, temporal, occipital.

Many areas of the cerebral cortex are involved in the processing of sensory information or motor commands, and are called *primary*. The primary visual cortex is in the occipital lobe, the primary auditory cortex is in the temporal lobe and the primary somatosensory cortex is in the parietal lobe. The primary motor cortex contains neurons that directly projects to the spinal cord and has a different meaning: it's the last site for the cortical processing of motor commands. Sensory information is processed along several parallel pathways from peripheral receptors through primary sensory cortex. Each primary area sends information to adjacent *unimodal* high-order areas. Sensory information representing different modalities converges upon *multimodal* association areas that integrate that information into a polisensory event. The last step is integrating these sensory information to plan a motor action: the posterior association areas are highly interconnected with the frontal association areas responsible for planning a motor action.

There are six organizing principles behind the cerebral cortex:

1. The cortex is composed of varying neuronal types.
2. The cortex is horizontally structured in layers.
3. The cortex is vertically organized into columns.
4. The cortex is organized into cytoarchitectonically unique regions.
5. Functional systems in the cortex are hierarchically organized, whereby cortical regions interact, either through direct connections or via sub-cortical mediation, to achieve higher-order mechanisms of sensori-motor and cognitive processing.
6. Structure-function relationship.

1. **The cortex is composed of varying neuronal types**

There are two main categories of neurons in the cerebral cortex: projection neurons and local inter-neurons (Kandel et al., 2000). Cortical neurons can be further classified into different types based on several criteria, such as cell form, usual position within the cortical laminae, type of synaptic terminals, direction of trans-synaptic action, and type of transmitter molecules. Two main types of synapses occur within the neocortex. The first are asymmetrical, excitatory synapses which make up about 75-80% of the total. The remaining synapses are symmetric and inhibitory (Mountcastle, 1998). Spiny pyramidal cells make up 70-80% of cortical neurons in mammals. They are located in different densities in all cortical layers except for layer I. Pyramidal cells in different layers have different targets and receive inputs from intrinsic cortical neurons, collaterals of other pyramidal cells, axonal terminals of pyramidal cells in other cortical areas, thalamic nuclei, brainstem monoaminergic systems, and from the claustrum (Mountcastle, 1998). Non-pyramidal excitatory neurons make up another 2-3% of the cortex

(Mountcastle, 1998). The remaining 20% of neurons in the cortex are non-pyramidal inhibitory neurons whose connections remain intrinsic to the cortex.

Neuron structure varies across the cortex, identified by three features: cell size, branching pattern, and number/distribution of inputs. These regional variation in structure underlie fundamental differences in cortical circuitry.

2. **The cortex is horizontally structured in layers.** T

The neocortex is organized into six layers (Brodmann, 1909). Layers are differentiated by cell composition and density. Layer I, the outermost layer, is called the *molecular layer* and is generally acellular, being occupied by dendrites of cells located deeper in the cortex. Layer II, the *external granule cell layer*, contains tightly packed small granule cells. Layer III, the *external pyramidal cell layer*, is comprised of pyramidal cells which increase in size towards the depth of the cortex. Layer IV, the *internal granule cell layer*, is similar to layer II, also mostly containing small granule cells. Layer V, the *internal pyramidal cell layer*, is similar to layer III, containing large pyramidal cells. Finally, layer VI, the *polymorphic, fusiform or multiform layer*, contains spindleform cells and gradually blends into the white matter. The layering of neurons provides means of organizing inputs and outputs of the cortex.

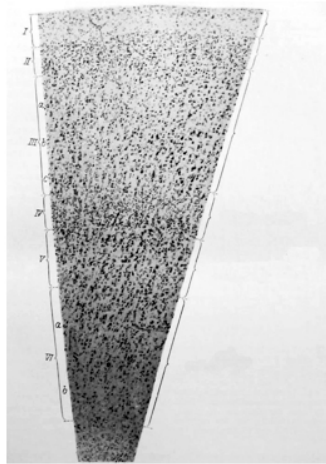


Figure 8: The six layers of the cortex illustrated on a single silver stained slice. Adapted from (Economo and Koskinas, 1925).

3. **The cortex is vertically organized into columns**

Along with the horizontal laminar pattern cortical neurons are also vertically or radially structured into columns. Columnar organization varies throughout the cortex, being prominent in the parietal lobes, less visible in parts of the frontal lobe (Economo e Koskinas 1925). Neurons within a particular column have similar response properties, likely being part of the same local processing network.

Evidence for the functional organization comes from microelectrode penetrations into the cortex along with transection and nerve regeneration studies. The primary visual cortex responds selectively to differentially oriented lines. Electrode penetration studies of the visual cortex found that perpendicular penetrations showed constant responses to a stimulus of a single orientation, whereas penetrations made nearly parallel to the surface found a consistent change in sensitivity to differently oriented stimuli (Obermayer e Blasdel 1993) (V. Mountcastle 1998)

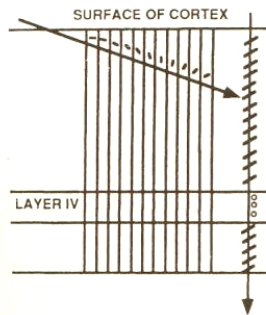


Figure 9: This figure shows orientation sensitivity of columns in the striate cortex. Vertical penetrations (rightmost arrow) show a single orientation, whereas parallel penetrations (diagonal arrow) show multiple orientations. The small lines above the diagonal penetration show the orientation of the line in the visual field which that particular column responds to. From (Mountcastle, 1998).

Figure 9 provides a schematic illustration of these results. Similarly, studies in the somatic sensory cortex found columns coding for both modality as well as location (point on finger). Evidence for columnar existence in the sensory cortex includes nerve regeneration experiments in monkeys. It was found that neurons in adjacent columns are related to adjoining and overlapping peripheral receptive fields.

4. **The cortex is organized into cytoarchitectonic areas**

Differential composition of neurons, along with varying lamination, subdivides the cortex into cytoarchitectonic areas, as mapped in figure 10. An example to illustrate the difference between two cytoarchitectonic areas is that of Brodmann Area (BA) 44 and 45, both part of Broca's area and implicated in language function. In BA 44 layer IV is dysgranular and barely recognizable, often invaded by pyramidal cells from layers III and V. BA 45 features a pronounced layer IV, though still less clear than its rostrally adjoining areas 46 and 10 (Economo e Koskinas 1925) (Amunts 1999).

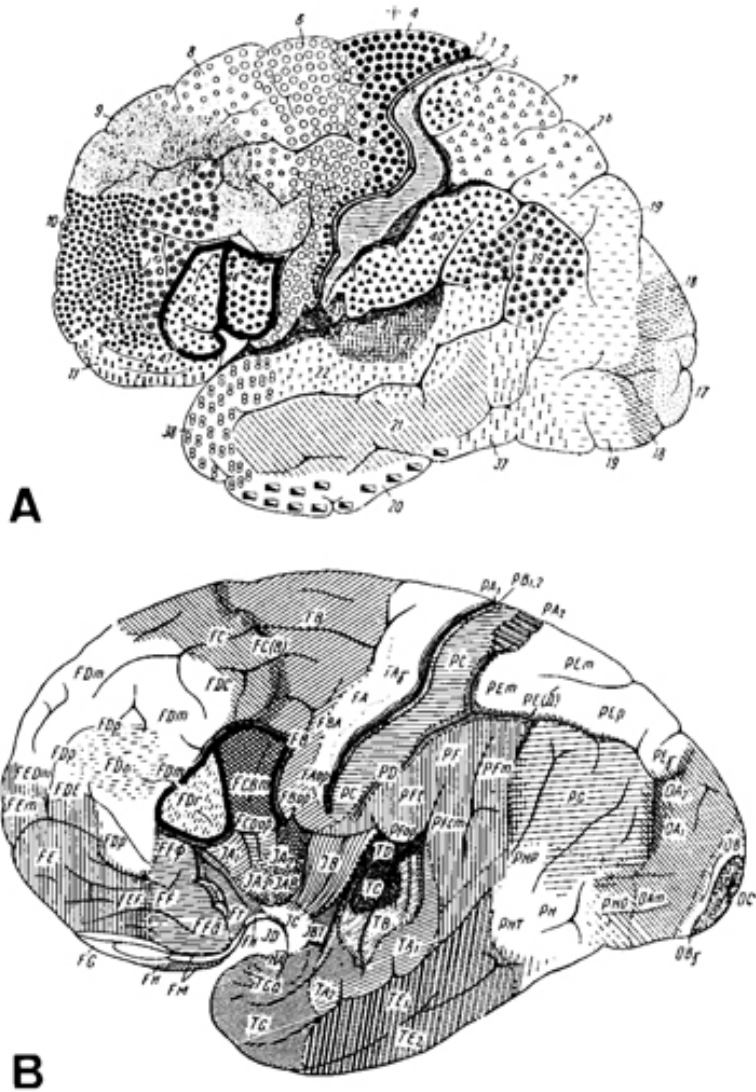


Figure 10: Two cytoarchitectonic maps dividing the cortex into morphologically similar areas are shown here. Part A shows the map from Brodmann, part B from Economo. Reproduced from (Amunts 1999). The boundaries for areas 44 and 45 are in bold. Economo–Koskinas with Cytoarchitectonic areas encompass the functional subdivision of the cortex.

The cellular, laminar, and columnar structures that are reflected in cytoarchitectonic boundaries clearly contribute to the functional specialization of different cortical areas.

5. **Functional systems are hierarchically organized**

Each cytoarchitectonic area is responsible for a set of functions; entire functional modalities, such as language or vision, need multiple cortical areas operating within a connected network. The classic example of such a cortical network comes from the vision literature. Two processing streams, the "what" and "where" streams, are believed to exist: the dorsal pathway, running from the primary visual cortex to the parietal lobes, is responsible for motion, depth, and spatial information. The ventral pathway, also originating in the primary visual cortex in the occipital lobes and extending to the temporal lobes, analyses form and color (Kandel et al., 2000). It is worth examining cortical processing of visual information in some more detail as it provides an excellent overview of some general properties of the cortex. Input from the retina is passed via the optic chiasm to the lateral geniculate nucleus (LGN). Information at this point is already separated into the parvocellular (P) pathway, responding to color, and the magnocellular (M) pathway, which processes. Output from the LGN is sent to the primary visual (striate) cortex - BA 17. Within the primary visual cortex, cortical columns code primarily for the orientation of the visual input, the eye from whence the input came (ocular dominance), as well as the color. Every part of the visual field is represented by multiple columns ultimately coding for all possible orientations, colors, and ocular inputs; the sum of these representations is often referred to as a *hypercolumn*. As alluded to earlier, the ventral visual pathway, running from the primary visual cortex to the interior temporal cortices, is responsible for form and color - the details of objects in the visual

field. The dorsal visual pathway, also originating in the striate cortex and progressing to the parietal lobes, analyses the location and movement. Neurons in the higher processing centers of either pathway have larger receptive fields than those in the lower cortical areas. Moreover, they respond to increasingly complex stimuli. Neurons in the inferior temporal cortex, for example, respond to a given shape at any position in the visual field, whereas neurons in the primary visual cortex only respond to a particular edge in a precise position within the visual field. Higher visual processing centers are also more dependent on selective attention than cortical areas lower in the pathway (Kandel et al., 2000). The structure of pyramidal neurons changes with cytoarchitectonic area, increasing their number of spines in areas subserving higher order visual processing tasks. This increase in spines raises the number of putative excitatory inputs along the dendrites. The pattern of connectivity of individual neurons changes as well, with higher order areas featuring neurons capable of sampling from larger areas of the visual field. The example of visual processing in the cortex highlights the significance of the structural elements of the cortex discussed above to its function. Laminar structure underlies local input processing and output redirection; cytoarchitectonic boundaries subserve different functions within the data processing network, and the structure of individual neurons is important for their participation in different tasks within the network.

6. Structure-function relationship

The cerebral cortex does not only follow a stereotyped pattern of development that can be altered through disease processes, it can also be changed with experience. Such plasticity can be due to recovery from injury as well as training within a functional paradigm. It is the latter of these two that can teach us the most about the structure function relationship in the cortex. Pascual-Leone and colleagues showed that five days of piano finger exercises

were sufficient to enlarge the cortical representation of the long finger flexor and extensor muscles (Pascual-leone 1995). Early acquisition of motor skills in string players also featured larger finger representations in the sensory-motor cortex. These types of changes in cortical representations are likely caused by a combination of formation of new synapses, recruitment of cortical tissue for a task that was previously not used for that purpose, as well as a strengthening of existing synapses. The brain is adaptable to change, and that task-specific specializations have their structural correlates. The microstructural component of these changes is not precisely known, though likely contains components of generations of new neurons (in the hippocampus at least), strengthening of existing synapses as well as the formation of new synapses. Changes in morphology based on functional adaptations suggest that the cortical thickness of areas subserving related functions might change in a correlated fashion.

2.2.1. Association areas

Association areas take up an increasingly larger percentage of the cerebral cortex as brain size increases among different species. The increasing size of association cortex correlates with the complexity of behavior and inferred mental functions that different species show.

Each sensory system has its own association areas on the cerebral cortex. The sensory systems (vision, hearing, etc.) each have their own primary area on the cortex, which gets the most direct connections from its sense. Each primary sensory area sends information to its own cortical association areas, which are next to their primary areas. The motor system is organized in the same way, but in the reverse direction: from motor association areas to the primary motor area to the motor systems in the brain stem and spinal cord.

The processing that occurs in the sensory association areas is the basis of complex mental processes associated with each sense. Each sensory

association area appears necessary for perception of objects and events in its sensory modality. The information that each sensory association area gets from its primary area is about simple contours, boundaries, and sensory qualities like color or pitch. Sensory association areas combine this kind of information to represent complex objects. For example, the visual association area on the lower part of the temporal lobe plays a primary role in your ability to recognize faces, dogs, cars, trees, etc., whereas the primary visual cortex is required for detecting basic features of the visual world: edges, light and dark, location, etc.

The activity of nerve cells in visual association cortex also shows that these areas are involved in a higher level of processing. For example, nerve cells in (a part of) the visual association area respond to visual stimuli that have some kind of complex pattern or structure. They usually respond only when the eye looks at complex patterns, such as images of objects, abstract forms, hands, faces, or even specific faces. This means that when such cells respond, the brain has information telling that the specific stimulus object that triggers the active cells is getting to the sense organ.

The same kind of effects appear in the somatosensory (touch) and auditory association areas. For example, damage to the auditory association cortex (around the primary auditory cortex on the top of the temporal lobe) leaves sensitivity to sound unaffected, but disturbs recognition of what sounds mean. Neurons in the auditory association areas respond much better to complex sound patterns like bird calls and speech sounds than to simple pure tones. Damage to the somatosensory association cortex (on the parietal lobe behind the primary somatosensory cortex) leaves sensitivity to touch unaffected, but disrupts ability to recognize objects by touch.

Higher order association cortex carries out complex mental processes not associated with any particular sense. Each sensory and motor association areas sends signals to higher order association areas, which combine this information to form the basis of the highest mental processes. These highest

mental processes, like language, thinking, and planning, do not depend on specific sensory information. For example, language can use vision (reading, sign language) and touch (Braille for the blind), as well as hearing.

The higher order association areas combine information from several sensory association areas.

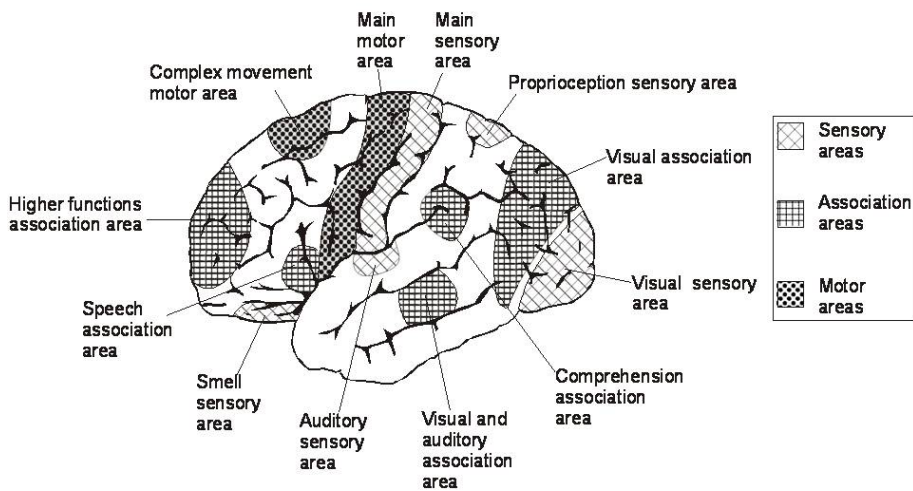


Figure 11: Main area in the brain, with particular interest on the association areas.

Associations areas are capable of mediating complex cognitive processes because they receive information from higher-order motor areas and convey information to high-order motor areas.

The link between specific mental functions and brain structure is quite obvious in the *posterior parietal cortex*: this association area is concerned with extrapersonal space and with creating a coherent whole from the details of a visual scene. Study of lesions in this area underlined problems with disorientation in the environment space, inability to discriminate between sensory stimuli, inability to locate and recognize parts of the body (Neglect), inability to recognize self, inability to write.

The parietal lobe is defined by four anatomical boundaries: the central sulcus separates the parietal lobe from the frontal lobe; the parieto-occipital sulcus separates the parietal and occipital lobes; the lateral sulcus is the most lateral boundary separating it from the temporal lobe; and the medial longitudinal fissure divides the two hemispheres.

2.3. Non-human primates vs. human brain

Monkeys have been used for studies of the neural mechanisms of cognition for over 70 years (Jacobsen 1936). Most of this work has been carried out on macaque monkeys. The assumption was that studies on monkeys will help us to understand the human brain. There could be two challenges.

The first accepts that these studies could be helpful but argues that they are no longer needed. The claim is that fMRI, MEG, TMS can now tell us everything that we need to know about the human brain for the purposes of cognitive neuroscience. However, this objection fails to distinguish between methods that record from whole populations of cells and methods that record from cells one at once or in small populations. The spatial resolution of imaging methods is adequate if one is interested in the functions of an area. But if one is interested in mechanism, that is in how the area does what it does, there is no alternative to using methods with a much finer spatial resolution. The reason is that one needs to know how the different cells interconnect within a module and how the differential coding of each cell within a module contributes to the population signal.

The second challenge is more serious. This is that the lines leading to modern monkeys and humans have been separated for 25 million years (Kumar 1998). Thus, one would expect to find significant differences between the brains of

monkeys and humans. Furthermore, there are very marked behavioural differences and these must depend partly on differences in the brain. For example, humans, but not monkeys, can speak and use grammar, can reflect on their own mental states and those of others and can achieve an explicit understanding of causes in the physical and mental world. We already know some of the specializations of the human brain that make this possible.

The physical difference are remarkable: the human brain is 4.8 times the size for a hypothetical monkey of the same body weight (Rilling 2006). But the human brain is not just a scaled up version of the monkey brain. The proportions of the human brain are not those that would be predicted by a plot of the changes in proportions in other primates as brain size increases. For example, the neocortex is 35% larger than predicted for a primate with as large a brain. The first consequence of an increase in size is that there is an increase in the number of specialized subregions, for example in the visual areas and in parietal cortex (Orban GA 2004). The second is that there are consequential changes in the microstructure.

Why using functional anatomic data from one species (macaque monkey) to make inferences about the functional organization of neural systems in another (human)?

We can learn a lot from animal models.

Macaque monkeys are widely used in order to understand some mechanisms of the human brain that would be unreachable otherwise.

The reason why a macaque model can still be valid for human brain is that evolution is opportunistic, as we know not only from comparative anatomy and embryology but also from recent comparisons of the coding sequences of the DNA in different animals. Evolution is a historical process. It works in

two ways. Where something works it retains it; where novel changes are required, they are typically made by adapting what was there in the first place. It is for this reason that the macaque monkey model can remain productive even in cases where humans have cognitive abilities that have not developed in other animals.

There are, of course, many respects in which human abilities can be found in monkeys. In these cases one can give the same tasks to monkeys and human subjects. Examples are visual conditional tasks, spatial working memory tasks or visual matching and non-matching rules.

Besides, recordings from electrodes in the human brain are always going to be restricted for ethical and practical reasons. For example, recordings can be taken for short periods during surgery for temporal lobe epilepsy and for longer periods with depth electrodes implanted so as to detect the source of the seizure onset. In these cases the aim of the recordings that are made for experimental purposes is not the clinical well-being of the patient, and there will always be strict limits to this type of research. However, recordings can also be taken so as to guide prostheses and here there is a clear clinical justification. Nonetheless, the basic work on decoding the activity of populations of cortical cells has first to be pioneered on macaque monkeys.

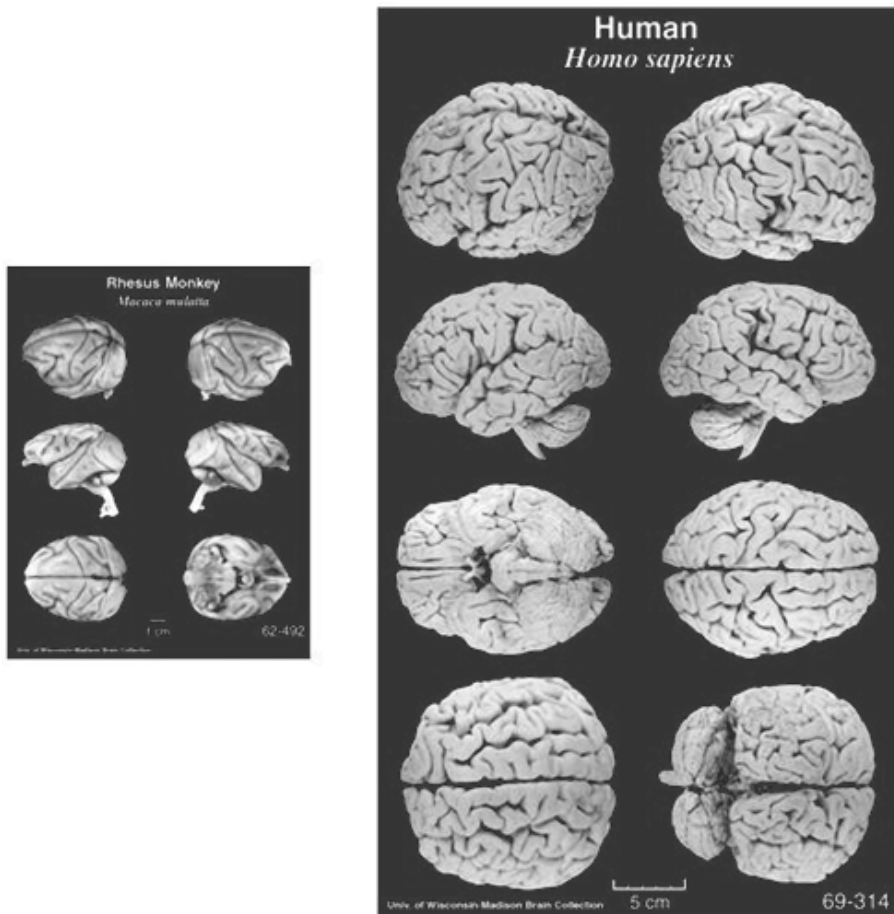


Figure 12: Comparison between human and macaque brains. The physical differences are remarkable.

We should not abandon the monkey model: whenever possible, it should be tested whether generalizations can be made. One useful strategy, that has been applied by scientists in the last years to verify the correctness of their assumption, is to use fMRI to visualize activations in humans, and compare these with activations in monkeys. Where the results are the comparable, it is possible to use information from single unit cellular

recording in those same areas to suggest the mechanisms by which functions are performed in the human brain.

2.3.1. Perception of motion in the macaque cerebral cortex

Motion is analyzed primarily in the dorsal pathway from the primary visual area to the parietal cortex. Motion is detected by comparing images recorded at different times. Most cells in the visual system are sensitive to retinal position and can resolve events separated in time by only 10-20ms, so most cells in the visual system may be able to extract information about the object that is moving and its position. Why is there any need of a specialized neural subsystem?

In the primary visual area V1 of the macaque brain cells respond to motion only in one direction. *Area MT* (middle temporal area, at the edge of parietal cortex) was the first area reported to respond to motion visual stimuli, while most of its cells do not respond to colors and shapes. MT has a retinotopic map of the contralateral visual field as V1, but the receptive fields are 10 times wider than those in the primary cortex. Cells in MT respond to motion of luminous bars but also to color in motion. In the human brain, a correspondent area devoted to motion has been identified at the junction of the parietal, temporal and occipital cortices.

The mechanism underlying motion perception, in particular self-motion perception, are not clear yet, but hypothesis has been made: the visual system analyzes the visual components of motion and then it combines them with other retinal and extraretinal signals (Lappe M. 1999). Another issue related to self-motion perception is the role of stationary and moving objects: self motion perception can be affected by these cues. Moving objects are part of the retinal flow and by analyzing the speed, location in space and in relation

with other objects and the observer, the system can calculate detailed information for heading perception (J. Cutting 1996) (e. a. Cutting 1999).

In monkeys, many areas show responsiveness to optic flow stimuli, but the tuning characteristics of the neurons may vary. Many studies investigated the progressive refinement of feature selectivity in the visual procession stream towards area MT (Lappe 2000) (C. Duffy 2000), but not much on the areas further in the dorsal pathway.

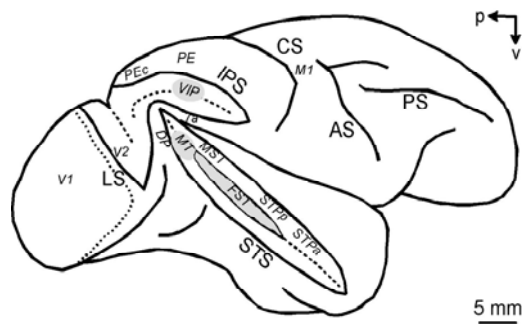


Figure 13: area MST, VIP, 7a, STP and PEc in the macaque brain

Area MST, found in the depths of the STS sulcus adjacent to MT, is considered part of the parietal stream and responds to visual motion as well in particular to stimuli of optic flow. The first studies on this area suggested that it performs a linear combination of motion information from MT (Saito 1986) (Tanaka 1989). Neurons in area MSTd are more responsive to large-field visual stimuli and give best responses to one type of optic flow (radial, rotation, spiral) (C. J. Duffy 1991) (C. & Duffy 1995) (C. J. Duffy 1997), are tuned with different speeds, are selective for the position of the FOE and also encode extraretinal signals (Shenoy 1999) of current eye position and speed or smooth pursuit movement, with or without visual stimulation. It seemed that

area MST could use vestibular signals in order to create a compensated heading representation while the body was moved with the visual stimulus.

Area VIP ventral intraparietal, in depth in the intraparietal sulcus, receives a direct projection from area MST. It has visual signal similar in many ways to those of MST: area VIP shows directional and speed selectivity to moving visual stimuli (C. Colby 1993) and it seems to be more responsive to expansion motion (Schaafsma e Duysens 1996) (Bremmer e Duhamel 2002). , RF are on average smaller than those of MST and highly directional for visual motion, and usually closely correspond to somatosensory RF (Duhamel e Colby 1998), and both are restricted in depth (Bremmer e Duhamel 1997). This is a difference between MST and VIP: MST seems to be involved in the analysis of heading perception in the far extrapersonal space, while some investigators to suggest that VIP is particularly involved in near-field motion analysis. Many VIP neurons show a RF that shift on the retina when the eyes move, as if the RF is transformed into head-centered coordinates.

In other cortical areas the representation of optic flow becomes more complex, in area 7A (Siegel e Read 1997) that shows several functional features important for spatial analysis. For example the response strongly depends on the speed of the stimulus (Siegel e Read 1997), neurons show a gain field mechanism (the activity in response to a visual stimulus is enhanced when the gaze in is in a particular zone of the visual field) (Andersen, et al. 1985). Motter and Mountcastle (Motter e Mountcastle 1981) described in 7a neurons called opponent vector: they respond to inward or outward moving stimuli with respect to the fovea. Studying motion response of area 7a, two new properties appear: some neurons are able to distinguish between particular types of optic flow (radial vs. rotational) while others are tuned for a particular direction (expansion vs. contraction) (Siegel e Read 1997). The second property is that they show angle of gaze tuning (Siegel e Read 1997). Neurons in 7a are also modulated by the retinotopic position of the stimulus. All these characteristics may leads to the conclusion that area 7a is not

involved in the perception of heading direction, but in the speed representation of multiple objects, to make a spatial representation of extrapersonal-space.

Area *STPa* neurons respond to visual moving stimuli (Bruce 1981) during object and self-motion when they are in the opposite direction, while they do not fire when self and object motion occur at the same speed in the same direction (Hietanen e Perrett 1996). This suggests they might process self-motion perception. Neurons in *STP* also respond to optic flow stimuli and they seem to prefer radial expansion , to control forward locomotion (Anderson e Siegel 1999).

Area PEc, in the dorso-caudal portion of the superior parietal cortex, has been for years considered part of the somato-sensory cortex (Duffy e Burchfiel 1971) (e. Mountcastle 1975), but recent studies demonstrated that neurons in this area also respond to optic flow stimuli (Raffi, Squatrito e Maioli 2002) and are involved in hands movements and reaching (e. Squatrito 2001) (Ferraina 2001). Area *PEc* is a multimodal area, some neurons are modulated by saccades and eye position (e. a. Raffi 2008), some neurons respond to proprioceptive stimulation (Breveglieri 2006). These studies may lead to the idea that neurons in area *PEc* are involved in the integration of visuo-motor signals and the optic flow processing takes part in linking visual input and motor output. Area *PEc* respond to both forward and backwards body movements and is selective for the FOE position: it could be a probable locus for integration and heading detection.

All these cortical functional features in different areas of the macaque brain likely indicate that motion perception and processing are very common in the cortex, they are used in planning actions and they evolve across various areas. Area *MST* might be involved in a first analysis of self-motion direction, area *VIP* seems to help guiding in near extrapersonal space, while *7a* creates an extrapersonal space representation concentrating on single objects motion.

Area STP is tuned with forward locomotion and area PEc could play a role in integrating visual information with motor planning. But the final location for the convergence of the signals into a coherent representation is unknown, and still much research needs to be done.

2.4. Electrophysiology

A typical neuron has four regions: the cell body (*soma*), dendrites, the axon and presynaptic terminals. The soma is where the DNA of the cells stays and metabolic processes occur. Dendrites are short branches that receive incoming signals from other cells, while the axon is a long fiber that carry signal to other neurons.

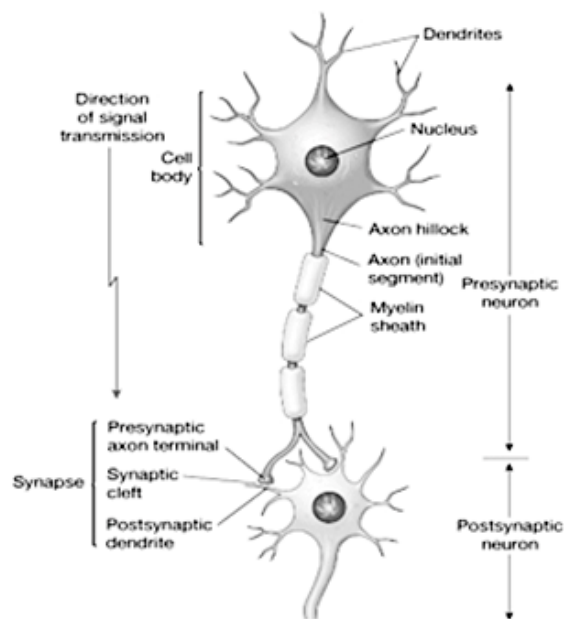


Figure 14: Typical neuronal physiology

The neuronal signal consists of short voltage pulses called action potentials or spikes and can be conveyed from 0.1mm to 3m. These pulses travel along the axon and are distributed to several postsynaptic neurons where they evoke postsynaptic potentials. If a postsynaptic neuron receives several spikes from several presynaptic neurons within a short time window, its membrane permeability to Na⁺ ions may increase, causing Na⁺ ions to enter in the cell and to change its potential. When the internal potential reaches a critical value (threshold) an action potential is triggered. This action potential is the output signal which is, in turn, transmitted to other neurons.

The action potential is a short transient all-or-none impulse with an amplitude around 100mV, a duration of 1ms that can propagate at 1-100m per second.

In vivo single-cell electrophysiology helps to study neural circuit function. For systemic cognitive neuroscience we need subjects who can solve cognitive tasks: awake, behaving subjects, with performance compatible to human behavior. We also need signals that are relevant for neural processing as neuronal spiking activity, field potentials and synaptic activity. The temporal precision of the recorded signal must be high, with a precise localization of the recorded signal. The sum of these requirements is only fulfilled in awake monkey electrophysiology based on intra-cortical microelectrode recordings.

Spatial scales for understanding brain functions

Structure	Size	Number	Method
Brain	10cm	1	fMRI,MEG,EEG,PET
Lobe	1-10cm	1-10	fMRI,PET,ECoG
Area	1-10mm	10-100	fMRI,ECoG,Optical Imaging
Layer	100µm	1-10	microelectrode
Column	100µm-1mm	Specific area	for microelectrode, Optical Imaging
Neuron	10µm	10^{11}	microelectrode
Synapse	1µm	10^{14}	Patch-clamp

Neuronal time scales

Event/signal	Duration	Method
Hemodynamic response	10s	fMRI-Bold, PET
Cortical/epidural/scalp field potentials	10-100ms	Microelectrode, ECoG,EEG, MEG
Post-synaptic potentials	10ms	Microelectrode
Spikes	1ms	microelectrode

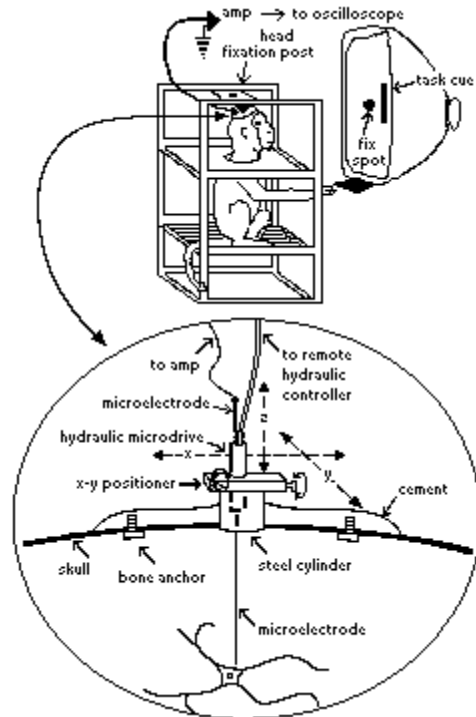


Figure 15: Schematic of recording technique used in behaving monkey. At top a monkey in a restraining chair with head fixed is shown. The monitor in front of the monkey displays a spot (target) that the animal must fixate to initiate each trial; this ensures that the animal is attending to the task when cues are presented. The animal also presses a nearby lever after target cues. The head-mounted assembly for recording impulse activity of brain neurons is shown in more detail below. A steel cylinder is cemented to the animal's skull and bone anchors. This cylinder is fitted with an X–Y positioner and a remotely controlled microdrive. The X–Y positioner allows lateral repositioning of the electrode between penetrations in the brain, while the microdrive lowers the electrode along each penetration. Electrical activity recorded on the electrode is relayed to amplifiers and other electronics for acquisition, storage and analysis.

Electrophysiological studies in behaving monkeys employ extracellular recordings from a metal microelectrode held in a miniature micropositioner on the animal's head. The micropositioner is typically attached to a chronically implanted steel chamber or cylinder that is stereotaxically positioned and permanently cemented to the skull in a prior surgery. These chambers often

allow lateral repositioning of the recording microelectrode for multiple penetrations, while the micropositioner allows the electrode to be lowered into the brain to the desired target along a particular track.

The most common types of microelectrodes used for recording from neurons in behaving animals are (a) etched tungsten or platinum–iridium wires, insulated with either glass or lacquer except for ~20 μm from the tip, or (b) thin micro wires that are typically 25–62 μm in diameter and lacquer-insulated except for the bluntly cut tip. Neurons of different brain areas are recorded more easily with one or another type of electrode. In general, micro wires are advantageous for experiments entailing long-term recordings from neurons in deep structures in behaving animals, whereas etched, stiff microelectrodes are advantageous for studies where penetration of the dura mater is needed or where numerous penetrations in a small area are desired.

Two general approaches are used with micro wire electrodes. Perhaps most commonly the microwires are simply implanted and glued in place with no further movement of the wires possible after surgery. In this method, a large number of wires (often more than 40) are implanted and each wire is monitored daily over the course of months for unit activity. Activity occurs on enough wires over time that many long-term and very stable recordings can often be obtained. The second method is to attach a small number of micro wires (two to six) to a movable microdrive which allows the wires to be repositioned vertically, and sometimes laterally as well, for new penetrations after surgery. This approach has the advantage of obtaining many more recordings from a single subject than the fixed wire approach, an important consideration when subjects are in limited supply (e.g., monkeys) or when extensive training is required for each animal recorded.

High-gain amplification of signals from the head of a moving animal often yields considerable movement related electrical artifacts; these are the bane of a behavioral electrophysiologist. These problems are typically overcome by

including a miniature first-stage amplifier in the fixed implant on the animal's head, so that recordings from the microelectrode can be amplified and converted to low-impedance signals before traveling over long distances of flexing cables.

As with all extracellular recordings, it is important to know whether activity seen on an individual electrode is generated from one neuron only, or from several nearby neurons simultaneously recorded. Results of the latter, termed *multiple-cell recording* or *multi-unit recording*, are more difficult to interpret because neurons in the multiple cell population may be physiologically heterogeneous. In that case, opposite changes in different cells recorded may appear as no change in the multiple-cell data. In addition, it is more difficult to ensure the stability of the recorded signal over time with multiple-cell activity.

The sequence of action potentials recorded with electrophysiology contains the information that is conveyed from one neuron to the next - but what is the code used by the neurons? Even though it is a question of fundamental importance the problem of neuronal coding is still not fully resolved.

2.5. Neural data analysis

The mammalian brain contains more than 10^{10} densely packed neurons that are connected to an intricate network. In every small volume of cortex, thousands of spikes are emitted each millisecond.

What is the information contained in such a spatio-temporal pattern of pulses?
What is the code used by the neurons to transmit that information?

How might other neurons decode the signal?

As external observers, can we read the code and understand the message of the neuronal activity pattern?

At present, a definite answer to these questions is not known.

They all point to the problem of neuronal coding, one of the fundamental issues in neuroscience. The aim is understanding brain processes, diagnose disorders, design prosthetic limbs and brain computer interface machines.

Spike train data is the primary data recorded during experimental neurophysiology. It has been shown that spikes from a single neuron are identical (Robinson 1998), thus the form of individual spikes is believed to carry little information. The spiking frequency and inter-spike intervals carry information and the synchronization of spikes with stimulus is of prime interest.

In this paragraph, the traditional procedures for the analysis of stimulus-correlated spike train data are reviewed. I will concentrate in procedures that attempt to extract most information about the underlying neuron, i.e. the excitability changes evoked by the stimulus. The stimulus is usually considered in a classical sense as a visual stimulus, but these general considerations are not restricted to this definition: other events such as the action potential occurrence of another neuron may be regarded as a stimulus.

The methods range from rather simple methods that require little computational effort to more sophisticated procedures that attempt to extract all information available in the recorded spike-train data.

In general the process of spike train analysis may be separated into several steps.

At first the raw experimental recording must be prepared for the detailed analysis by extracting single unit action potential occurrence times and must be synchronized with the stimuli occurrence.

As the extracellular waveforms recorded have a non-zero duration it is essential to choose a salient feature of the waveform as the instant of action potential occurrence. This is usually the first crossing of a threshold or the location of a prominent maximum or minimum..

The second step consists on calculations over these spike train times that indicate stimulus-induced excitations and inhibitions.

Thirdly, the observed output features need to be verified statistically.

In this paragraph, I will concentrate mainly on the methodology for the second step, while I'll focus on the third when explaining the analysis carried on in particular for our experiments.

Having detected all the desired timings of action potentials, it is proper to display this data at first with as little post processing as possible. The easiest graph that may be constructed from stimulus-correlated spike train data is a so called *raster plot*. In such a diagram the abscissa is the spike detection time relative to the stimulus. The ordinate (each row) is the number of the trial in which the action potential was observed: usually the same stimulus is presented several times (at least 10). To create the raster plot, a little line is drawn for each spike timing. The raster plot has the main advantage that the spike timing information is condensed extremely and thus responses to a huge number of stimuli are visible at one time. This allows for example the detection of a 'silent period' following a discharge.

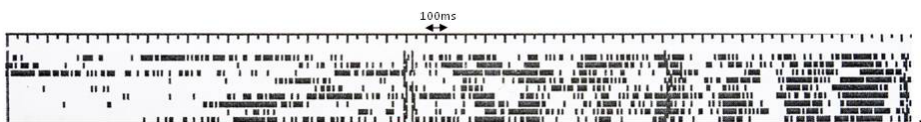


Figure 16: Example of a raster plot. Each vertical line represent a spike, each row is a repetition of the same trial with the same stimulus.

Additional raw display of the spike train data is called *interspike-interval superposition plot* and is only applicable for a continuously discharging neuron. The IISP contains a dot for each action potential with the abscissa denoting its detection time relative to the stimulus. The ordinate of each dot is the preceding interspike interval, i.e., the time interval between the detection times of the spike and the one immediately preceding it in the same trial.

Traditionally it has been thought that most, if not all, of the relevant information of the activity of a neuron is contained in the *mean firing rate*. It dates back to the pioneering work of Adrian (Adrian 1928). In the following decades, measurement of firing rates became a standard tool for describing the properties of all types of sensory or cortical neurons (Hubel 1959) (V. Mountcastle 1957), partly due to the relative ease of measuring rates experimentally. It is clear, however, that an approach based on a temporal average neglects all the information possibly contained in the exact timing of the spikes. It is therefore no surprise that the firing rate concept has been repeatedly criticized and is subject of an ongoing debate.

A glance at the experimental literature reveals that there is no unique and well-defined concept of mean firing rate. In fact, there are at least three different notions of rate which are often confused and used simultaneously.

The three definitions refer to three different averaging procedures: either an average over time, or an average over several repetitions of the experiment, or an average over a population of neurons.

- Is a mean over time really the code used by neurons in the brain? In other words, is a neuron which receives signals from a sensory neuron only looking at and reacting to the number of spikes it receives in a time window of, say, 500 ms? From behavioral experiments it is known that reaction times are often rather short. Temporal averaging can work well in cases where the

stimulus is constant or slowly varying and does not require a fast reaction of the organism - and this is the situation usually encountered in experimental protocols, when the interest is in isolating the response of a neuron to one stimulus. Real-world input, however, is hardly stationary, but often changing on a fast time scale. For example, even when viewing a static image, humans perform saccades, rapid changes of the direction of gaze. The image projected onto the retinal photo receptors changes therefore every few hundred milliseconds.

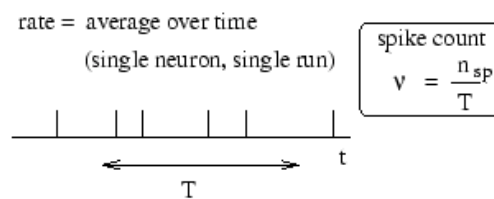


Figure 17: temporal averaging of neural spikes to calculate mean firing rate.

- There is a second definition of rate which works for stationary as well as for time-dependent stimuli and is the most common technique. The experimenter records from a neuron while stimulating with some input sequence, the same stimulation sequence is repeated several times and the neuronal response is reported in a *Peri-Stimulus Time Histograms* (PSTH). The spike train has to be aligned with the stimulus onset, for each of the repetitions of the same stimulus condition (at least 10). The aligned sequences are then superimposed in time, and used to construct a histogram: the stimulus period T is divided into N bins of size Δ and the number of spikes that belong to each Δ is calculated. The method requires the choice of this parameter that is called binwidth and that influences the shape and the resolution of the PSTH. The bar-graph histogram is drawn with the bar-height of bin i given by $R_i / n \Delta$ in units of estimated spikes per second at time $i \Delta$. Sometimes the result is smoothed to get a continuous 'rate' variable. The spike density of the PSTH

is usually reported in units of Hz and often called the (time-dependent) firing rate of the neuron. The obvious problem with this approach is that it cannot be the decoding scheme used by neurons in the brain. Consider for example a frog which wants to catch a fly. It cannot wait for the insect to fly repeatedly along exactly the same trajectory. The frog has to base its decision on a single 'run' - each fly and each trajectory is different. Nevertheless, the experimental spike density measure can make sense, if there are large populations of independent neurons that receive the same stimulus. Instead of recording from a population of N neurons in a single run, it is experimentally easier to record from a single neuron and average over N repeated runs.

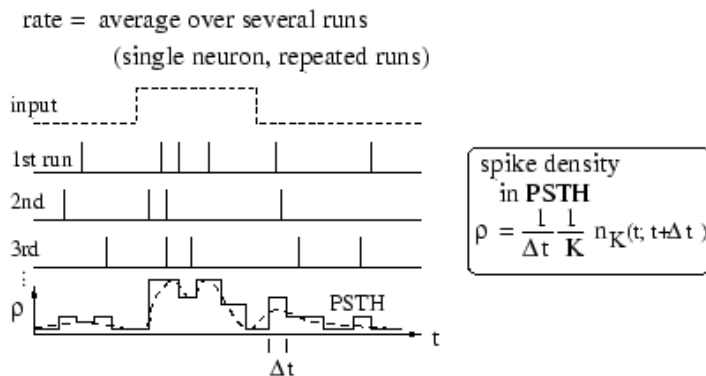


Figure 18: mean firing rate calculated over several trials, of the same neuron

In 1978 Ellaway (Ellaway 1978) proposed a simple post-processing procedure for a PSTH called CUSUM (cumulative sum of PSTH). To construct the CUSUM first you need to estimate the mean content of the pre-stimulus bin. Then, this value is subtracted from all post-stimulus bins. The resulting function is integrated with respect to time (simply summing the content of consecutive bins in case of a histogram). Since the CUSUM is the time integral of the PSTH, the measure unit is impulses per stimulus.

- The third definition of mean rate counts on the fact that the number of neurons in the brain is huge. Often many neurons have similar properties and respond to the same stimuli. Let us idealize the situation and consider a population of neurons with identical properties. In particular, all neurons in the population should have the same pattern of input and output connections. The spikes of the neurons in a population m are sent off to another population n . In our idealized picture, each neuron in population n receives input from all neurons in population m .

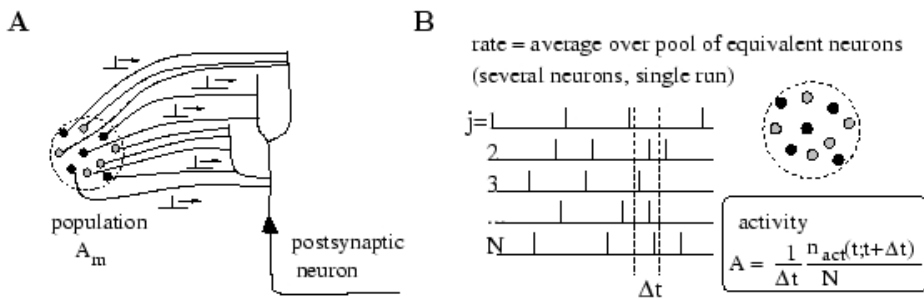


Figure 19: example of a neuronal network in which spikes of a population are all sent off to another population.

The relevant quantity, from the point of view of the receiving neuron, is the proportion of active neurons in the presynaptic population m . Formally, we define the population activity as:

$$A(t) = \frac{1}{\Delta t} \frac{n_{\text{act}}(t; t + \Delta t)}{N} = \frac{1}{\Delta t} \frac{\int_t^{t+\Delta t} \sum_j \sum_f \delta(t - t_j^{(f)}) dt}{N}$$

where N is the size of the population, $n_{\text{act}}(t; t + \Delta t)$ the number of spikes (summed over all neurons in the population) that occur between t and $t + \Delta t$ and Δt a small time interval; this eq. defines a variable with units s^{-1} - in

other words, a rate. The population activity may vary rapidly and can reflect changes in the stimulus conditions nearly instantaneously (Brunel 2001) (Gerstner 2000). The population activity does not suffer from the disadvantages of a firing rate defined by temporal averaging at the single-unit level. A potential problem with this definition is that we have formally required a homogeneous population of neurons with identical connections which is hardly realistic. Real populations will always have a certain degree of heterogeneity both in their internal parameters and in their connectivity pattern. Nevertheless, rate as a population activity (of suitably defined pools of neurons) may be a useful coding principle in many areas of the brain.

During recent years, more and more experimental evidence suggests that a straightforward firing rate concept based on temporal averaging may be too simplistic to describe brain activity. One of the main arguments is that reaction times in behavioral experiments are often too short to allow long temporal averages. Humans can recognize and respond to visual scenes in less than 400ms (Thorpe 1996). Recognition and reaction involve several processing steps from the retinal input to the finger movement at the output. If, at each processing step, neurons had to wait and perform a temporal average in order to read the message of the presynaptic neurons, the reaction time would be much longer. New techniques to analyze spike train need to concentrate on synchronization between neurons.

Connections between neurons fall into two general groups: direct synaptic coupling and common input coupling. In the direct coupling, when neuron A fires neuron B has increased probability of firing. In common input coupling, neuron B and C have increased probabilities of firing synchronously, when A fires.

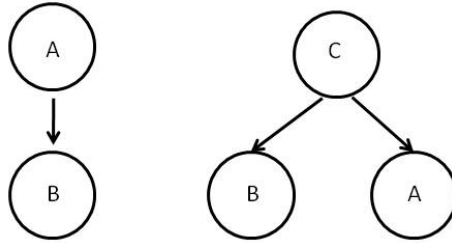


Figure 20: Two general kinds of connections between neurons: direct coupling and common input.

The *cross-correlogram* is one of the most common method to analyze multi-dimensional spike train data and measures the temporal correlation of one spike train with another. The time axis is divided into time bins whose length is set by the operator. One neuron is set as the reference neuron and time zero is aligned with the first spike of this neuron. Then, we observe how many spikes of the other neuron (target neuron) fall into the bins we set. The purpose is to see if a spike in the reference neuron at time t affects the probability of the target neuron to have a spike at time $t+k$. k may be negative, positive or zero. When evaluating cross-correlograms, there are certain interesting patterns.

- If k is close to zero and the cross-correlogram is symmetric, the target neuron is more likely to fire immediately after the reference neuron: we can suppose a correlation between the two and they fire in synchrony.

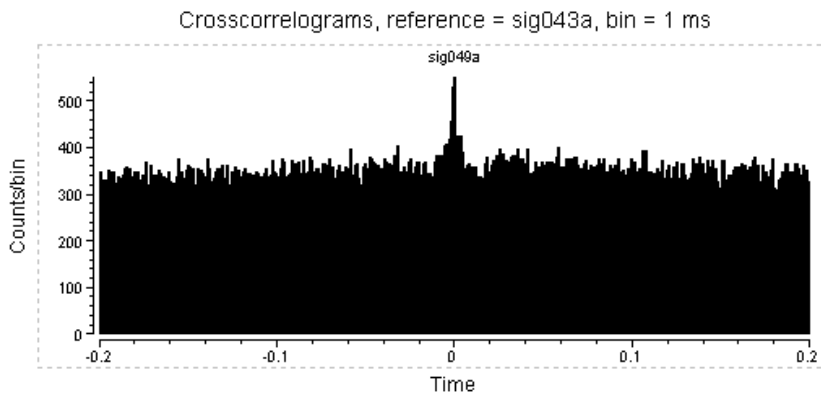


Figure 21: Symmetric crosscorrelogram that can be interpreted as a sign of synchrony between neurons.

One might guess that Neuron A forms a direct excitatory connection on Neuron B. However, looking at the cross-correlogram we see that B experiences an increase in firing *prior* to the zero point. If A directly excites B, then how would Neuron B experience an increase in firing *before* Neuron A even fires? Obviously this cannot be the case. For the same reason we can conclude that Neuron B does not form a direct excitatory connection on Neuron A. Instead, the most likely scenario is that there is another Neuron C that feeds into both Neuron A and Neuron B. This would explain the symmetrical peak: when Neuron C fires, it sends excitatory post-synaptic potentials to both A and B. Thus, when there is a symmetrical peak, one could hypothesize that Neurons A and B share a **common input**, in this case Neuron C.

- Occasionally one might see a **symmetrical trough** around $k=0$, as shown below; this means that Neuron B is *less* likely to fire when Neuron A spikes. Again, the symmetry of the peak precludes the possibility of a direct inhibitory connection between A and B. Instead, a likely explanation is that both A and B receive input from Neuron C, but B receives *inhibitory* input while A receives *excitatory* input. So when C fires, it sends an excitatory

potential to Neuron A, increasing its likelihood of firing, while sending an inhibitory potential to Neuron B, decreasing its likelihood of spiking.

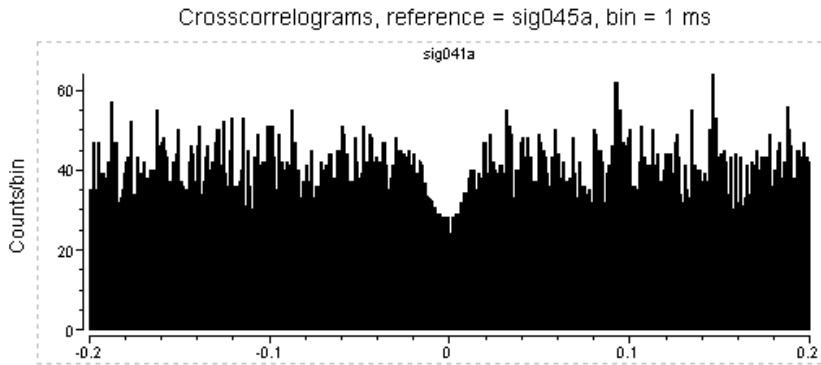


Figure 22: Symmetric cross-correlogram that can be interpreted as a sign of synchrony between neurons but with an inhibitory signal.

- A **direct excitatory connection** between Neurons A and B produces a peak that is offset from zero.

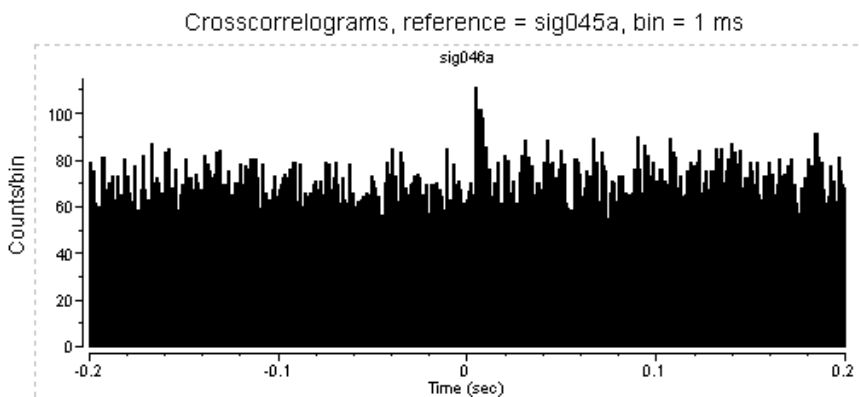


Figure 23: Cross-correlogram that can be interpreted as a direct excitatory connection between neuron.

3. Hardware and software for neurophysiologic experiment with behaving monkey

3.1. Hardware for neural data acquisition

Nowadays, new techniques allow to acquire data from multiple neurons: they are multielectrode and multispikes acquisition systems. AlphaOmega (Alpha Omega Eng. Israel) is one of them.

The equipment for recording electrophysiological data our lab includes:

EPS: electrode positioning system

MCP: a modular amplification and filtering system

MSD: multi-spike detector

ALPHAMAP: hardware that can record from 16 channels simultaneously. The computer system that is used to acquire and analyze the data in behavioural electrophysiology is a key element, because many events are typically recorded simultaneously (e.g., two or more cells activity, markers for different sensory stimuli and behavioral events, video time markers, X and Y eye positions), it is necessary to have a system that can rapidly record large amounts of data on-line with millisecond temporal resolution.

To test the performance of this system, we created some .wav file that reproduced wave forms similar to action potentials maximum frequency (1Khz). Results in the accuracy of acquisition were very satisfying.

In addition, sophisticated software is required so that neuronal activity or other data can be tabulated (typically in PSTHs) with respect to an arbitrarily chosen type of event out of the many recorded. The most challenging (but important) aspect of developing such software is to make it easy to use and easy to abstract results from very large data files, but also make it sufficiently

flexible so that new subroutines can be written and integrated to analyze as many aspects as possible from electrophysiological data.

The choice we made was to implement all data analysis with home-made routines in MATLAB®, a high-level language and interactive environment that enables you to perform computationally intensive tasks. Brief description of all routines will follow in the Appendices.

During experiments, eye position should be continuously monitored. It's performed by means of an infra-red video eye-tracker (Arrington Research, AZ, USA). This eye tracker has its own calibration software, but it cannot be used with non-human primates because it's a different paradigm they are not trained for.

The calibration paradigm was very simple for the animals, because it was similar to tasks they usually performed. By means of a C routine written as a *.tim* file for VCortex (see Ch. 3.2. for details on behavioural control during experiments), at the beginning of each trial a red small dot was presented in different points of a grid on a screen, while the monkey had to perform a reaction time task. When the target appeared, the monkey had to push a button and start fixating. When the target changed color, the monkey had to release the button in a maximum reaction time. In the meanwhile, eye X and Y position was acquired with the video eye-tracker. If this calibration is done at the beginning of each recording session, the monkey is very concentrated and most probably would execute the trial correctly. Knowing each position of the target and the correspondent signal acquired, it was possible to calculate two parameters that allowed later to reconstruct the correct eye position.

Considering a grid of 5 point on the screen, we could calculate the calibration parameter with a first order linear model:

$$\begin{cases} s_x = a_0 + a_1x; \\ s_y = b_0 + b_1y; \end{cases}$$

(s_x, s_y) were the target coordinates while (x, y) the acquired eye position signals.

The four coefficients were optimized by means of the least squares model. If a 9 points grid was used, the calibration model would be a second order one and the calibration coefficients would become 12.

3.2. Behaviour control during experiments

Electrophysiological studies on behaving monkeys need a careful and precise control of all the behaviours of the animal. Monkey are trained to execute a fixation task, while they sit on a chair in front of a screen. When a target (two small red lines) appears on the screen, the monkey has to push a button in a maximum reaction time, and start the fixation. Only when the target becomes green, the monkey can release the button as quickly as possible. The fixation is necessary to maintain the attention on the screen while visual stimuli are presented. If the task is executed correctly, the monkey receives as reward some drops of fruit juice. During all the task, eye position is monitored with an eye tracker: if the eye position shifts from the target of more than 2° of visual field, the trial is aborted.

The behavior control in our lab is performed by means of VCortex v2.2., a software from Salk Institute, CA, USA and a CIO-DAS1602/12 data acquisition board. The data acquisition board is connected to the graphical board to present the visual stimuli, but has also many channels to monitor the button the monkey has to push, the eye position and the reward.

To create the desired experimental set-up and behavior control it's necessary to write 3 text files that the compiler inside VCortex interprets: an *item file*, *condition file* and *timing file*.

The item file is simply a list of objects (they can be shapes, sounds, pictures or movies) with their characteristics (starting position, length, width, path), that'll be used during the experiment.

The condition file is a list of condition, each of which contains some objects. It helps putting together different objects that'll be used simultaneously, and also permits to handle the randomization of the stimuli presentation.

The timing file is the real core of the behavioural control: it has to be written in C language and manages both the stimuli visual presentation and the monkey behavior. It should include the handling of all possible behaviours and situations that can happen during a trial: it controls when the button is pushed and if the timing is correct or not, it monitors eye position, it sends "time markers" to the acquisition hardware to synchronize data with events in the post-processing of data and it controls when and if to give the reward to the monkey. The result of the behavior is coded in the variable *state*.

This is the flow of the events to be managed during a single trial:

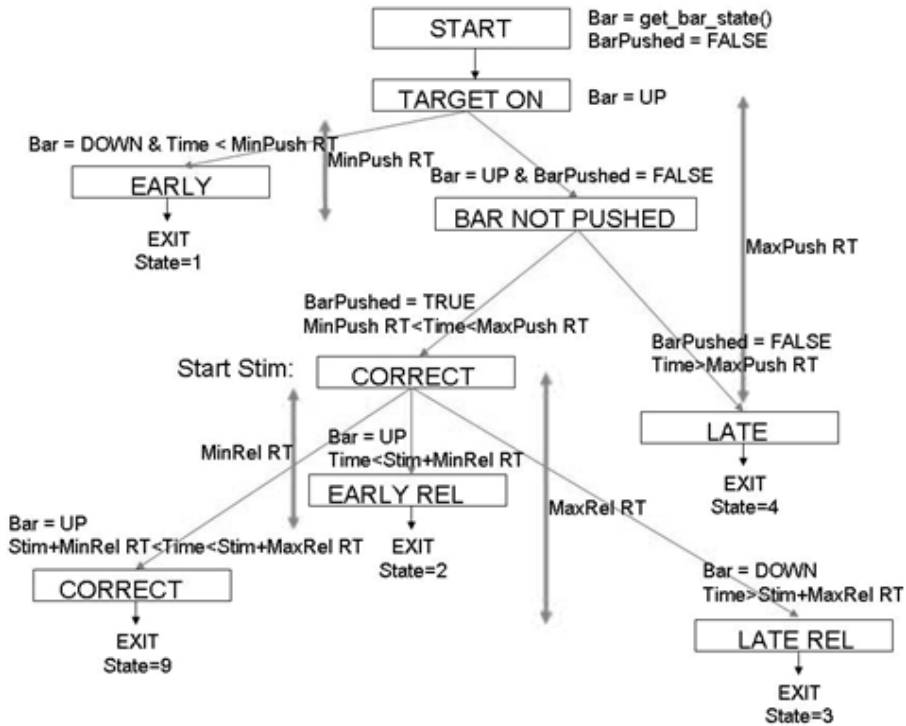
- At the beginning, the timing file should check the status of the button. If it's pushed, nothing should appear on the screen and a sound should make the trained monkey understand that he has to release the button.
- When the target (of fixation point *FP*) appears, the monkey has a `maxPushReaction Time` to push the button, otherwise the trial will be aborted and labeled as `LatePush (state = 4)`.
- If the monkey pushes the button in the correct time, the trial starts and the visual stimuli are presented on the screen.
 - If the button is released before the visual cue that indicates the end of the trial, the trial is aborted as an `EarlyRelease (state = 2)`
 - If the monkey keeps pushing the button after the maximum reaction time, the trial is aborted as `LateRelease (state = 3)`

- If the button is release in the correct time, the trial is correct (state = 9) and the monkey receives the reward.

During all the duration of the trial, saccades are not permitted, so eye position has always to remain inside a window around the target, whose dimension is set by the operator. Otherwise, the trial will be aborted and labeled as eyeOff (state = 5).

It is important, especially during monkey training to consolidate and help learning, that every times a mistake is made the trial is instantaneously aborted, everything disappears from the screen and different sounds are presented. All aspects that are controlled in the timing file.

Another role of the VCortex software, controlled in the timing file, is the possibility to send “time markers” to the acquisition hardware, when important events happen: the post-processing of data needs these information to synchronize spikes with the visual stimuli. In our data acquisition hardware, only 3 channels were left for this aim: a 3 bit coding of the event is necessary to identify all the numerous possible events.



3.3. Visual stimuli presentation

In a similar way as for the behavioural control, visual stimuli presented on the screen are generated by a C routine saved in the .tim file as the behavioural control.

The experiments are usually divided in two parts:

- In the first one, when a cell is isolated, its visual responsiveness is initially assessed, by moving a luminous bar (3 cd/m^2) on a dark background, with different speeds, sizes and peripheral locations around the screen, in order to outline the receptive field. The speed usually used in the following experiments is $30^\circ/\text{s}$.

The receptive field map is calculated as the area where the cell appears to increase its activity. The monkey has always to fixate the FP. There are two ways of running this part of experiment with VCortex routines: it's possible to decide by the control of the keyboard in which direction to move the luminous bar, or either run the automatic version of the programs that moves the bar randomly in all previously selected directions.

Both the luminous bar and the target are objects whose characteristics (dimensions, initial position) are set in the .itm file of VCortex, while the bar sweeping on the screen is controlled by the .tim file in VCortex.

- After the mapping of its own the receptive field, each neuron is tested with optic flow stimuli.

Optic flow is the pattern of apparent motion of objects, surfaces, and edges in a visual scene caused by the relative motion between an observer and the scene. The "focus of expansion" or *FOE* tells in which direction the observer is moving. For example, if you are travelling in a straight line, the optic flow is zero in the directly forward direction.

Our optic flow stimuli are formed by 1000 randomly distributed luminous dots. Each dot subtended 0.06° , with a luminous intensity of 3 cd/m^2 . The dots moved radially in order to simulate expanding and contracting fields, or in a translational motion in eight directions at 45° angular intervals. The apparent average speed is $\sim 10^\circ/\text{s}$ for radial optic flow and $\sim 15^\circ/\text{s}$ for translational. For each dot moving out of the screen a new dot is placed in a random position inside the flow.

These visual stimuli are created offline with MatLAB routines, saved as movies and then showed on the screen by means of VCortex routines, to simultaneously control the behavior of the monkey. The number and the dimensions of the dots can be controlled by the operator while generating the movies.

We use many different experimental paradigms, to explore as many combination as possible of FOE and FP positions.

The sensitivity to this type of stimulus is assessed by positioning the FOE usually in a 3 x 3 grid at 15° distance from each point: to be able to understand if eye position modifies the optic flow selectivity and which is the exact relationship between FOE and eye position, we vary the spatial position of FOE and FP. Five different stimulation paradigms are used in the following studies. In the first test, the retinotopic organization of FOE neuronal selectivity is tested presenting FP in the center of the screen and FOE in one of nine locations in a 3x3 grid at 15° distance each . In the second test, to assess the influence of the eye position upon the optic flow and retinotopy selectivity, we reverse the FP/FOE positions by presenting the FOE in the center of the screen, while FP is in one of the same nine locations as before. In addition, in the third test, the eye position effect irrespective of retinotopy is studied by presenting FP and FOE in the same position in each of the nine locations. Finally, when recordings are stable enough, response selectivity for translational stimuli is tested. The random dot background is moved tangentially to the frontoparallel plane, in eight directions at 45° angular interval. For the translational stimulus the speed is 15°/s. Trials are recorded in blocks, stimuli order are randomly selected. Each stimulus is repeated at least eight times.

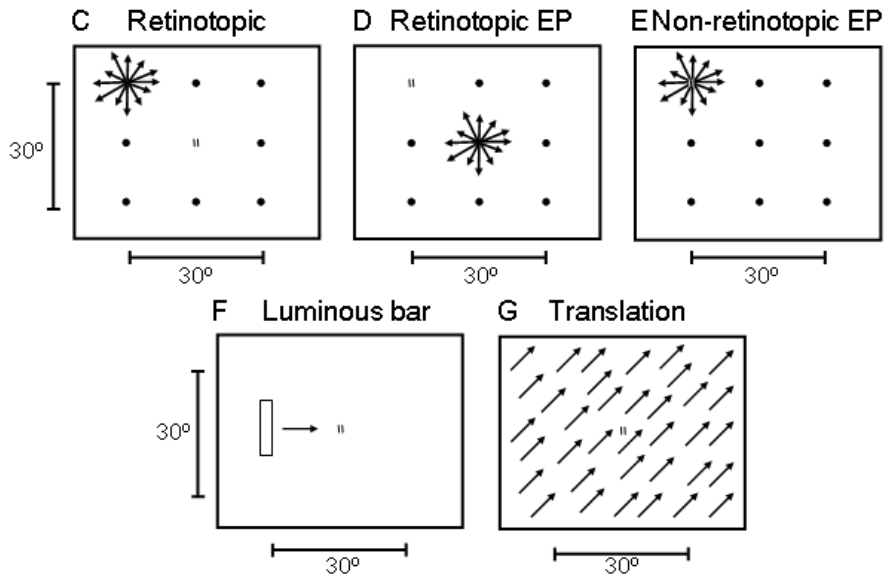


Figure 24: Retinotopic test. The FP presented in the center of the screen and FOE in one of nine locations in a 3x3 grid at 15° distance each. Black dots indicates other FOE peripheral positions. D. Retinotopic EP test. The FOE in the center of the screen, while FP in one of the nine locations. Black dots indicates other FP peripheral positions. E. Non-retinotopic EP test. FP and FOE displayed concentric in one of the nine locations. Black dots indicates other FP/FOE peripheral positions. F. Receptive field mapping. A luminous bar moving across the screen in eight directions at 45° angular intervals. G. Translation test. The random dot background moved tangentially to the frontoparallel plane, in eight directions at 45° angular interval. FP: fixation point; FOE: focus of expansion; EP: eye position, RdT: random time.

4. Multimodal representation of optic flow processing in monkey area PEc

During locomotion, the visual perception of self-motion is mainly provided by optic flow. The optic flow pattern is not always simple: the eyes usually scan the environment so the gaze is not always directed to the focus of expansion (FOE) of the flow field. These movements have the effect to change the retinal FOE position with respect to the fovea. As seen in Ch. 2.3.2., area PEc of the macaque monkey, in the dorsal parietal cortex, is a good candidate multimodal signal integration, especially during self motion and arm movement planning. The aim of this research was to assess whether optic flow selective neurons in parietal area PEc are modulated by eye position. We recorded single neuron activity during optic flow stimulation in two monkeys, varying eye and retinal FOE positions. We found that the majority of PEc neurons are modulated by the FOE retinotopic position with different tuning for expansion and contraction. Although many neurons did not show any gaze field without visual stimulation, the eye position modulated optic flow responses in about half of neurons. These novel results suggest that PEc neurons integrate both visual and eye position signals and allow to hypothesize a role in guiding locomotion being part of a cortical network involved in FOE representation during self-motion. Visual and eye position interaction in this area could be seen as a contribution to the building of the invariant space representation necessary to motor planning.

4.1. Methods

4.1.1. Experimental paradigm and stimuli

Experiments were performed on three hemispheres of two male macaques (*M. fascicularis*) 8 and 9 years old. Monkeys were bought from “R.C. Hartelust B.V., P.O. Box 2170, 5001 CD Tilburg”, The Netherlands. All experimental procedures were performed with the control of the veterinary staff of the University of Bologna, after receiving approval by the Committee on Ethics in Animal Experimentation of Bologna University and governmental approval, in compliance with the Italian guidelines for care and use of laboratory animals (Italian Legislative Decree 116/92; in accordance with the European Community Council Directive 86/609/EEC on animal welfare). All efforts were made to minimize animal suffering and to reduce the number of animals used.

Surgery

A metal recording chamber of 18 mm inner diameter was placed on the skull midline above the Parieto-occipital Sulcus (POS). The chamber center was placed at stereotaxic coordinates AP-13, ML 0 in the first monkey (MF) and using MRI guidance in the second (MG). MF was also used in previous studies (Raffi, Squatrito e Maioli 2002) (e. a. Raffi 2008). At the same time, a metal holder for restraining the head was also implanted by using metal screws and bone cement (Palacos®). Surgical procedures were performed under general anesthesia (Thiopentotal Sodium 15 mg/Kg i.v.). Analgesic and antibiotics were given for several days after surgery (Ketorolac tromethamine, 30 mg/die i.m.; Benzathine Benzylpenicillin 0.1 ml/Kg i.m.).

After recovering from surgery, extracellular recordings of single neurons were performed on both hemispheres of MF and in the right hemispheres of MG using glass-coated elgiloy or tungsten microelectrodes passing through the

dura mater. The monkey's head was fixed at the experimental apparatus. Data acquisition was made by a multi spike-sorter system for electrophysiological recordings (Alpha-Omega Inc.), storing the output on a PC hard disk. At the end of the recording sessions, electrolytic microlesions were performed in MF to be later used as landmarks for the anatomical reconstruction of the recording sites. After perfusion, the brain was sectioned for histology. Coronal sections 60 μ m in thickness were made and the cytoarchitecture was examined after staining with toluidine blue. Electrode tracks and the locations of recorded units were then reconstructed with the help of the coordinates of each penetration and the electrolytic microlesions. Electrolytic microlesions were not done in MG, in which the recording sites reconstruction has been performed based on the chamber location and electrode coordinates.

Experimental paradigm and stimuli

Extracellular activity of single neurons was recorded from the dorsal surface of the superior parietal lobule.

The monkeys performed a reaction time task while fixating a red target, consisting of a square pattern formed by two luminous vertical bars (0.17° wide) separated by a dark gap (0.17° wide). The target was presented on a 19" computer monitor placed 28.5 cm from the eyes.

The trial temporal sequences were as follow: at the FP onset the monkeys had to push a lever beginning fixation (time 0). Such fixation lasted for 1000 ms, then a cloud of dots randomly distributed appeared. After 1000 ms the dots cloud started moving with radial expansion direction and after about 1000 ms the dot cloud moved in contraction (Fig. 26A). Trial duration was random, and varied between 4000 and 6000 ms. In longer trials, after contraction, expansion stimulation started again. The monkeys had to detect a change in target orientation and release the lever within 500 ms. A drop of juice or water was the reward for each correct trial. Eye position was monitored

monocularly, with a resolution of 0.1° , by an optoelectronic system that uses the corneal reflection of an infrared light beam (Bach 1983). The eye position was checked off-line and trials with incorrect fixation or saccades were discarded.

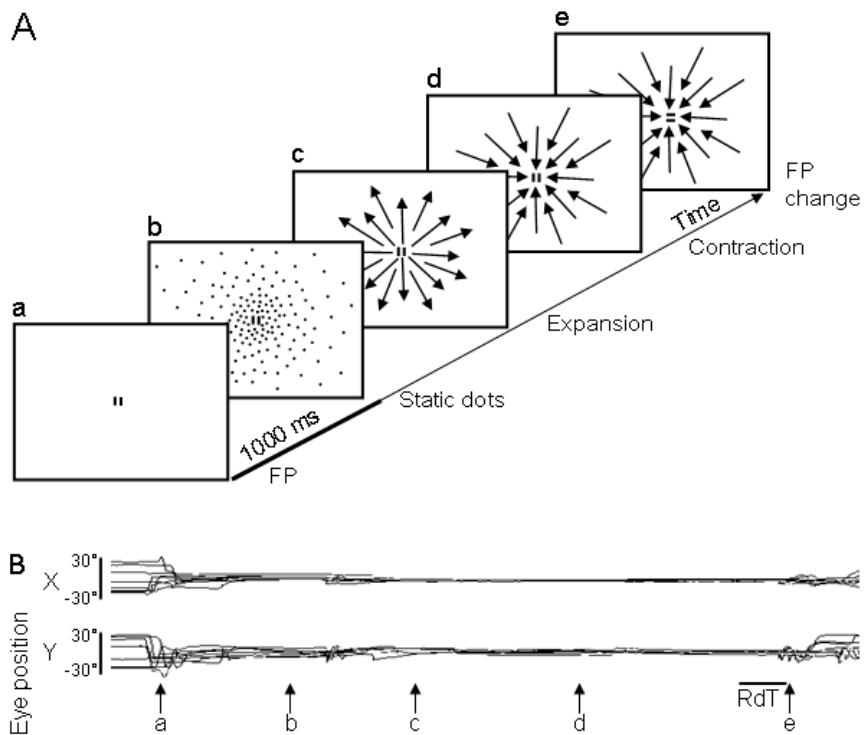


Figure 25: Behavioral protocol. A. Temporal sequence of the behavioral task. Full screen optic flow stimuli consisted of 1000 moving dots with an apparent average speed of $10^\circ/\text{sec}$. At the onset of the fixation point (a) the monkey pushed a lever. After one second, the cloud of dots appeared (b) and after about one second it began its expansion motion (c). After about one second, the optic flow stimulus began its contraction motion (d). Then the monkey had to detect a change in target orientation (e) and release the lever within a maximum reaction time of 500 ms. B. Superimposed X and Y eye traces for fixation in the central position ($0^\circ, 0^\circ$). Conventions as in part A.

Extracellular activity of single neurons was recorded, during daily experimental sessions, from both the dorsal and the medial surface of the superior parietal lobule. When a cell was isolated, its visual responsiveness was initially assessed, by moving a luminous bar (3 cd/m^2) on a dark background, with different speeds, sizes and peripheral locations around the screen, in order to outline the receptive field. After the mapping each neuron was tested with optic flow stimuli formed by 1000 randomly distributed luminous dots. Each dot subtended 0.06° , with a luminous intensity of 3 cd/m^2 . The dots moved radially in order to simulate expanding and contracting fields. The apparent average speed was $\sim 10^\circ/\text{s}$. The sensitivity to this type of stimulus was assessed by positioning the FOE usually in a 3×3 grid at 15° distance from each point. When the FOE was positioned in peripheral locations, for each dot moving out of the screen a new dot was placed in a random position inside the flow. Occasionally, wider inter-point distances were tested. For each cell, the random dot background was also moved tangentially to the frontoparallel plane, in eight directions at 45° angular intervals. For the planar stimulus the speed was $15^\circ/\text{s}$. Each neuron was also tested by the luminous bar, moving in eight directions at 45° angular intervals in order to compare the directional selectivity to the bar stimulus with the selectivity to the optic flow and planar motion. Each stimulus was repeated at least eight times. The dimension of the receptive field of each cell was determined by the response duration along the preferred direction (e. a. Squatrito 2001).

To be able to understand if eye position modifies the optic flow selectivity and which is the exact relationship between FOE and eye position, we varied the spatial position of FOE and FP. Five different stimulation paradigms were used in this study. Three of them were aimed at studying the interactions between FOE retinotopy and eye position. In first test (test 1 or “retinotopic”), the retinotopic organization of FOE neuronal selectivity was tested presenting FP in the center of the screen and FOE in one of nine locations in a 3×3 grid at

15° distance each (Fig. 26C). In the second test (test 2 or “retinotopic EP”), to assess the influence of the eye position upon the optic flow and retinotopy selectivity, we reversed the FP/FOE positions by presenting the FOE in the center of the screen, while FP was in one of the nine locations (Fig. 26D). In this way we obtained a set of stimulations with same retinotopy as in the first test but different eye position. In addition, in the third test (test 3 or “concentric”), the eye position effect irrespective of retinotopy was studied by presenting FP and FOE in the same position in each of the nine locations (Fig. 26E). Each neuron was also tested by the luminous bar, moving along the screen in eight directions at 45° angular intervals, in order to compare the directional selectivity to the bar stimulus with the optic flow selectivity (Fig. 26F). The bar had a constant speed of 30°/s. Finally, when recordings were stable enough, response selectivity for translational stimuli was tested. (Fig. 26G). The random dot background was moved tangentially to the frontoparallel plane, in eight directions at 45° angular interval. For the translational stimulus the speed was 15°/s. Trials were recorded in blocks, stimuli order were randomly selected. Each stimulus was repeated at least eight times.

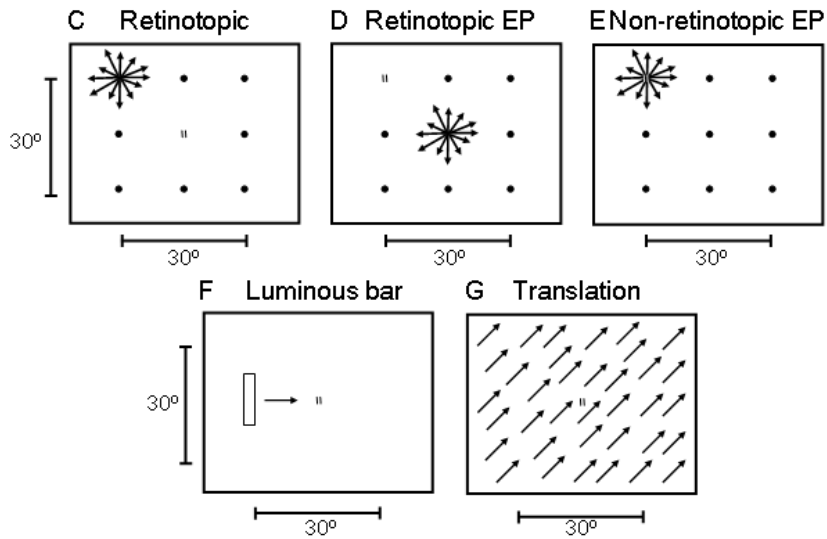


Figure 26: C. Retinotopic test. The FP was presented in the center of the screen and FOE in one of nine locations in a 3x3 grid at 15° distance each. Black dots indicates other FOE peripheral positions. In this test, the FOE was also positioned in the central position concentric with the fixation point. D. Retinotopic EP test. The FOE was in the center of the screen, while FP was in one of the nine locations. Black dots indicates other FP peripheral positions. E. Non-retinotopic EP test. FP and FOE were displayed concentric in one of the nine locations. Black dots indicates other FP/FOE peripheral positions. F. Receptive field mapping. A luminous bar moving across the screen in eight directions at 45° angular intervals. G. Translation test. The random dot background was moved tangentially to the frontoparallel plane, in eight directions at 45° angular interval. FP: fixation point; FOE: focus of expansion; EP: eye position, RdT: random time.

4.1.2. Data analysis

All data analysis were performed by means of MatLAB routines.

- The activity of a cell is recorded by the acquisition system as ISI (*inter-spike intervals*):

```

1 1 E 155
0      104    123    10    68    61    8    57    161    26    30    124    2    79    120
-192  33    14    18    147    31    61    47    23
-224  70    9     8     30    56    43    16    8    44    39    17    14    15    28    5
-240  13    7     65    46    2     23    68    91    65    4     23    12    3
-208  14    18    22    27    36    2     5     20    23    6     18    61    29    20    24
-80   214

1 2 H 217
0      34    139    63    7     171   137    9     59    48    34    34    37    40    106
-192  31    5     127   121   59    74    148
-224  4     102   19    349   86    27    93    81    72    65    137   283   92    168   14
-240  2
-240  40    1     2     76    29    2     48    30    21    4     7     2     17    8     17
-232  2     15    50    55    36    57    54    17    10    16    72    24    30    17    13
-236  192   2     37    28    14    25
-244  10    8     13    10    7     4     20    3     11    14    3     35    3     6     2
-212  7     0     8     4     24    13    25    7     31    31    68    223   208   120   57
-84   165

```

Figure 27: Text file format generated by the acquisition system. Inter-spike intervals are stored.

Number “1” is a code for the kind of stimulation that’s being applied for that set of trials, number “2” is the current trial number for that set, “H” indicates the result of the performance of the monkey. “H” is a correct trial, “E” is an early release of the button and “L” is a late release of the button.

The number that follows the result of a trial indicate show many ms passed since the end of the previous trial until the beginning of the current trial. Every following number indicates a spike event.

Negative numbers are the time markers that allows to synchronize cell activity with visual stimuli presentation:

-192 → target on

-224 → target on + bar down

-240 → start stimulus Expansion

-232 → change stimulus to Contraction

From these raw data, the next necessary step is to select only correct trials, excluding those in which the button was pushed earlier than the minimum reaction time or later than the maximum reaction time, and those in which the eye exited from the window around the target.

This needs to be done off-line because the hardware and software used in this experiment couldn't abort trials on the basis of the performance of the monkey. One of the aims of the new hardware and software is to resolve this issue.

- Single-cell neural data are first analyzed calculating the *mean firing rate* (see Ch. 2.5. for details) in four epochs. As mean firing rate, we intended the average frequency of a neuron over time.

- 1) the baseline activity was computed when the monkey fixated FP at the beginning of the trial, with no visual stimuli presented on the screen. The spiking activity of the first 100 ms was discarded from the computation to avoid the effect of the saccade made to reach the FP.

- 2) The neural activity during the static dots presentation was computed in an epoch of 900 ms, starting 100 ms after the onset of the stimulus.

- 3) During dots in expansion the mean firing rate was computed for 900ms of stimulation, as well as

- 4) During dots in contraction, to have all epochs analyzed uniformly.

For each trial recorded with the luminous bar and translation, the mean firing rate was computed for 900 ms for fixation in the primary position and each of the eight tested directions. The dimension of the receptive field of each cell was determined, during luminous bar stimulation, by the response duration along the preferred direction (e. a. Squatrito 2001).

The output file contains the mean frequency for each epoch of stimulation, for each repetition of the same trial. The classes indicate the kind of stimulation, as before.

```

classe 7
freq.fase 1: 35.8343,34.3643,23.4899,8.9686,14.6396,8.8692,13.3333,7.1006
freq.fase 2: 80.1394,50.4587,44.0476,48.9845,51.3141,50.6329,14.5414,39.7196
freq.fase 3: 112.865,81.3135,81.9543,79.5199,80.1556,65.3188,70.3364,78.208
freq.fase 4: 77.2231,55.9796,58.6265,57.4818,64.5657,49.0654,59.9688,56.9423
classe 18
freq.fase 1: 27.5545,17.9372,9.1429,10.8696,5.7078,5.4446,7.9787,19.3182
freq.fase 2: 27.8422,45.614,25.3456,30.1275,55.2291,28.4238,36.1582,42.7447
freq.fase 3: 56.3821,74.2424,49.8442,69.4127,85.0898,52.7523,55.9496,65.7792
freq.fase 4: 54.6401,51.2025,67.0194,73.6301,43.7342,50.7614,53.9174,36.4059

```

Figure 28: output text files with mean frequencies over time, over $n=8-10$ trials

- For the characteristic of the visual stimuli used, and the aim of the study, there are two independent variables that may modulate cell activity and we would investigate: the combination of the FOE and FP position (identified by the number of the class) and the epoch (only target, static dots, OF in expansion and contraction).

It's appropriate to perform a *two way unbalanced ANOVA* statistical analysis to highlight which factors modulate the cell activity, for each cell. This initial analysis allows to select on which neurons to carry forward a more focused analysis.

There are three sets of hypothesis with the two-way ANOVA.

The null hypotheses for each of the sets are:

1. The population means of the first factor are equal. This is like the one-way ANOVA for the row factor.
2. The population means of the second factor are equal. This is like the one-way ANOVA for the column factor.
3. There is no interaction between the two factors. The interaction is the effect that one factor has on the other factor.

All differences in firing rates were assessed with stimuli (static, expansion and contraction, or translation direction) and eye or FOE position as two factors. The ANOVA were run in those neurons recorded with at least 6 FOE and/or FP positions, or 6 bar and/or fronto-parallel stimuli directions.

This analysis allowed to determine whether the firing rates depended on the kind of stimulus motion or its retinal position. Then, for all significant neurons, a one-way ANOVA was performed in each epoch (fixation, static dots, expansion, contraction, luminous bar and translation) to determine the selectivity of a particular cell for each stimulus. The ANOVA were run in those neurons recorded with at least 6 FOE and/or FP positions, or 6 bar and/or translational stimuli directions.

- Only neurons with significant differences in stimuli and/or eye position were further analyzed using a *multiple linear regression* and a stepwise fit.

Multiple regression is a method used to examine the relationship between one dependent variable Y and one or more independent variables X_i .

The regression parameters or coefficients b_i in the regression equation are estimated using the method of least squares, by solving the linear model $Y = X\beta + \epsilon$ for β , where: Y is the dependent variable, X is the independent

variable, β is the vector with the regression coefficients and ϵ is the error term. In this method, the sum of squared residuals between the regression plane and the observed values of the dependent variable are minimized. The regression equation represents a (hyper)plane in a $k+1$ dimensional space in which k is the number of independent variables $X_1, X_2, X_3, \dots, X_k$, plus one dimension for the dependent variable Y .

The estimated b coefficients (b_1 , b_2 and b_3) were calculated along with their 95% confidence intervals, to model the results as:

$$Y_i = b_1 + b_2X(i, 2) + b_3X(i, 3)$$

for the i -th element of the observation vector.

The stepwise procedure was used given that leaves only the coefficients that are significant in the final model of the data. The R^2 coefficient of determination is a statistical measure of how well the regression plane approximates the real data points. The coefficient of determination R^2 has also the purpose of predicting future outcomes on the basis of other related information. It provides a measure of how well future outcomes are likely to be predicted by the model. R^2 is the square of the sample correlation coefficient between the outcomes and their predicted values.

- To determine which mathematical model better explains PEc neural activity, we also used a *quadratic multiple regression model*, with six estimated b coefficients to model the data as:

$$Y_i = b_1 + b_2X(i, 2) + b_3X(i, 3) + b_4X(i, 2)^2 + b_5X(i, 3)^2 + b_6X(i, 2)X(i, 3)$$

for the i -th element of the observation vector.

- To better assess in which particular cases the angle of gaze influenced the optic flow responses, we selected and compared for every neuron the responses to couples of stimuli in which the retinotopic position was the same, but the eye position changed.

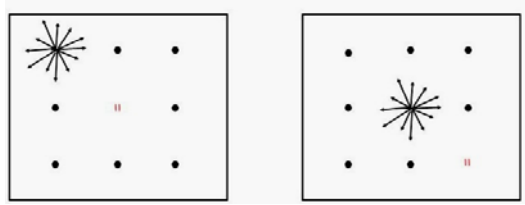


Figure 29: two conditions of stimulation in which the FOE position respect to the eye is equivalent. Eye position is different.

We performed a *t-test* for each couple to determine whether these two samples from a normal distribution (x and y) could have the same mean, with a 0.05 significance level. If the two responses are statistically different, we may assume that the neuron, in that particular combination of FOE and FP positions, is modulated by eye position.

- Then, we run a further analysis of the eye position effect on optic flow retinotopy. To reduce the number of independent variables, we transformed the FOE/FP coordinates in a single angle coding (i.e. a horizontal FOE position on the screen of 15° to the right, was coded as a 0° angle, while a position of 15° to the right and 15° upward, was coded as a 45° angle). To compare the same FOE retinal position in two different conditions in which the eye position is different, FP position angles where flipped by 180° (i.e. when the eye was in a 0° angle position, or to the right, the FOE was at 180° with respect to the eye). We then performed a linear regression based on *orthogonal least squares*. This method is a data modeling technique in which observational errors on both dependent and independent variables are taken into account and it gives the two coefficients of the linear model. The goodness of fit was computed as the sum of the squared distances between the data and the model. This analysis was carried out for expansion and contraction stimuli, to assess the eye position modulation upon motion perception. In particular, it is sufficient to look and the *slope* of the linear model, to evaluate whether the cell is modulated by eye position or not: if for

the two combination of stimuli the response of the cell remains similar, the slope would be positive, while if the eye modulates cell activity the slope would be negative.

4.2. Results

We performed 70 electrode penetrations in three hemispheres of two monkeys. The visual responsiveness of each isolated neuron was tested presenting either the luminous bar motion along eight directions or an optic flow stimulus in random positions. We found 86 non-visual neurons and 111 that seemed to show visual responsiveness. The statistical analysis performed after recordings showed that 108 neurons were significantly activated by at least one type of optic flow stimulation (two-way ANOVA, $p < 0.05$) (Fig. 30A).

Receptive field mapping was completed in 60 neurons. The majority of neurons (38/60, 63%) stimulated with a luminous bar showed a significant effect of the moving stimulus in some directions; only 2 neurons did not show any modulation (Fig. 30B). All receptive fields (RFs) were very large, usually extending more than 30° with a broad directional selectivity. We also found 9 that showed a foveal-sparing RF with a robust response to both inward and outward directions (see below the example in Fig. 31A), 2 neurons that showed a foveal-sparing RF with selectivity for outward directions and 1 neuron that showed an outward-vector circular RF.

The fronto-parallel stimulus was tested in 31 neurons, and 26 of them (84%) showed a significant stimulus effect. About a third of the responsive neurons showed an interaction effect between stimulus and direction, and, about a third showed a dependence on stimulus and direction (Fig. 30B). The regression models have been applied to the responsive cells, but only 7 of them (27%) presented a significant directional tuning. Neuronal responses to

fronto-parallel stimuli however, were much weaker than those to luminous bar or optic flow stimuli.

The majority of PEc neurons recorded in this experiment showed a different responsiveness to the optic flow tests. Figure 6C shows the optic flow test types that significantly modulated PEc neuronal activity (two-way ANOVA, $p < 0.05$). The majority of neurons recorded with the optic flow tests showed a significant interaction effect between optic flow type (expansion or contraction) and FOE position in space (Fig. 30C). A very few neurons were not responsive to these tasks. Multiple linear and quadratic regression methods were applied to those neurons that showed significant modulation by one, two or all tests. Considering the spatial tuning of the whole set of recorded neurons, 37% of neurons (22/59, including only retinotopic EP and concentric stimuli) showed a spatial tuning for the eye position, 58% (63/108) for the static stimulus, 51% (55/108) for expansion and 56% (60/108) for contraction.

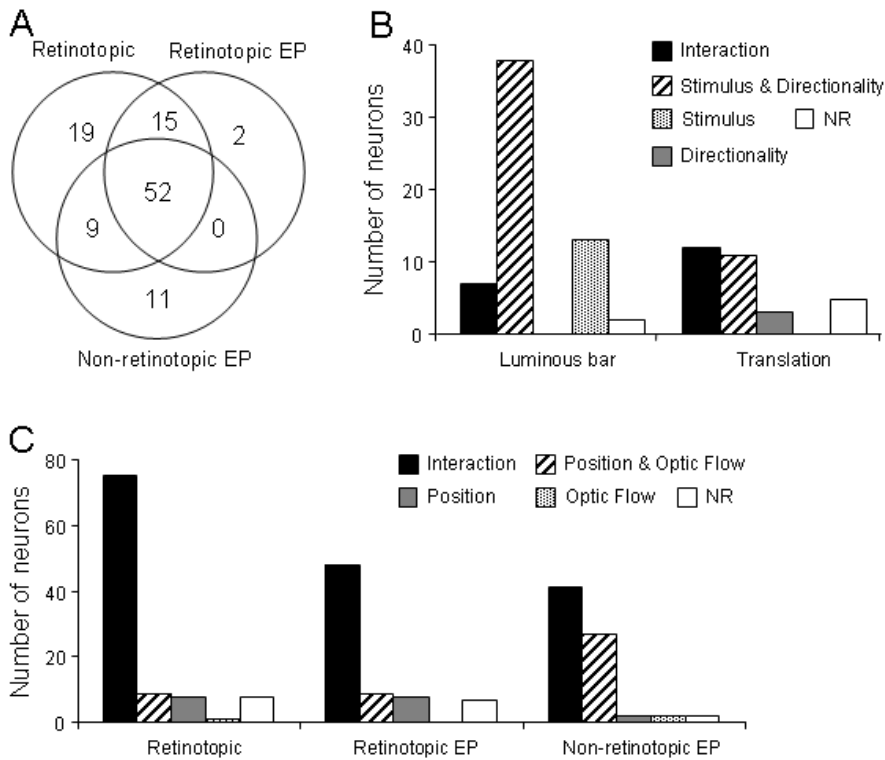


Figure 30: A. Venn diagram of responsive neurons to at least one type of optic flow stimulation (n=108). B. Results for the ANOVA in the luminous bar and translational stimulation; FD: n=60, BD: n=31. C. Results for the ANOVA in the three optic flow tests; Retinotopic: n=101, Retinotopic EP: n=75, Non-retinotopic EP: n=72. EP: eye position, FD: figure direction, BD: background direction.

An exemplary repertoire of responses of a PEc neuron to the whole set of visual stimuli is presented in Figure 31 and 32. The one-way ANOVA used for the directionality analysis showed that this neuron had a robust response to the luminous bar in both inward and outward directions sparing the fovea ($p < 0.001$). The RF extended for the whole visual field that could be mapped with our procedure. Note that the screen covered $60 \times 70^\circ$ of visual field, thus,

it is likely that the RF of this neuron exceeded those dimensions given also that the neuronal response onset to the stimulus motion started abruptly (Fig. 31A). Concerning fronto-parallel motion, there was a significant effect of the dots direction in the left visual field (one-way ANOVA, $p < 0.001$). The two-way ANOVA used for stimulus epoch comparisons showed no significant difference in firing rate between static dots and fixation period ($p = 0.36$) (Fig. 31B). This cell, however, did not show a significant fit with the regression model used for defining the directional tuning ($R^2 = 0.34$, $p = 0.34$, not shown). As a result, the directionality of the fronto-parallel stimuli is not explained by the RF features given that the latter did not show any preferred direction.

Furthermore, we found different neuronal responses to the three optic flow tests. The two-way ANOVA showed a significant difference across all trial conditions in the retinotopic test (interaction $p = 0.01$) (Fig. 32Cs). We found a significant effect of both optic flow stimuli ($p < 0.001$), while there was no significant difference in firing rate between static dots and fixation ($p = 0.26$). This means that the radial flow field motion is the appropriate stimulus for this neuron rather than a static visual stimulus. The cell showed a significant fit with the regression model used for defining the spatial tuning for contraction in the vertical axes ($R^2 = 0.49$, $p = 0.03$), while it did not show any tuning for the static stimulus ($R^2 = 0.15$, $p = 0.60$) and for expansion ($R^2 = 0.07$, $p = 0.78$).

As for the eye position organization of the optic flow tuning (Fig. 32Ds), the two-way ANOVA showed a significant difference across all trial conditions in the neuron's activity (interaction $p < 0.001$). A significant stimulus effect was found for static dots ($p < 0.001$) as well as a significant effect of the optic flow stimulus (interaction $p = 0.007$). The cell showed a significant spatial tuning for expansion ($R^2 = 0.76$, $p = 0.01$) and contraction ($R^2 = 0.94$, $p = 0.03$), while there was no tuning for fixation ($R^2 = 0.25$, $p = 0.41$) and static dots ($R^2 = 0.13$, $p = 0.65$).

The two-way ANOVA performed on concentric stimuli test (Fig. 32Es) showed a significant difference across all trial conditions (interaction $p=0.03$). A significant stimulus effect was found for static dots ($p<0.001$) and optic flow type and FOE position ($p<0.001$). There was a significant spatial tuning for contraction ($R^2=0.93$, $p=0.05$) and no tuning for fixation ($R^2=0.12$, $p=0.66$), static stimulus ($R^2=0.34$, $p=0.28$) and expansion ($R^2=0.19$, $p=0.52$).

In summary, the activity was strongly influenced by eye position during optic flow stimulation but with a different spatial tuning of the FOE retinotopy. The simple eye position displacement in peripheral locations without optic flow stimulation did not modulate the cell's activity.

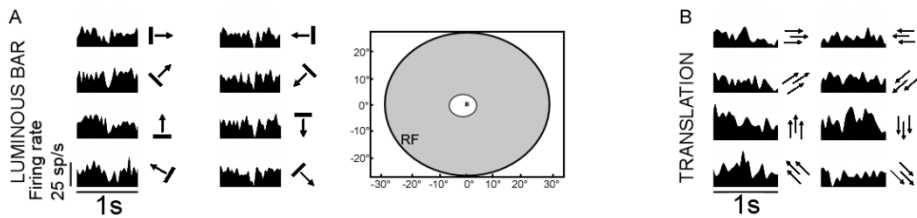


Figure 31: Response of a PEc neuron to all stimuli. A. Spike density plot (50 ms bin) for responses to the luminous bar. Arrows show the direction of motion. Vertical bar shows the neuron's firing rate and it is identical for all plots shown. On the right of the spike density plot, receptive field drawing. B. Spike density plot for responses to the translational dots. Arrows show the dots direction.

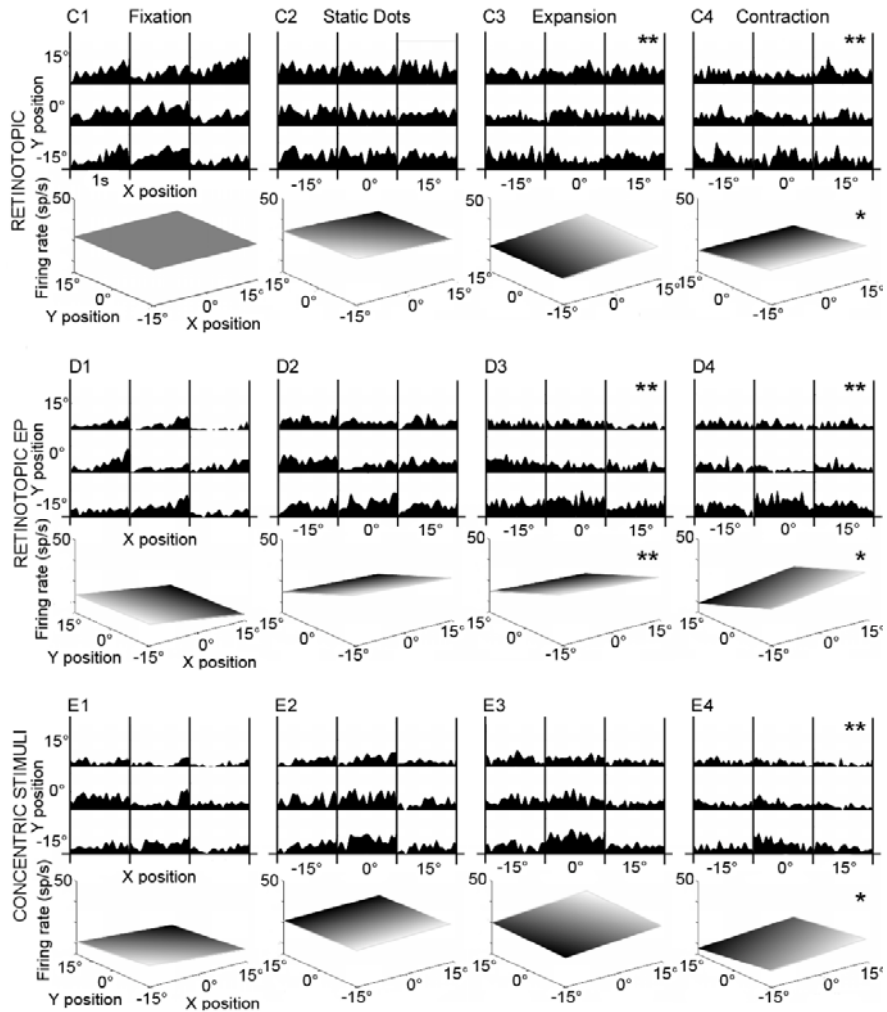


Figure 32: C. Retinotopic test. On the top, Spike density plot for response in the nine FOE positions. On the bottom, linear regression planes computed according to *eq. 1*. ANOVA significance values followed by the regression coefficients are reported for each stimulus. Asterisks show the significant effects (* $p < 0.05$, ** $p < 0.01$). C1. Fixation: $p = 0.29$ (in this paradigm FP was always presented in the center, the plane is shown for uniformity). C2. Static Dots: $p = 0.21$; $R^2 = 0.15$ $p = 0.60$ C3. Expansion: $p < 0.001$; $R^2 = 0.07$ $p = 0.78$ C4. Contraction: $p < 0.001$; $R^2 = 0.49$ $p = 0.03$ D. Spike density plot and regression planes for the retinotopic EP test. D1. Fixation: $p = 0.26$; $R^2 = 0.25$ $p = 0.41$ D2. Static Dots: $p = 0.56$; $R^2 = 0.13$ $p = 0.65$ D3. Expansion: $p < 0.001$; $R^2 = 0.76$ $p = 0.01$ D4. Contraction: $p < 0.001$; $R^2 = 0.94$ $p = 0.03$ E. Spike density plot and regression planes for the non-retinotopic EP. E1. Fixation $p = 0.20$; $R^2 = 0.12$

p=0.66 E2. Static Dots: p=0.69; $R^2=0.34$ p=0.28 E3. Expansion: p=0.15; $R^2=0.19$ p=0.52 E4. Contraction: p<0.001; $R^2=0.93$ p=0.05. Data set: Unit MF271.

FOE retinotopy

A total of 101 visual neurons were recorded with the retinotopic test and 95 (95%) were modulated by the optic flow stimulus in at least one epoch of the task. Only 6 neurons were not responsive to this task. Having FOE position as single factor, results of the one-way ANOVA run in each epoch separately showed that 72 neurons (71%) were modulated by expansion, 79 (78%) by contraction, and 37 (36%) by static dots presentation. Results of the two-way ANOVA, having FOE position and optic flow type as factors, showed that 74% of neurons (75/101) had an interaction effect between the two conditions (Fig. 30C). Responsive neurons were then analyzed by both regression models: 28% of neurons (26/95) showed a spatial tuning for the static stimulus, 29% (28/95) for expansion, and 28% (26/95) for contraction. In both optic flow stimuli, the majority of neurons showed preference for a peripheral FOE positions (n=18 for expansion, n=19 for contraction). These results indicate that the activity of this population of visual neurons is powerfully modulated by the optic flow stimuli with shifted FOE position w weakly modulated by static stimuli. Furthermore, about one third of the visually activated neurons showed a significant spatial organization of the FOE.

As for the directionality of the optic flow stimuli (expansion vs contraction), results of the one-way ANOVA (p<0.05) showed that the activity of 64 neurons (63%) was modulated by both directions, 8 (8%) by expansion only and 15 (15%) by contraction only. Within the sample of 64 neurons modulated by both stimuli, the b coefficients for the horizontal and vertical modulation of the firing rate of the multiple linear regression showed that 39 (61%) had a spatial tuning with a different orientation in space in the two directions.

Change in FOE retinotopy with different angle of gaze (retinotopic EP test)

A total of 72 visual neurons were recorded with the retinotopic EP test and 69 of them (95%) showed eye position modulation in at least one epoch of the task. Only 3 neurons were not responsive to this task. Results of the one-way ANOVA for each epoch, with a FP position as single factor showed that 55 neurons (76%) were modulated by expansion, 54 (69%) by spatial tuning for contraction, while only 21 neurons (29%) by FP position and 24 neurons (33%) by the static dots presentation. Results of the two-way ANOVA, having FP position and optic flow type as factors, showed that the majority of neurons (48/72, 66%) had an interaction effect between optic flow type and eye position in space (Fig. 30C). These responsive neurons were then analyzed by both regression models: 36% neurons (25/69) showed a spatial tuning for expansion, 42% (29/69) for contraction, 19% (13/69) for the eye position and 23% (16/69) for the static stimulus. These results reveal that this population of visual neurons shows a strong modulation of its responsiveness to retinotopic position of FOE related to the different angle of gaze.

With regard to stimulus direction, the activity of 47 neurons (65%) was modulated by both optic flow stimuli, 5 (7%) by expansion and 7 (9%) by contraction (one-way ANOVA, $p < 0.05$). The analysis of the b coefficients showed that within the sample of 47 neurons modulated by both stimuli, 29 (62%) had a spatial tuning with a different spatial orientation.

Concentric stimuli

A total of 75 visual neurons were recorded with the concentric stimuli test and 72 (96%) showed a modulation of eye position and/or optic flow stimulus in at least one epoch of the task.

Only 3 neurons were not responsive to this task. Results of the one-way ANOVA run for each epoch separately, with FP/FOE position as single

factor, showed that 47 neurons (62%) were modulated by expansion, 56 (74%) by contraction, while only 13 neurons (17%) by fixation and 23 (30%) by the static dots presentation. Results of the two-way ANOVA, with FP/FOE position and optic flow type as factors, showed that 55% of neurons (41/75) had an interaction effect between stimulus type and FOE position. A good portion of cells showed a dependence on stimulus type and eye position (27/75, 36%) (Fig. 30C). These responsive neurons were then analyzed by both regression models: 28% of them (20/72) showed a spatial tuning for expansion, 25% (18/72) for contraction, 14% (10/72) for the eye position, and 26% (19/72) for the static stimulus. Figure 33 shows other examples of the eye position effect on responses to radial optic flow stimuli centred on the fovea. Both neurons had a significant difference in firing rate in expansion and contraction (one-way ANOVA, $p < 0.05$), however, the first neuron (Fig. 33A) showed a similar and significant spatial tuning for both expansion ($R^2 = 0.68$, $p = 0.03$) and contraction ($R^2 = 0.60$, $p = 0.02$), while the second neuron (Fig. 33B) showed a different tuning in both phases and is significant only for expansion ($R^2 = 0.86$, $p = 0.003$) (contraction $R^2 = 0.23$, $p = 0.44$). Similar features can be seen in the neuron shown in Figure 32Es. These results strongly indicate that these PEc neurons are powerfully modulated when gaze and optic flow stimuli are simultaneously presented in the same spatial location, while weakly modulated by eye displacement per se. It is important to underline that retinotopic neurons with the best response in the concentric FP/FOE position in the center of the screen ($n = 10$ for expansion, $n = 9$ for contraction), did not show any spatial tuning when recorded with the concentric stimuli task.

The study of the directional analysis showed that the activity of 41 neurons (55%) was modulated by both optic flow stimulus directions, 5 (6%) by expansion only and 15 (20%) by contraction (one-way ANOVA, $p < 0.05$). Differently from the other two tests, in which the majority of neurons showed different spatial orientation for expansion and contraction, here the responses

to the two directions did not change substantially. In fact, the analysis of the b coefficients showed that within the sample of 41 neurons modulated by both directions, only 12 (29%) had a spatial tuning with a different spatial orientation.

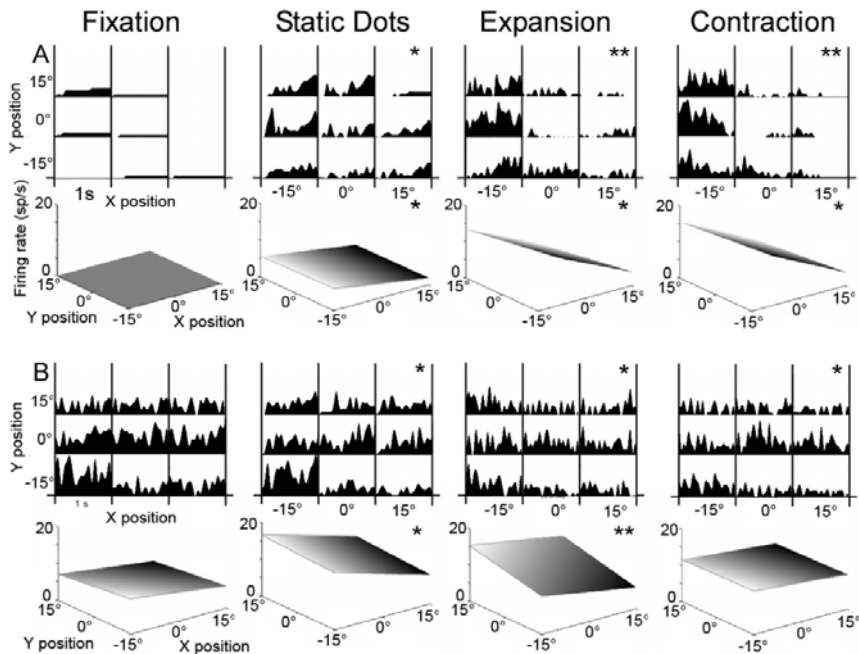


Figure 33: Spike density plot (50 ms bin) and regression planes for FP/FOE positions of non-retinotopic EP test in two cells (A,B). ANOVA significance values and regression coefficients: A. Fixation $p=1$; $R^2=0$ $p=0$; Static Dots: $p=0.02$; $R^2=0.48$ $p=0.03$; Expansion $R^2=0.68$ $p=0.03$; Contraction $R^2=0.60$ $p=0.02$ B. Fixation $p=0.25$; $R^2=0.48$ $p=0.14$; Static Dots: $p=0.01$; $R^2=0.7$ $p=0.02$; Expansion $R^2=0.86$ $p=0.003$; Contraction $R^2=0.23$ $p=0.44$. Asterisks show the significant effects (* $p < 0.05$, ** $p < 0.01$). Data set: A: Unit MF212, B: Unit MG015.

Eye position effect upon FOE retinotopy

The eye position effect upon the FOE retinotopy was examined in detail by comparing the response of each cell to the same retinal stimulation with a different eye position. Each comparison pair has been firstly analyzed by a t-test ($p < 0.05$). Figure 34A shows the spike density plots for the activity of the eight comparison pairs of a single neuron (the central position is identical in both tests). Straight lines in Figure 34A indicate the spike density plots for the FOE retinotopic position, dashed lines the response for the eye position. The specific FP/FOE positions are illustrated for each pair. A significant difference in firing rate was found in almost all pairs for expansion (5/8) and for contraction (7/8). Only two fixation and only one static dot position differently modulated this cell. This comparison analysis has been performed in 68 neurons recorded with at least four pairs of positions in both paradigms. Almost all neurons showed a significant difference in firing rate in at least one pair (66/68, 97%). The population data for the numbers of significant pairs for fixation and static dots are shown in Figure 34B, for expansion and contraction in Figure 34C. The different eye position significantly modulated the neural activity during both expansion and contraction, and, as clearly noticeable, the great majority of neurons were not modulated, or only one pair was, by the different fixation or static dots presentation.

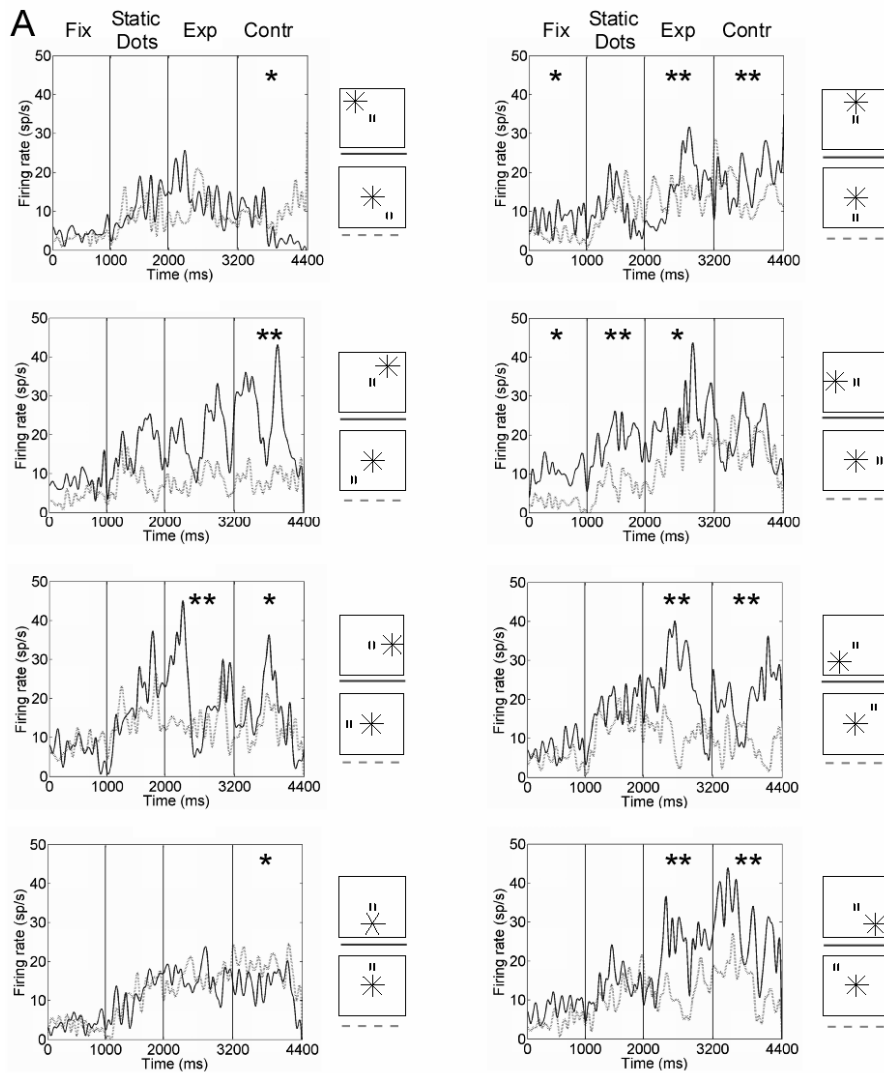


Figure 34 A: Comparison of the same retinal stimulation at different eye positions. A. Spike density plot (50 ms bin) for responses of a cell to the same retinal position of the stimuli with different eye position. The t-test significance values (* $p < 0.05$, ** $p < 0.01$) are shown on the top of each. The couples of FOE/FP position are shown to the right.

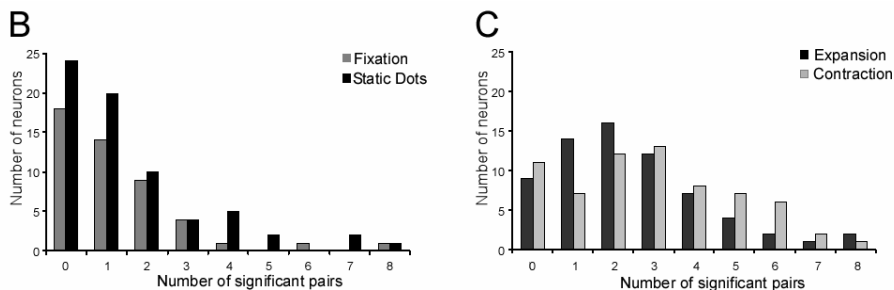


Figure 35 B,C: B. Frequency histograms of t-test population data. Number of neurons that show statistically significant different response during fixation and static stimuli. C. Number of neurons that show statistically significant response with different eye positions for expansion and contraction stimuli. Fix: fixation; Exp: expansion; Contr: contraction. Data set: Unit MF255.

To quantify the number of neurons that showed an eye position effect on the FOE retinotopy, we used a linear regression method based on orthogonal least squares. The criteria for choosing the significant cells was based on the sum of the square distance between the model and the data. Looking at the sign and value of the slopes of the linear regression given by the model (m coefficients), we could compare the differences in neuronal activity between the retinotopy test and the retinotopic EP test. Positive m coefficient means that the trend of the two responses of the cell during a particular epoch, over the FOE position, is similar indicating no eye position effect. An example of this analysis is shown in Figure 35. This neuron had a different trend in activity in both expansion and contraction (Fig. 35A) confirmed by negative slopes: expansion $m=-0.8$, contraction $m=-4.24$ (Fig. 35B). This model could be applied to 53 neurons that had a sufficient number of pairs in which FP and FOE orthogonal positions were transformed in a single angle coding (see Methods). The model could fit the data in 39 neurons (74%) for expansion and 46 (87%) for contraction (Fig. 35C). Results show that 22 neurons followed similar trend in the activity for expansion stimuli, meaning that there

is no or little eye position modulation on the FOE retinotopy, while 17 neurons have opposite trend indicating an effect due to different eye position in space. For contraction stimuli, no eye position modulation was seen in 26 neurons (positive m coefficients), while 20 showed an effect (negative m coefficients).

Figure 36 shows two examples of spatial tuning with different characteristics. Note that the eye position plane has been corrected by a factor of -1 to have in the same spatial location the same retinal stimulation with different eye position. Parallel plane orientation indicates no eye position effect on the optic flow retinotopy, as it is the case shown in Figure 36B3. Furthermore, this neuron showed significant retinotopic spatial tuning in all pairs (t-test, $p < 0.05$). Opposite planes imply the eye position effect on the optic flow retinotopy. Within this population, it is possible to see different types of optic flow selectivity. The spatial tuning of the exemplary neuron shown in Figure 36A3,114 differs along both axes in both expansion and contraction, while the tuning of the cell shown in Figure 36B3,B4 is similar in expansion while differs in contraction. Note that the cell's planes shown in Figure 36A are the same shown in Figure 32E1-4.

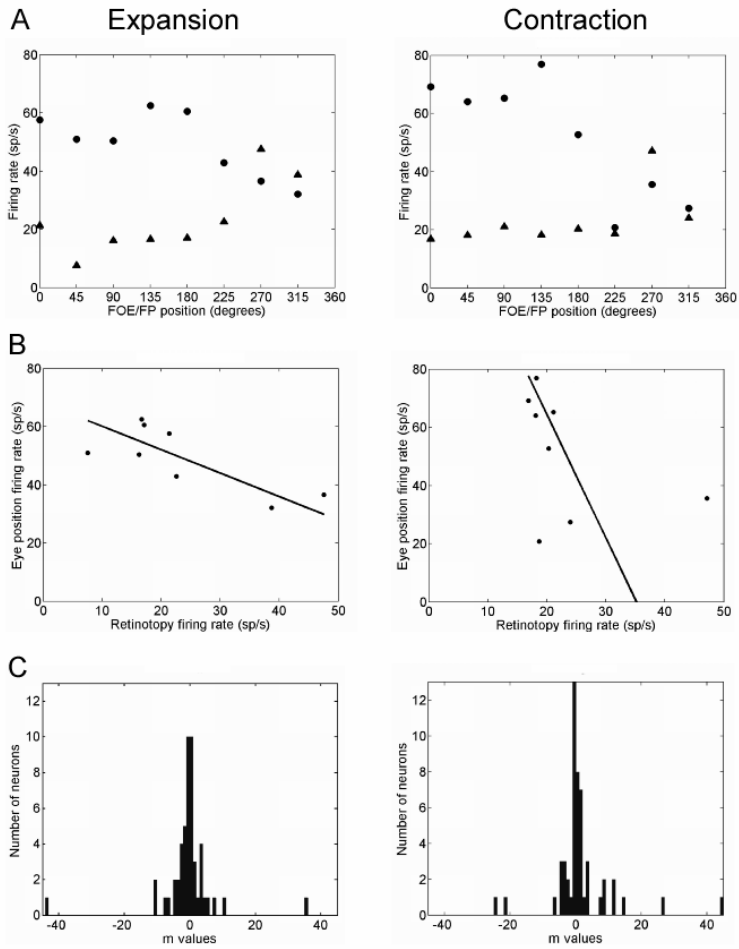


Figure 36: Comparison of the same retinal stimulation at different eye positions, by means of a total least square linear regression method. A. Retinotopic (circles) and retinotopic EP (triangles) firing rates with respect to the FOE retinal position, during expansion and contraction. B. Total least square linear regression model of the Retinotopic vs. retinotopic EP firing rate. Circles marks the data points, the line indicates the linear fit of the model. C. Population data (n=53). Frequency histograms of the number of neurons with the corresponding m coefficients calculated by the model. Data set: Unit MF194.

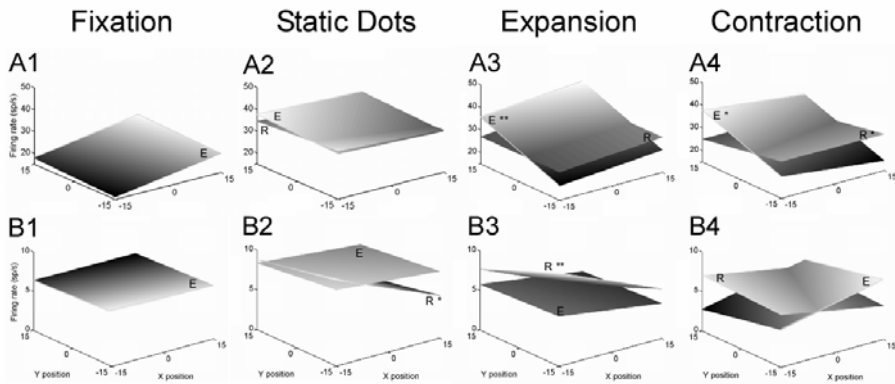


Figure 37: Comparison of regression planes in retinotopic and retinotopic EP tests, in four cells. A-B Regression planes of responses to the Retinotopic (R) and the Retinotopic EP (E) tests to the four epochs of the task. Eye position regression planes are shown corrected by a factor of -1 to have in the same spatial location the same retinal stimulation with different eye positions (see Methods). Asterisks show the significant spatial tuning (* $p < 0.05$, ** $p < 0.01$). Regression coefficients: Retinotopic static dots A. $R^2=0.15$ $p=0.6$ B. $R^2=0.64$ $p=0.04$; Retinotopic expansion: A. $R^2=0.07$ $p=0.78$ B. $R^2=0.88$ $p=0.001$; Retinotopic contraction: A. $R^2=0.49$ $p=0.03$ B. $R^2=0.31$ $p=0.31$; Retinotopic EP fixation: A. $R^2=0.25$ $p=0.41$ B. $R^2=0.03$ $p=0.9$; Retinotopic EP static dots A. $R^2=0.07$ $p=0.78$ B. $R^2=0.19$ $p=0.52$; Retinotopic EP expansion: A. $R^2=0.76$ $p=0.01$ B. $R^2=0.08$ $p=0.76$; Retinotopic EP contraction: A. $R^2=0.51$ $p=0.05$ B. $R^2=0.60$ $p=0.06$ Data set: A: Unit MF271, B: Unit MG008.

Anatomical reconstruction

The anatomical reconstruction of the recording sites of visual neurons recorded in area P_{Ec} was performed on the basis of cytoarchitecture (Pandya e Seltzer 1982) (Paxinos 2000). Figure 37A,B represents the orthogonal projections on the dorsal surface of the superior parietal cortex of each recording site of visual neurons recorded in both monkeys. Visual neurons were mostly found in the antero-lateral part of area P_{Ec}. We searched for a potential topography of eye head frames of reference of optic flow neurons by marking each recording site of the 66 neurons in which the comparison was possible with the preferred frame of reference. Results seem to indicate that

neurons with the same preferred frame of reference tend to be clustered. This might suggest a possible columnar or patchy organization of these representations (Fig. 37C,D). However, this study was not aimed at uncovering area P_{EC} neuronal topography, so the electrode penetrations were randomly performed. These results might be a good starting point for a research aimed at uncovering the cortical topography of area P_{EC} optic flow neurons possibly studying the specific connections with target premotor neurons.

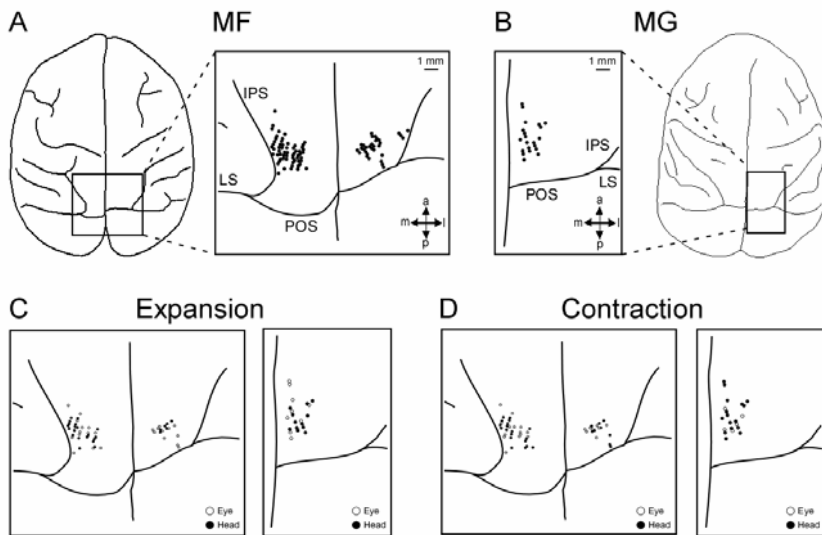


Figure 38: Anatomy of the recording regions. A. The right panel shows the silhouette of the dorsal view of MF. The recording regions in both hemispheres are shown enlarged in the inset to the left panel. The dots mark the orthogonal projection of each recording site on the cortical surface. B. The left panel shows the silhouette of the dorsal view of MG. The inset shows the recording regions in the right hemisphere. C-D. Each dot marks the recording site of the 66 neurons in which the comparison between FOE retinotopy and eye position effect was possible. Empty circles represent neurons that showed the eye-centered coding, black circles the head-centered coding. *IPS*, intraparietal sulcus; *LS*, lunate sulcus; *POS*: parieto-occipital sulcus; *m*: medial; *a*: anterior; *l*: lateral; *p*: posterior.

4.3. Conclusions and discussion

The neuronal responses to the visual paradigms used in the present study highlight complex functional features of area PEc neurons. This study demonstrates that the firing rate of PEc neurons is modulated by optic flow stimuli, signalling the flow direction. In agreement with results of a previous study (Raffi, Squatrito e Maioli 2002), the optic flow selectivity is not always predictable from the RF features. Some neurons of this population are tuned to the FOE retinal position, and for some of them the responses to identical FOE spatial position are modulated by eye position.

Although we did not test PEc neurons with rotatory stimuli or with other elementary components of flow field associated with heading perception, it is likely that the responses to radial optic flow, with selectivity for FOE retinal position of area PEc neurons are suited for contributing to cortical mechanisms of heading perception.

Eye position effect within the optic flow selectivity

The FOE retinotopic representation implies that PEc neurons could signal the offset between line of gaze and heading direction. The main result of this research is that the response of many PEc neurons to optic flow radial stimuli is strongly influenced by eye position. This finding demonstrates that FOE representation in area PEc might integrate retinal and extraretinal signals, in order to stabilize FOE spatial representation when the angle of gaze is shifted. Due to our experimental paradigm we cannot say whether this mechanism can be interpreted as a dynamic post-saccadic change in neuronal response, like the spatial map update after an eye movement (Colby e Duhamel 1996) (C. e. Colby 2005). At present, it must be intended as a steady gaze modulation of PEc firing activity during optic flow stimulation. It is feasible that eye position signals come to these cells from other PEc non-visual neurons whose

activity is modulated, with directional tuning, by both phasic and tonic eye displacement (e. a. Raffi 2008). The described dependence of visual responses on eye position is in line with the neural mechanisms taking place in the posterior parietal cortex, which play a crucial role in the integration of sensory signals to motor output generation. Comparing the neuronal responses to the same retinal FOE position at different angle of gaze in both stimuli, we found two different subpopulations of neurons: one responding similarly to FOE independently from eye position, the other modulated by the combination of FOE and eye position. These results, together with those demonstrating a pure response to eye position but not to visual stimuli (e. a. Raffi 2008), could support the hypothesis that intra-areal neuronal connections within PEc could enforce the integration between retinotopic information and eye position.

Although we did not perform data analysis suited to directly measure the spatial reference frame of neuronal tuning as has been done in other studies of spatial reference frames (Avillac 2005) (Fetsch 2007), nevertheless, our results demonstrate some sort of gain field effect on FOE spatial representation in PEc. Thus, visual and eye position interaction in this area should be seen as a contribution to the building of the invariant space representation necessary to motor planning

It is noteworthy that the spatial organization of expansion and contraction stimuli is different in the majority of neurons tested with the retinotopic tests (tests 1 and 2) (cfr. Figs. 34,35,36). The comparison between the FOE retinotopy and the eye position effect on such retinotopy shows that eye position differently affect FOE spatial representation for both expansion and contraction stimuli, in terms of gradient orientation (Figs. 35,36A3,36B3). In contrast, in most neurons tested with the concentric test (test 3) the spatial orientation of expansion and contraction stimuli is similar. On a general point of view, one can consider expansion and contraction associated to opposite heading directions. So, the responses of neurons likely related to heading perception should be opponent to the two directions. The fact that some

neurons show similar responses to both expansion and contraction may mean that actual heading direction is not coded by single neurons. Future research should address this problem, studying with a more ethological approach the heading perception at cell population level. The observed changes in spatial tuning orientation of FOE representation with different gaze angles should be considered in this framework.

Functional role of area PEc in heading perception

It is well known that besides PEc, many other cortical areas are possibly involved in heading perception processing, such as MST, VIP, 7a, DP, STPa and M1 (see (Raffi e Siegel 2004) (Britten 2008) for review). It has been suggested that heading perception might be a distributed cortical function that depends on sensory signal integration during optic flow processing and a substantial mediation by feed-forward and feed-back cortico-cortical circuits (Raffi e Siegel 2004). Area PEc receives the visual input mainly from areas V6, V6A, MST, 7a and VIP (Marconi 2001) (Shipp 1998) and directly project to area F2 (Marconi 2001) (Matelli 1998).

It has been reported that neurons in PMd encode sensory signals in head-centered coordinates (Boussaoud 1998). More recent studies showed that PMd neurons encode the locations of reach targets relative to arm, hand and eye. Some neurons encode reach goals using limb-centered reference frames, whereas others employ eye-centered reference frames (Pesaran, Nelson e Andersen 2006) (Batista 2007) (Wu e Hatsopoulos 2006). Recording sites reported in those studies are likely located in the projection region of area PEc (Marconi 2001) (Matelli 1998). Area PEc directly projects to the caudal portion of PMd (PMdc, also named area F2). Thus, areas PEc and PMd may form a cortical network involved in spatial stimuli location during self-motion and/or body movement programming. A recent fMRI study on human subjects identified a parieto-frontal network, including the homologues of

areas PEc and dorsal premotor cortex (PMd), involved in spatial updating representation in parietal cortex and motor act generation in premotor cortex during presentation of self-motion stimuli (Wolbers 2008). The human premotor cortex, including more than the homologues of area PMd, is activated by optic flow stimuli. Thus, it would be possible to assume that this optic flow activity would likely be found in the monkey premotor cortex as well given that both its input neurons (area PEc) and its target neurons (area M1) are activated by optic flow stimuli (Merchant 2001) (Raffi, Squatrito e Maioli 2002). So one can speculate that PEc contributes to spatial updating during self-motion and, on the basis on PMd data, its cortical output might be directly used for movement planning perhaps in head-centered coordinates.

Area PEc is an important node in the visuo-motor integration of hand and arm movements (Battaglia-Meyer 2001) (Ferraina 2001). Area PEc also possesses somatosensory neurons that have RFs placed in the arm, many of those are bimodal: visual and somatosensory (Breveglieri 2006) (Breveglieri 2008). From these and the data of the present study it is possible to hypothesize that optic flow processing in area PEc might serve the occipito-frontal circuit that control limb movements during locomotion.

4.4. Model of a neuronal network for eye position coding

Current computational models of heading perception attempt to reproduce the human psychophysical findings using the properties of MT and MST neurons. These models typically consist of two layers of neuron-like elements which represent the retinal flow as input (MT layer) and the computed heading as output (MST layer). The computation of heading and the properties of the neurons in the second (MST) layer mainly depend on the setup of synaptic connections with the first layer. In the model, populations of optic-flow processing neurons compute the mean-squared differences for a large number of possible headings in parallel. Each population estimates the current likelihood of a specific heading. This results in a heading map, the elements of which are populations of neurons. The most likely heading direction is equated with the peak of activity in this map. Extra retinal eye movement signals are easily combined with this approach to provide better estimates of heading when direct visual estimation is difficult. As in model neurons, individual MST cells cannot unambiguously specify the focus. A population code based on actual responses of MST neurons can locate the focus with an accuracy near that obtained by human observers. It's known that neurons in area PEc encode signals from different modalities, such as visual, extra retinal and somatosensory, probably combining them to encode spatial parameter of extrapersonal space to prepare body movements. Raffi et al. (e. a. Raffi 2008) report the characterization of the functional properties of PEc non-visual neurons that showed saccade-related activity. They analyzed the pre- and post-saccadic firing activity in 189 neurons recorded in five hemispheres of three behaving monkeys. Spiking activity of PEc single neurons was recorded while the monkeys performed visually-guided saccades in a reaction time task.

The idea of this neuronal network starts from the results of a previous study (Raffi, Squatrito e Maioli 2002).

It's known that neurons in area PEc encode signals from different modalities, such as visual, extraretinal and somatosensory, probably combining them to encode spatial parameter of extrapersonal space to prepare body movements. Raffi et al. report the characterization of the functional properties of PEc non-visual neurons that showed saccade-related activity. They analyzed the pre- and post-saccadic firing activity in 189 neurons recorded in five hemispheres of three behaving monkeys. Spiking activity of PEc single neurons was recorded while the monkeys performed visually-guided saccades in a reaction time task.

4.4.1. Experimental paradigm

The monkeys were trained in a visually guided saccades task. Experiments were performed in the dark. The monkeys began the task by fixating a red square (fixation point, FP) always positioned in the center of the screen. At the FP onset, the animals pushed a button beginning static fixation (FP_{FIX}) for a variable time of at least 1000 ms; then FP disappeared from the center (beginning of the fixation point movement, FP_{MOV}) and simultaneously reappeared in the periphery. The monkey had to make a saccade to reach the FP in the new peripheral position. Saccades were made along one of eight directions with an angular separation of 45° (Fig.38A,B). A 90° flip in FP orientation was the cue (Fig.38C) for the animal to release the lever (cue) in a maximum reaction time of 400 ms. The eye position was checked off-line and trials with incorrect fixation or saccades were discarded. Trial duration was randomized and varied between 4500 and 7100 ms. Trials were recorded in blocks, saccade directions were randomly selected. Saccades were made at 20° eccentricities. Eye position was recorded with a sample rate of 62.5/s; it

was monitored monocularly, by an optoelectronic system that uses the corneal reflection of an infrared light beam, with a resolution of 0.1°

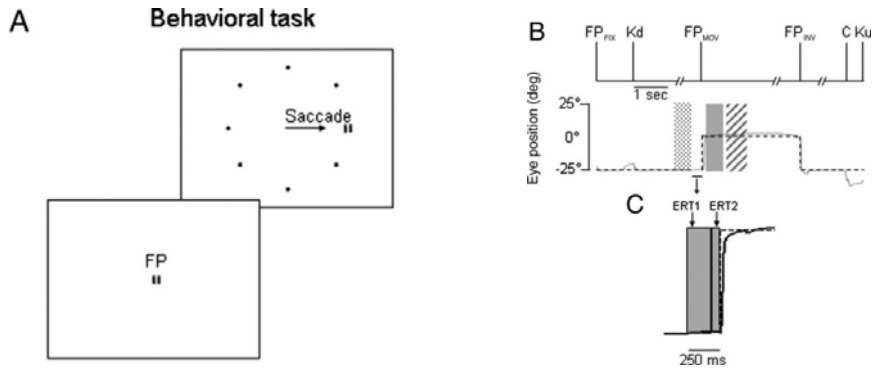


Figure 39: A. Saccade behavioural task: the fixation point disappears from the centers and then appears in a random peripheral position. B,C. Eye position during while performing a saccade and relative reaction times ERT.

4.4.2. Data analysis

The mean firing rate was calculated in several epochs for each trial. The baseline activity was computed in the last 500 ms of FP_{FIX} (Fig. 38B, dotted box). A pre-saccadic epoch was analyzed by computing the mean firing rate from FP_{MOV} to the saccade. This is a measure of the eye reaction time (ERT), (i.e. the time period from the FP disappearance to the beginning of the saccade). To better characterize the pre-saccadic period, the computation of ERT was performed in two sub-epochs: a first part of eye reaction time (called ERT1), from FP disappearance until 50 ms before the saccade onset, and a second part of ERT (called ERT2), the last 50 ms before the saccade onset (Fig. 38C, gray boxes). The saccade onset was considered the instant when the eye velocity reached 10% of the maximum velocity. This analysis of the pre-saccadic epoch is useful in testing if these cells play a role in saccade programming, because in this period the eye was still fixating the center of the screen but the FP was already in the peripheral position (i.e. the eye was

fixating a dark spot but the monkey already knew where to make the eye movement). Furthermore, the motor planning of the saccade occurs, approximately, within the last 50 ms preceding the saccade onset, so the contrast between ERT1 and ERT2 allows separation of the effect of the decision phase from those of the motor programming phase.

The mean firing rate in the post-saccadic period was computed in two epochs: 1) from 50 to 550 ms after the end of the saccade (phasic activity, Fig. 38B gray box); and, 2) from 600 to 1200 ms (eye position activity, Fig. 38B dashed box). All differences in firing rate across saccade directions and/or saccade epochs were assessed for statistical significance using analysis of variance (ANOVA). Directional tuning curves of each cell were determined by fitting the experimental data with a von Mises circular distribution, modified with a corrective factor, computed by the formula:

$$M(\theta) = A \cdot \frac{1}{2\pi I_0(k)} e^{[k \cos(\theta - \gamma)]}$$

where A is the corrective factor with a value of 0.8, $I_0(k)$ is the Bessel function, k is the parameter of concentration indicating the amplitude of the tuning curve, θ is the stimulus direction (in radians) and γ is the preferred direction (in radians). The preferred direction of each cell was determined using the sum of each angular value (degrees) divided by the length of the mean resultant of the units vectors. The von Mises distribution is the most commonly used distribution model for circular data. It is a unimodal symmetrical distribution similar to the normal distribution in linear data. It has been described as the best fitting model function for single unit orientation tuning curves. This analysis was performed on cells that showed a significant difference (ANOVA, $P < 0.05$) in firing rate during the different epochs of the eye movement when compared with the baseline activity. The goodness of fit was assessed by a χ^2 test ($P < 0.05$). The bandwidth of each tuning curve, taken as half-width at the half-height, was determined using the equation:

$$\theta_{0.5} = 0.5 \arccos \left[\frac{\ln 0.5 + k}{k} \right]; \quad k > -0.5 \ln 0.5$$

In the post-saccadic epochs, we analyzed the influence of eye position on the neural activity using a linear regression method, having firing activity as dependent variable with horizontal and vertical eye positions as independent variables.

4.4.3. Results and neuronal model

Raffi et al. found that 84% of neurons recorded from area P_{EC} showed pre-saccadic activity with directional tuning. In 26% of neurons, we found inhibition of activity in the pre-saccadic period. The onset of this “pause” always started before the saccade and, in 51% of neurons, it was invariant among different gaze directions. The post-saccadic activity in these cells was either a phasic response with directional tuning (77%) and/or an eye position tuning (75%). The analysis of the preferred direction did not show hemispheric preference, however, for the majority of neurons, the angular difference in the preferred direction, in the pre- and post-saccadic period, was more than 60°. By confirming, therefore, that P_{EC} neurons carry information about eye position, these novel findings open new horizons on P_{EC} function that, to date, is not well documented. The pre-saccadic activity may reflect an involvement in saccade control, whereas post-saccadic activity may indicate a role in informing on the new eye position. These novel results about saccade and eye position processing may imply a role of area P_{EC} in gaze direction mechanisms and, possibly, in remapping visual space after eye movements.

The aim of this model is to simulate, with a neuronal network, the pre-saccadic and post-saccadic activity of non-visual neurons in area P_{EC}. These neurons are fundamental because they seem to encode the saccade metrics and might be involved in gaze control.

The number of neurons of the network can be selected by the operator. Each neuron respond to some “preferred” saccade direction while is silent or inhibited for opposite directions. Each neuron may also interact with neighboring neurons by means of lateral sinapses, that can be both excitatory and inhibitory. The network input is the peripheral retinoic position of the fixation point in the instant that precedes the saccade.

The output might be either: *i)* the simulated pre-saccadic response *ii)* the post-saccadic response.

In the first case, the network simulates the condition in which the subject is still looking at the center of the screen, but knows that has to perform a saccade. In particular, the network simulated the neuronal response while planning a future eye saccade. In the second condition, the network simulates the coding of the new eye position after the saccade is ended and the eye is fixation the FP in a peripheral position.

The characteristics of the responses of the cells of this neuronal network are very similar to the real data.

For the simulation in Fig. 39, the network was constituted by 24 neurons.

Other parameters were the following:

excitatory sinapses $\sigma = 45^\circ$; inhibitory sinapses $\sigma = 90^\circ$;

excitatory sinapses $L_0 = 4.4$; inhibitory sinapses $L_0 = 4$;

sigmoid threshold = 10; euler integration step = 0.1;

gaussian bandwidth = 23; sigmoid parameter = 30;

baseline activity = 10sp/s;

We also carried on some simulation in which baseline neuronal activities were random. The response of the network was chosen with the *winner takes all* rule.

The aim of this simple neuronal network is to be a starting point for a more complex network that would be able to simulate physiological neuronal response of area Pec to Optic flow stimuli, with different eye position. The model can help understanding the mechanism underlying eye position and visual stimuli information integration.

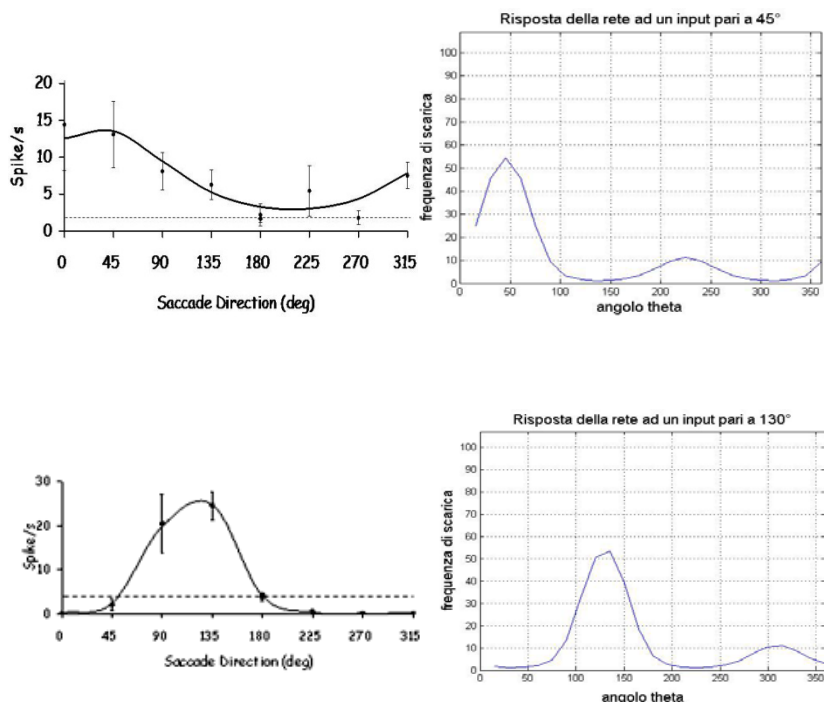


Figure 40: Directional curve of real data on the left and simulated on the right

5. Spike train oscillation modulated by optic flow stimuli in area PEc

Brain rhythms arise through the synchronization of neurons and their entrainment in a regular firing pattern. In this process, networks of reciprocally connected inhibitory neurons are often involved, but what mechanism determines the oscillation frequency is not completely understood.

Theories of brain function are based on the fact that information is carried by the electrical activity of neurons. What is the neural code of information, and how is it used by the brain to achieve perception, action, thought, and consciousness? In other words, which aspects of a neuron's electrical activity convey information about the environment and our mental states? This neural activity appears as a sequence of very brief events, the action potentials, separated by gaps of variable duration. The intervals between spikes can be as long as a few tenths of a second or shorter than a hundredth of a second. The spikes and the intervals between them codify the neuron's message. It is well established that the only type of message that a neuron can send to another neuron must be represented in the sequences of spikes that are transmitted along its axon. The time-scale for neural computations involved in perception and action is too short to allow gene expression, protein synthesis, and chemical cascades to play a part in carrying information. Spikes are all-or-none events, size does not matter.

The information lies in spikes sequences. The question is how to read this sequence of spikes emitted by neurons as a function of time. What are the properties of the neural spike trains that provide the possibility to carry the information or take part in information processing? What is the information

contained in such a spatio-temporal pattern of pulse? What is the code used by the neurons to transmit that information? How might other neurons decode the signal? The above questions point to the problem of neuronal coding. At present, an answer to these questions is not known. In the theory of neuronal information processing, there are two main hypotheses with respect to where in the spike train the neural information is encoded, whether in the neural firing rate or in the precise timing of the spikes.

Until recently, the most popular hypothesis is that most of, if not all, the relevant information is contained in the mean firing rate of the neuron, defined by the number of spikes that occur in a time window, divided by the length of the window. The concept of mean firing rates has been successfully applied during the last 80 years.

The definition of the rate has been applied to the discovery of the properties of many type of neurons in the sensory, motor, and central nervous system, by searching for those stimuli that make neurons fire maximally. Since Adrian's studies (Adrian 1928) the rate coding hypothesis has been dominant in the neural computational field. Rate coding explains how the presentation and intensity of the stimulus can influence neural activity but this coding neglects the temporal organization of spike trains. For this reason, the firing rate concept has been criticized and it is subject of an ongoing debate, stimulated also by experiments showing the importance of the temporal dimension in neural information processing.

Recently, more and more experimental evidences suggested that a straightforward firing rate concept based on temporal averaging may be too simplistic to describe brain activity. Indeed, for any rate there are an infinite number of possible temporal distributions of spikes. Vice versa, it has been experimentally showed that different stimuli or tasks can elicit different patterns of activity that have the same firing rate. In principle, taking into

account the temporal structure of a spike train would expand the alphabet that brain uses to encode information.

Recent observations on the behavior of cortical visual neurons demonstrated a precision in brain function timings higher than would be predicted from frequency coding. Humans, for example, can recognize and respond to visual scenes in less than 400ms. Recognition and reaction involve several processing steps from the retinal input to the finger movement at the output. If at each processing step neurons had to wait in order to perform a temporal average, the reaction time would be much longer. This result suggests the existence of computational processes based on the precise timing of spikes in neuronal ensembles. In the last decade, the focus of attention in experimental and computational neuroscience has therefore shifted towards the exploration of how the timing of single spikes is used by the nervous system.

There is evidence of precise temporal correlations between pulses of different neurons and stimulus dependent synchronization of the activity in neuronal populations. These results suggest that the exact timing of spikes should play an important role.

Looking at the raster plot of the data we acquired and analyzed during the previous experiment (see Ch. 4.), it was clear to us how the response of most of cells was not constant in the 1s period when the visual stimulation was the same, either with expanding and contracting optic flow. There might be two reason for a behavior like this: it could be an intrinsic behavior of a cell, or determined by the connections between cells of the same area integrating different information. The previous study, based on mean firing rate, had lost these details.

The aim of this further analysis on the data shown in Ch. 4 was to investigate the different behaviors of the cell instantaneous frequency oscillations in time. Unfortunately, all these cells were recorded in different experimental sessions, so it was meaningless to study the correlation and cross-correlation between

different response pattern recorded, as usually done with simultaneous recordings. This analysis will be carried on in future studies, when recording of multiple cell will be performed simultaneously.

5.1. Methods

5.1.1. Experimental paradigm and stimuli

For the in depth experimental paradigm and stimuli see chapter 4.1.1.

In brief: extracellular activity of single neurons was recorded from the dorsal surface of the superior parietal lobule. The monkeys performed a reaction time task while fixating a red target presented on a computer monitor and while different visual stimuli were shown. The eye position was checked off-line and trials with incorrect fixation or saccades were discarded. Five different stimulation paradigms were used. In first test, the FP was presented in the center of the screen and FOE in one of nine locations in a 3x3 grid at 15° distance each (Fig. 40C). In the second test the FOE was presented in the center of the screen, while FP was in one of the nine locations (Fig. 40D). In addition, in the third test, the eye position effect was studied by presenting FP and FOE in the same position in each of the nine locations (Fig. 40E). Each neuron was also tested by the luminous bar, moving along the screen in eight directions at 45° angular intervals (Fig. 40F). Finally, when recordings were stable enough, response selectivity for translational stimuli was tested. (Fig. 40G).

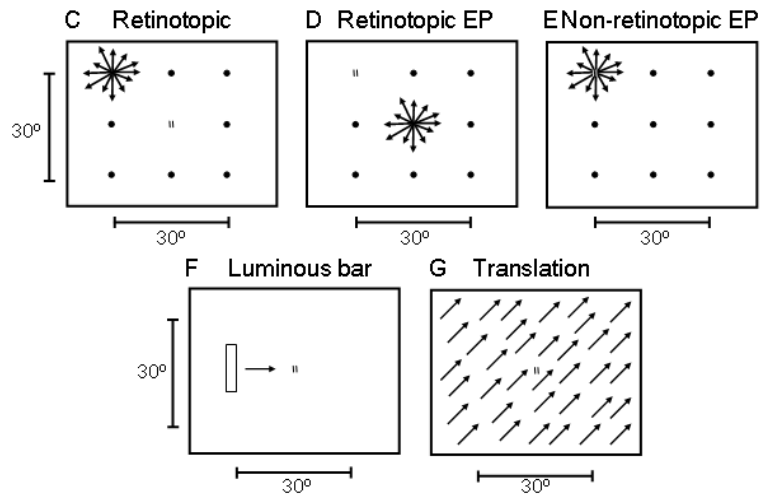


Figure 41: C. Retinotopic test. The FP was presented in the center of the screen and FOE in one of nine locations in a 3x3 grid at 15° distance each. Black dots indicates other FOE peripheral positions. In this test, the FOE was also positioned in the central position concentric with the fixation point. D. Retinotopic EP test. The FOE was in the center of the screen, while FP was in one of the nine locations. Black dots indicates other FP peripheral positions. E. Non-retinotopic EP test. FP and FOE were displayed concentric in one of the nine locations. Black dots indicates other FP/FOE peripheral positions. F. Receptive field mapping. A luminous bar moving across the screen in eight directions at 45° angular intervals. G. Translation test. The random dot background was moved tangentially to the frontoparallel plane, in eight directions at 45° angular interval. FP: fixation point; FOE: focus of expansion; EP: eye position, RdT: random time.

5.1.2. Data Analysis

All data analysis were performed by means of MatLAB routines.

- The activity of a cell was recorded by the acquisition system as ISI (*inter-spike intervals*):

```

1 1 E 155
0
-192 33      104      123      10      68      61      8      57      161      26      30      124      2      79      120
-224 70      9       8       30      56      43      16      8       44      39      17      14      15      28      5
-240 13      7       65      46      2       23      68      91      65      4       23      12      3
-208 14      18      22      27      36      2       5       20      23      6       18      61      29      20      24
-80  214

1 2 H 217
0
-192 31      5       127      121      59      74      148
-224 4       102      19      349      86      27      93      81      72      65      137      283      92      168      14
-240 2
-240 40      1       2       76      29      2       48      30      21      4       7       2       17      8      17
-232 2       15      50      55      36      57      54      17      10      16      72      24      30      17      13
-236 192      2       37      28      14      25
-244 10      8       13      10      7       4       20      3       11      14      3       35      3       6       2
-212 7       0       8       4       24      13      25      7       31      31      68      223      208      120      57
-84  165

```

Figure 42: output text file of the acquisition system. Every number represents an event, than can be a spike or a time marker to synchronize cell activity with the behavioural experiment.

- From the ISI we plotted the correspondent raster plot, that showed the response of neurons of area P_{Ec} to radial optic flow stimuli. From the raster plot observation, it was noticeable that many neurons did not maintain a constant activity while the same visual stimulus was presented.

As example, see Fig.42.

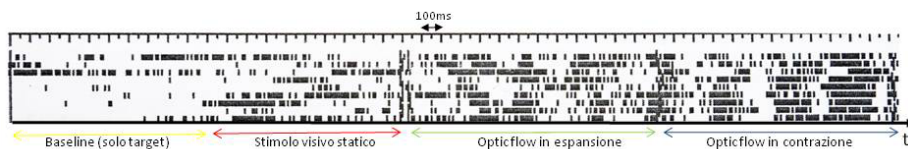


Figure 43: Raster plot of the activity of a neuron during the presentation of a particular combination of FOE/FP positions. Every vertical line corresponds to a spike in time and every row is a repetition of the same visual stimulation.

In addition to mean rate analysis, it was therefore interesting to try to characterize the trend of these activity oscillations in time. The main aim were: to find a relationship between the response pattern and the visual stimuli/eye positions, to look for typical pattern that may repeat in different conditions and to investigate the interactions between neurons.

- For each cell and each combination of stimulation, the PSTH was calculated (see Ch. 2.5. for details). Spike train were aligned with stimulus onset, for each of the n ($n \cong 10$) repetitions of the same trial. The stimulation interval T was divides into N bins of length Δ . We calculated the number of spikes happening in each Δ , for every repetition of the trial, and normalized by n . To improve the temporal resolution of the PSTH, we calculated it with a time window of 40ms sliding along the time axis of 5ms each iteration.
- We interpolated the PSTH discrete values (\bullet) with splines. A cubic spline is a spline constructed of piecewise third-order polynomials which pass through a set of control points, the PSTH discrete values. The second derivative of each polynomial is commonly set to zero at the endpoints, since this provides a boundary condition. In this way, we obtained a continuous function of neuronal activity, during the presentation of a visual stimulus.

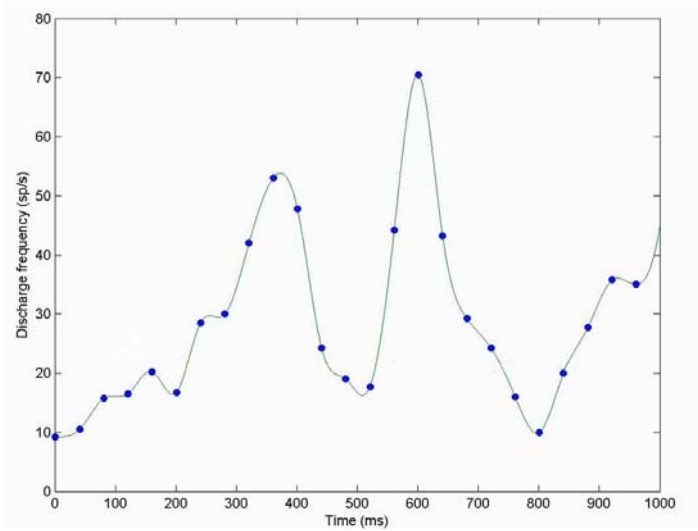


Figure 44: Spline interpolation of the PSTH discrete values, for the response to expansion optic flow of the same cell as before.

● discrete values every 40ms of the PSTH

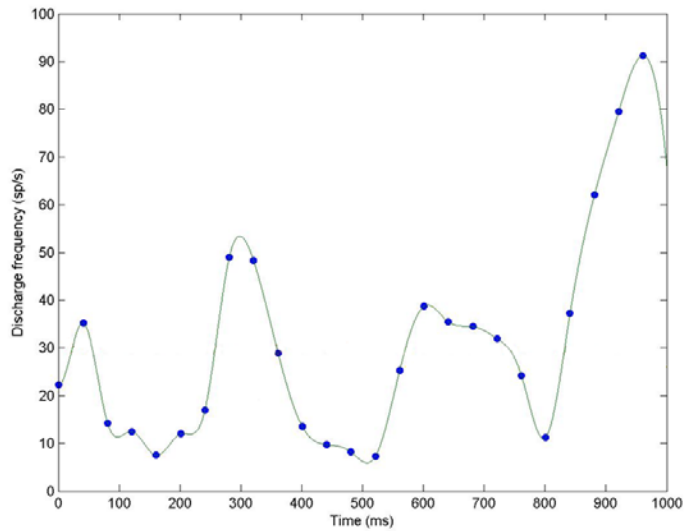


Figure 45: Spline interpolation of the PSTH discrete values, for the response in 1s to contraction optic flow, of the same cell as before.

● discrete values every 40ms of the PSTH

- We then defined a threshold value: if the cell activity was over this value, we considered the cell discharge frequency increased by the stimulus presentation. This threshold value depended on: the mean baseline discharge rate, that is the mean activity when no visual stimuli are presented, and the maximums and minimums of the PSTH values during visual stimuli presentation.

b : baseline mean frequency rate

f : spline of PSTH values

s : threshold value defined as

$$s = b + 40\%(\max(f) - b)$$

- We calculated the time intervals when the spline function of the cell activity is over/under the threshold value. We also considered appropriate to leave out the time intervals shorter than 50ms, as we assumed they were not significant enough.

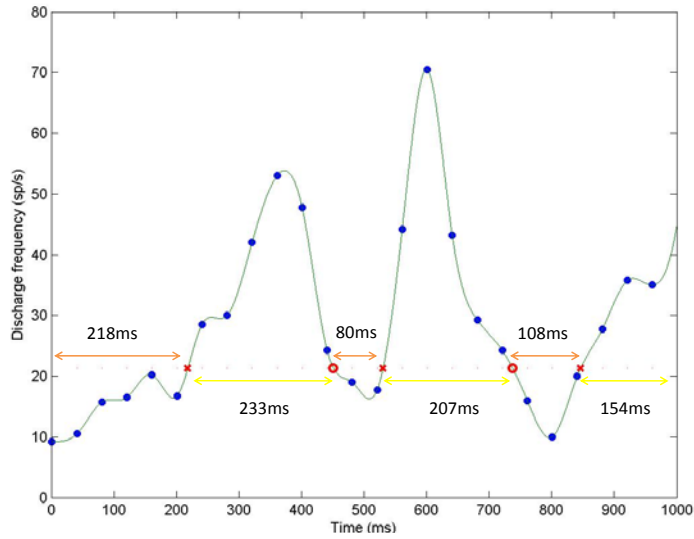


Figure 46: Spline interpolation of the PSTH discrete values, for the response to expansion optic flow of the same cell as before.

● discrete values every 40ms of the PSTH. X,O. intersections between the spline and the threshold value.

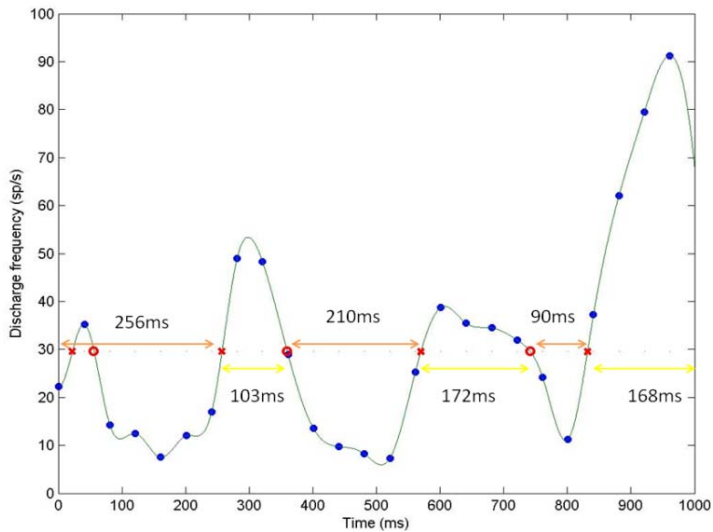


Figure 47: Spline interpolation of the PSTH discrete values, for the response to contraction optic flow of the same cell as before.

● discrete values every 40ms of the PSTH. X,O. intersections between the spline and the threshold value.

- At last, we applied a K-Means cluster analysis to the data achieved with the previous steps. The term *cluster analysis* encompasses a number of different algorithms and methods for grouping objects of similar kind into respective categories. Cluster analysis is an exploratory data analysis tool which aims at sorting different objects into groups in a way that the degree of association between two objects is maximal if they belong to the same group and minimal otherwise. In particular, we are interested in grouping cells for similar “oscillations” behavior, and understanding if a particular combination of FOE/FP position arise similar oscillations in more than one cell.

In the analysis carried on, we considered separately optic flow in expansion and contraction, and different stimuli positions.

- The variables for the first clustering were the latencies (ms from the stimulus onset and the threshold overcoming) and the integral of the spline function in the time interval when the activity is over the threshold. Results might be interesting to quantitatively distinguish different behaviours: some cells might change their oscillations characteristics with the changing of the stimulus position, while other might retain the same oscillation not regarding the stimulus position.
- The variable for the second clustering was how many times the activity of a cell overcame the threshold value.

5.2. Results

With the cluster analysis based on when the cells activity overcomes the threshold value and for how long it remains over the threshold, we tried to characterize different behaviors of the cells. This is what cluster analysis was for: understanding how many different behaviours, during the same stimulation, the recorded cells showed, and whether there was one “most common” behaviour.

- The results of the first clustering considered as variables the latency and the integral of the spline function in the time interval when the activity is over the threshold. We considered separately optic flow in expansion and contraction, and the three experimental paradigms. Results showed that there was not only one more common behavior between cells, but two.

Half of the cells changed their firing pattern characteristics with the changing of the stimulus position, the FOE/FP position or both. This was noticed for both expansion and contraction, almost in the same way. This behavior is a significant clue that can be explained in two ways: as seen in the background chapter, one question is still open for researchers: where does neuronal signal coding lies? These results suggest that signal coding might lie also in the oscillations of the spike train. The second hypothesis is that these particular patterns of oscillations were produced by the connections with other cells.

The other half of cells retained almost the same oscillation pattern, not regarding the stimulus position or paradigm.

- The second clustering considered only how many oscillations in time the activity of the cell showed, considering expansion and contraction separately. These results are useful in evaluating common behavior of the cells, not including the stimuli modulation. We chose to separate cell in three groups: cell that showed only 1 main period over-threshold, two oscillations and more than two.

As expected, we found that 42% of cells during expansion and 45% during contraction had only one phase over-threshold. This is the most common behavior, that in some way reinforces the significance of the analysis we made based on mean frequency (see Ch.4). Calculating the mean frequency over time causes the loss of details, that may be significant, but doesn't completely change the meaning of the results. The latencies of these periods over-threshold went from few ms to 300ms and more. The mean latency for expansion and contraction together is 156ms.

The second group of cells, who showed two oscillations over-threshold, was populated by 25% for expansion and 24% for contraction. The mean latency was usually slightly shorter than the previous group, and the mean latency was 103ms.

At last, we have the group of the cells that showed more than two oscillations in 1s of the same visual stimulation, 33% for expansion and 31% per contraction. As noticeable, a quite big percentage of cells falls in this group: it would be interesting to further investigate these different behaviors in an ad hoc study. Unfortunately, these data were not recorded with this aim, and this particular cellular behavior was discovered only later. Simultaneous recording of groups of cells would add a lot of information.

5.3. Conclusions and Discussion

This more in depth analysis of the same data as in Ch.4 started from the awareness that neuronal coding is complex, and most probably doesn't lie completely in mean firing rate. Many studies in recent years have been devoted to the detection and interpretation of them as synchronizing devices. Plus, looking at the raster plot of the data, it was clear how the response of most cells was not constant in the 1s period when the visual stimulation was the same, either with expanding and contracting optic flow.

The results of this study are still preliminary, in the sense that they do not expect to be exhaustive and they cannot answer to which is the reason why these cells respond to visual stimuli with these different patterns. For sure, a more targeted experiment should be soon carried on, with simultaneous recording of multiple cells.

In the future study, it'll be interesting to study the cells interconnection with the "gravitational transformation". This model studies synchronism between spike trains of different neurons, recorded simultaneously. From the information regarding synchronism, it's possible to make some hypothesis on neuronal connections in small recorded networks.

The basic idea of the gravitational model (Gerstein e Aertsen, Representation of cooperative firing activity among simultaneously recorded neurons. 1985) (Gerstein, Perkel e Dayhoffs 1985) is to represent each neuron of a network as a particle that can move in a virtual Euclidean space. If we have N neurons in the network, we would have N particles and a N-dimensional euclidean space. Whenever a neuron generates a spike, its corresponding particle increment its fake "charge", and after its charge decades exponentially in time. Particles may move in the space and attract each other proportionally to the product of their charges. We're not interested In following the dynamics of the movements, but in how they aggregate after some time. The equation that controls the i-th particle (i.e. neuron) moving is:

$$d\bar{x}_i/dt = \sigma q_i(t) \bar{f}_i(t)$$

With:

$$q_i(t) = q_i(0)e^{-t/\tau} : \text{charge exponential decay}$$

$$\bar{f}_i = \sum_{j \neq i} q_j \bar{r}_i(j) : \text{field that moves the particles}$$

$$\bar{r}_i(j) = \frac{(\bar{x}_j - \bar{x}_i)}{\|\bar{x}_j - \bar{x}_i\|^2} \text{ direction of the field}$$

By means of an Euler integration of the differential equation, it's possible to follow particles motion whenever a spike happens. For the simulation, it's possible to fix two parameters: σ regulates the mobility of the particles in a viscous environment, τ controls how much two spikes should be synchronous if we want two particles to attract each other.

Until now the model has been implemented in a MatLAB routine, but it's been applied only to simulated trains of spikes, with Poisson distribution. The reason is that we didn't record any neurons simultaneously, yet.

The idea for future data analysis is to: first, select with the same cluster analysis as in this study groups of neurons that can be good candidates for synchronism, and then apply the gravitational model to these data.

Results will be very interesting, because detecting synchronism between some neurons may imply synaptic connections between them.

Future ideas to improve the gravitational model are: to increment the fake charge in a different way for each neuron, to consider more neuron variability, and to contemplate that if a neuron fires and another not, not only they do not attract each other, but they should repulse.

7. Overall Conclusions and Discussion

The principal subject of this work is the investigation of the mechanism of the visual perception of space and motion. There's a question researcher and scientists of many fields have tried for a long time to address: how do we see the world around us? And, how can men perceive the direction of their motion?

The visual information during locomotion, called Optic Flow (OF), is very important to perceive heading direction. When we move, for example flying on a plane or driving a car, distant objects like clouds and mountains move so slowly they appear still. The objects that are closer, such as buildings and trees, appear to move backwards, with closer objects moving faster than distant objects. Very close objects, such as grass or small signs by the road, move so fast they whiz right by us. In addition, when we interact with the environment our head never remains in a fixed position and the adjustments in posture produce some changes in the position of our eyes in space.

All these information are important to determine what is called *heading direction*. Heading perception is the process of inferring the speed and direction of elements in a scene based on visual, vestibular and proprioceptive inputs. Although this process appears straightforward to most observers, it has proven to be a difficult problem from a computational perspective, and extraordinarily difficult to explain in terms of neural processing.

This thesis was aimed to investigating a still open question about motion perception.

It's well known from neurophysiologic researches that motion is analyzed primarily in the dorsal pathway from the primary visual area to the parietal cortex. Most cells in the visual system may be able to extract information

about an object that is moving and its position. Why do scientists suppose the existence of a specialized neural subsystem? Is there any need of it?

In monkeys, many areas show responsiveness to optic flow stimuli, but the tuning characteristics of the neurons may vary. Area MT, MST, VIP, 7a, STPa are known for taking part in motion processing.

Area PEc, in the dorso-caudal portion of the superior parietal cortex, has been for years considered part of the somato-sensory cortex but recent studies demonstrated that neurons in this area also respond to optic flow stimuli and are involved in hands movements and reaching.

Our research project started from the hypothesis that neurons in area PEc might be involved in the integration of visuo-motor signals and that optic flow processing takes part in linking visual input and motor output.

- In details, the main aim of this research was to assess whether optic flow selective neurons in parietal area PEc are modulated by eye position. We recorded single neuron activity during optic flow stimulation in two monkeys, varying eye and retinal FOE positions, while they were fixating in particular position of the screen. The experimental paradigm included three main tasks: the *retinotopic* organization of FOE neuronal selectivity was tested presenting FP in the center of the screen and FOE in one of nine locations, the *retinotopic eye position* task assessed the influence of the eye position upon the optic flow and retinotopy selectivity with FP/FOE positions reversed by presenting the FOE in the center of the screen, while FP was in one of the nine locations; in the last task the eye position effect irrespective of retinotopy was studied by presenting FP and FOE in the same position in each of the nine locations.

The main result of this research is that the response of many PEc neurons to optic flow radial stimuli is strongly influenced by eye position, with different tuning for expansion and contraction. This finding demonstrates that FOE

representation in area PEc might integrate retinal and extraretinal signals, in order to stabilize FOE spatial representation when the angle of gaze is shifted.

Although many neurons did not show any gaze field without visual stimulation, the eye position modulated optic flow responses in about half of neurons. Comparing the neuronal responses to the same retinal FOE position at different angle of gaze in both stimuli, we found two different subpopulations of neurons: one responding similarly to FOE independently from eye position, the other modulated by the combination of FOE and eye position.

These novel results suggest that PEc neurons integrate both visual and eye position signals and allow to hypothesize a role in guiding locomotion being part of a cortical network involved in FOE representation during self-motion. Visual and eye position interaction in this area could be seen as a contribution to the building of the invariant space representation necessary to motor planning.

- The second aim of this study started from the knowledge that brain rhythms arise through the synchronization of neurons and their entrainment in a regular firing pattern. In this process, networks of reciprocally connected inhibitory neurons are often involved, but what mechanism determines the oscillation frequency is not completely understood. Moreover, a question still open is which aspects of a neuron's electrical activity convey information about the environment and our mental states. It's well known that the information lies in spikes sequences, but the question is how to read this sequence of spikes emitted by neurons as a function of time. Recently, more and more experimental evidences suggested that a straightforward firing rate concept based on temporal averaging may be too simplistic to describe brain activity. Looking at the raster plot of the data we acquired and analyzed during the previous experiment, it was clear how the response of most of cells was not constant in the 1s period when the visual stimulation was the same,

either with expanding and contracting optic flow. The aim of this further analysis on the neuronal data was to investigate the different behaviors of the cell instantaneous frequency oscillations in time. With a cluster analysis based on when the cells activity overcomes the threshold value and for how long it remains over the threshold, we tried to characterize different behaviors of the cells. This is what cluster analysis was for: understanding how many different behaviours, during the same stimulation, the recorded cells showed, and whether there was one “most common” behaviour. Results showed that half of the cells changed their firing pattern characteristics with the changing of the stimulus position, the FOE/FP position or both. The other half of cells retained almost the same oscillation pattern, not regarding the stimulus position or paradigm. These results suggest that signal coding might lie also in the oscillations of the spike train.

The second clustering considered only how many oscillations in time the activity of the cell showed, considering expansion and contraction separately. Most of cells (over 40%) showed only one long period overthreshold, the second group of cells showed two oscillation over-threshold (25%) and then other cells showed up to four oscillations in 1s time. The results of this study are still preliminary, in the sense that they do not expect to be exhaustive and they cannot answer to which is the reason why these cells respond to visual stimuli with these different patterns. For sure, a more targeted experiment should be soon carried on, with simultaneous recording of multiple cells.

Bibliography

Adrian, E.D. *The basis of sensation: The action of the sense organs*. New York: Norton, 1928.

Amunts, V.V. "A structural organization of the sensory projections on a reticular formation of the brain stem." *Zh Nevrol Psikhiatr*, 1999.

Andersen, R.A., C. Asanuma, C.K. Essick, and R.M. Siegel. "Encoding of spatial location by posterior parietal neurons." *Science*, 1985.

Anderson, K.C., and R.M. Siegel. "Optic flow selectivity in the anterior superior temporal polysensory area, STPa, of the behaving monkey." *J. Neurosci.*, 1999.

association, American medical. *L'uso degli animali nella ricerca scientifica*. Bologna: Esculapio, 1995.

Avillac, et al. "Reference frame for representing visual and tactile locations in parietal cortex." *Nat Neurosci*, 2005.

Bach, M. "An accurate and linear infrared oculometer." *J. Neurosci. Methods*, 1983.

Banks, et al. "Estimating heading during real and simulated eye movements." *Vis. Res.*, 1996.

Banks, M.S., and C.S. Royden. "Estimating heading during eye movement." *Vis. Res.*, 1994.

Batista, et al. "Reference frames for reach planning in macaque dorsal premotor cortex." *J. Neurophysiol.*, 2007.

Battaglia-Meyer, et al. "Eye-hand coordination during reaching. An analysis of the relationships between visuomanual signals in parietal cortex and parieto-frontal associations projections." *Cereb. Cortex*, 2001.

Boussaoud, D. "eye position effects on the neuronal activity of dorsal premotor cortex in the macaque monkey." *J Neurophysiol*, 1998.

- Bremmer, F., and J. Duhamel. "Heading encoding in the macaque ventral intraparietal area (VIP)." *Eur. J. Neurosci.*, 2002.
- Bremmer, F., and J.R. Duhamel. "The representation of movement in near extrapersonal space in the macaque ventral intraparietal area (VIP)." *Exp. Brain Res.*, 1997.
- Breveglieri, et al. "Visual, somatosensory, and bimodal activities in the macaque parietal area PEc." *Cereb Cortex*, 2008.
- "Somatosensory Cells in Area PEc of Macaque Posterior Parietal Cortex ." *J. Neurosci.*, 2006.
- Britten, K.H. "Mechanism of self-motion perception." *Annu rev neurosci*, 2008.
- Bruce, C. "Visual properties of neurons in a polysensory area in the superior temporal sulcus of the macaque." *J. Neurophysiol.*, 1981.
- Brunel, L. "Effects of synaptic noise and filtering on the frequency response of firing neurons." *Phys. Rev. Lett.*, 2001.
- Clocksink, W.F. "Determining the orientation of surfaces from optical flow." *Proc Conf AISB*, 1980.
- Colby, C.L. et al. "Corollary discharge and spatial updating:when the brain is split in space still unified?" *Prog Brain Res*, 2005.
- Colby, C.L. "Ventral intraparietal area of the macaque: anatomic location and visual response properties." *J. Neurophysiol.*, 1993.
- Colby, C.L., and J.R. Duhamel. "Spatial representations for action in parietal cortex." *Brain Res Cogn Brain Res* , 1996.
- Crowell, et al. "Perceiving heading with different retinal regions and types of optic flow." *Percept. Psychol.*, 1991.
- In *Perception with an eye for motion.*, by et al. Cutting. MIT press, 1986.

"Human heading judgements and object-based motion information." *Vision Res.*, 1999.

Cutting, J.E. "Wayfinding from multiple sources of local information in retinal flow." *Percept. Perform.*, 1996.

Duffy, C. J., & Wurtz, R. H. "Sensitivity of MST neurons to optic flow stimuli. I. A continuum of response selectivity to large field stimuli.II. Mechanism of response selectivity revealed by small-field stimuli." *J. Neurophysiol.*, 1991.

"Medial superior temporal area neurons respond to speed patterns in optic flow." *J. Neurosci.*, 1997.

Duffy, C.J. & Wurtz, R. H. "Response of monkey MST neurons to optic flow stimuli with shifted centers of motion." *J. Neurosci.*, 1995.

Duffy, C.J. "Optic flow analysis for self-movement perception." *Neuronal processing of optic flow.*, 2000.

Duffy, F.H., and J.L. Burchfiel. "Somatosensory system: organizational hierarchy from single unit in monkey area 5. ." *Science*, 1971.

Duhamel, J.R., and C.L. Colby. "Ventral intraparietal area of the macaque: congruent visual and somatic response properties." *J. Neurophysiol.*, 1998.

Economo, C. von, and G.N. Koskinas. "Die cytoarchitektonik der Hirnrinde des erwachsenen menschen." *Textband Und atlas*, 1925.

Ellaway, P.H. "Cumulative sum technique and its application to the analysis of peristimulus time histograms." *Electroencephalogr. Clin. Neurophysiol.*, 1978.

Fajen, B.R., and W.H. Warren. "Go with the flow." *Trends in cogn Science*, 2000.

Ferraina, et al. "Early coding of visuomanual coordination during reaching in parietal area PEc." *J. Neurophysiol.*, 2001.

Fetsch, et al. "Spatial reference frames of visual, vestibular and multimodal heading signals in the dorsal subdivision of the medial superior temporal area." *J Neurosci*, 2007.

Gerstein, G.L., and M.H.J. Aertsen. "Representation of cooperative firing activity among simultaneously recorded neurons." *J. Neurophys.*, 1985.

Gerstein, G.L., D.H. Perkel, and J.E. Dayhoffs. "Cooperative firing activity in simultaneously recorded populations of neurons: detection and measurement." *J. Neurosci.*, 1985.

Gerstner, W. "Population dynamics of spiking neurons: fast transients, asynchronous states and locking." *Neural. Comp.*, 2000.

Gibson, J. *The perception of visual world*. Cambridge: The riverside press, 1950.

Grigo, A., and M. Lappe. *An analysis of heading towards a wall, in Vision and Action*. Cambridge University Press, 1998.

Hadani, I., G. Ishai, and M. Gur. "Visual stability and space perception in monocular vision: a mathematical model." *J Opt. Soc. Am*, 1980.

Harris, M.G., and G. Carrè. "Is optic flow used to guide walking while wearing a displacing prism?" *Perception*, 2001.

Hietanen, J.K., and D.I. Perrett. "A comparison of visual responses to object- and ego-motion in the macaque superior temporal polysensory area." *Exp. brain res.*, 1996.

Hubel, D. H. Wiesel, T. N. "Receptive fields of single neurons in the cat's striate cortex. ." *J. Physiol.*, 1959.

Jacobsen, J.F. "The functions of the frontal association areas in monkeys." *Comp Psychol Mon*, 1936.

Koenderink, J.J., and A.J. van Doorn. "Spatial noise for virtual research." *Vision Res*, 1974.

- Kumar, S. "A molecular timescale for vertebrate." *Nature*, 1998.
- Lappe M., Bremmer F., Van der Berg A.V. "Perception of self motion from visual flow." *Trends. Cogn. Science*, 1999.
- Lappe, M. "Computational mechanism for optic flow analysis in primate cortex. ." *Neuronal processing of optic flow.*, 2000.
- Lee, D.N. "The optic flow field: the foundation of vision." *Philos Trans. R. Soc. London Ser.* , 1980.
- Longuet-Higgins, H.C., and K. Prazdny. "The interpretation of a moving retinal image." *Proc R Soc Lond Biol Sci*, 1980.
- Marconi, et al. "Eye-hand coordination during reaching. I. Anatomical relationships between parietal and frontal cortex. ." *Cereb. Cortex*, 2001.
- Matelli, et al. "Superior area 6 differs from the superior parietal lobule in the macaque monkey." *J. Comp. Neurol.*, 1998.
- Merchant, et al. "Effects of optic flow in motor cortex and area 7a." *J. Neurophysiol.*, 2001.
- Motter, B.C., and V.B. Mountcastle. "The functional properties of the light-sensitive neurons of the posterior parietal cortex studied in waking monkeys: foveal sparing and opponent vector organization." *J. Neurosci.*, 1981.
- Mountcastle, et.al. "Posterior parietal association cortex of the monkey: command functions for operations within extrapersonal space." *J. Neurophysiol.*, 1975.
- Mountcastle, V.B. "Perceptual neuroscience." *Cereb cortex*, 1998.
- "Modality and topographic properties of single neurons of cat's somatosensory cortex." *J. Neurophysiol.*, 1957.
- Obermayer, K., and G.G. Blasdel. "Geometry of orientation and ocular dominance columns in monkey striate cortex." *J Neurosci*, 1993.

Orban GA, Van Essen D, Vanduffel W.: "Comparative mapping of higher visual areas in monkeys and humans." *Trends Cogn Sci*, 2004.

Pandya, D.N., and B. Seltzer. "Intrinsic connections and architectonics of posterior parietal cortex in the rhesus monkey." *J Comp Neurobiol*, 1982.

Pascual-leone, et al. "Procedural learning and prefrontal cortex." *Ann NY acad sci*, 1995.

Paxinos, G. *The rhesus monkey brain: in stereotaxic coordinates*. Boston: Academic press, 2000.

Pesaran, B., M.J. Nelson, and R.A. Andersen. "Dorsal premotor neurons encode the relative position of the hand, eye, and goal during reach planning." *J. Neurophysiol.*, 2006.

Prokop, et al. "Visual influence on human locomotion: modulation to changes in optic flow." *Exp.Brain Res.*, 1997.

Raffi, et al. "Neuronal responses in macaque area PEc to saccade and eye position." *J. Neurosci.*, 2008.

Raffi, M., and R.M. Siegel. "Multiple cortical representation of optic flow processing." In *Optic flow and beyond*, by L.M. Vaina, S.A. Beardsley and S.K. Rushton. 2004.

Raffi, M., S. Squatrito, and M.G. Maioli. "Neuronal responses to optic flow in the monkey parietal area PEc." *Cereb. cortex*, 2002.

Rieger, et al. "Human visual navigatin in the presence of 3D rotations." *Biol. Cybern.*, 1985.

Rilling, J. "Human and nonhuman primate brains: are they allometrically scaled versions of the same design?" *Anthropol.*, 2006.

Robinson, D. (Neurobiology. Springer, The) 1998.

Rogers, B.J., and C. Dalton. "The role of perceived direction and optic flow in the control of locomotion and for estimating the point of impact." *Investigative ophthalmology and visual science*, 1999.

Rogers, B.J., and R.S. Allison. "When do we use optic flow and when do we use perceived direction to control locomotion?" *Perception*, 1999.

Rushton, S.K., and D.D. Salvucci. "An egocentric account of the visual guidance of locomotion." *Trends in cognitive science*, 2001.

Rushton, S.K., J.M. Harris, M.R. Lloyd, and J.P. Wann. "Guidance of locomotion on foot uses perceived target location rather than optic flow." *Curr Biol.*, 1998.

Saito, H. "Integration of direction signals of image motion in the superior temporal sulcus of the macaque monkey." *J. Neurophysiol.*, 1986.

Schaafsma, S.J., and J. Duysens. "Neurons in the ventral intraparietal area of awake macaque monkey closely resemble neurons in the dorsal part of the medial superior temporal area in their responses to optic flow patterns." *J. Neurophysiol.*, 1996.

Shenoy, K. V., Bradley, D. C., & Andersen, R.A. "Influence of gaze rotation on the visual response of primate MSTd neurons." *J. Neurophysiol.*, 1999.

Shipp, et al. "A visuo-somatomotor pathway through superior parietal cortex in the macaque monkey: cortical connections of areas V6 and V6a." *Eur J Neurosci*, 1998.

Siegel, R.M., and H.L. Read. "Construction and representation of visual space in the inferior parietal lobule." *Cereb. Cortex*, 1997.

Squatrito, et al. "Visual motion responses of neurons in the caudal area PEc of the macaque monkeys." *J. neurosci.*, 2001.

Squatrito, et al. "Visual motion responses of neurons in the caudal area PE of the macaque monkeys." *J. Neurosci.*, 2001.

- Stone, L., and J. Perrone. "Human heading estimation during visually simulated curvilinear motion." *Vis. Res.*, 1997.
- Tanaka, K. "Underlying mechanisms of the response specificity of expansion/contraction and rotation cells in the dorsal part of the medial superior temporal area of the macaque monkey." *J. Neurophysiol.*, 1989.
- Thorpe, S., Fize, D., and Marlot, C. "Speed of processing in the human visual system. ." *Nature*, 1996.
- Turano, K., and X. Wang. "Visual discrimination between a curved path and straight path of self motion: effects of forward speed." *Vis. Res.*, 1994.
- van den Berg, A.V. "Human heading perception." *Neuronal Processing of Optic Flow*, 2000.
- W.H., Warren. "Perception of circular heading from optic flow." *J. Exp. Psychol. Hum. Percept. Perform*, 1991.
- Warren, et al. "Perception of translational heading from optic flow." *J. Exp. Psychol. Hum. Percept. Perform*, 1988.
- Warren, et al. "On the sufficiency of the velocity field for perception heading." *Biol. Cybern.*, 1991.
- "Optic flow is used to control human walking." *Nature Neuroscience*, 2001.
- Warren, W.H., and D.J. Hannon. "Eye movements and optical flow." *J. Opt. Soc. Am. Ser.*, 1990.
- Wolbers, et al. "Spatial updating: how the brain keeps track of changing object location during observer motion." *Nat Neurosci*, 2008.
- Wood, et al. "Weighting to go with the flow?" *Current Biol*, 2000.
- Wu, W., and N.G. Hatsopoulos. "Coordinate system representations of movement direction in the premotor cortex. ." *exp Brain res.*, 2006.

